

**CHARACTERISTICS OF ROMAN MORTARS  
PRODUCED FROM NATURAL AND ARTIFICIAL  
POZZOLANS IN AİGAİ AND NYSA**

**A Thesis Submitted to the  
the Graduate School of Engineering and Sciences of  
İzmir Institute of Technology  
in Partial Fulfillment of the Requirements for the Degree of**

**DOCTOR OF PHILOSOPHY**

**in Architecture**

**by**

**Elif UĞURLU SAĞIN**

**July 2012**

**İZMİR**

We approve the thesis of **Elif UĞURLU SAĞIN**

**Examining Committee Members:**

---

**Prof.Dr. Hasan BÖKE**

Department of Architectural Restoration, İzmir Institute of Technology

---

**Prof.Dr. Başak İPEKOĞLU**

Department of Architectural Restoration, İzmir Institute of Technology

---

**Assoc.Prof.Dr. Şebnem YÜCEL**

Department of Architecture, İzmir Institute of Technology

---

**Assoc.Prof.Dr. Selim Sarp TUNÇOKU**

Department of Architectural Restoration, İzmir Institute of Technology

---

**Assoc.Prof.Dr. Ahmet GÜLEÇ**

Department of Conservation and Restoration of Movable Cultural Assets,  
İstanbul University

**10 July 2012**

---

**Prof.Dr. Hasan BÖKE**

Supervisor,  
Department of Architectural Restoration  
İzmir Institute of Technology

---

**Assoc.Prof.Dr. Şeniz ÇIKIŞ**

Head of the Department of Architecture

---

**Prof.Dr. R.Tuğrul SENGER**

Dean of the Graduate School of  
Engineering and Sciences

## ACKNOWLEDGMENTS

First and foremost, I would like to express my deepest gratitude to my supervisor Prof.Dr. Hasan Bke for his scientific guidance, concern and unfailing support throughout this thesis. His knowledge and encouragement always enrich my development as a student; and I am much indebted to him for all my graduate education period. I have to mention that, it has been an honor for me to be his first PhD student.

I especially wish to thank Prof.Dr. Bařak İpekoęlu, head of the Department of Architectural Restoration, for her support and tolerance, and also for constructive comments about the thesis.

I gratefully acknowledge my thesis committee, Assoc.Prof.Dr. Selim Sarp Tunçoku and Assoc.Prof.Dr. řebnem Ycel for their valuable contributions in the progress of this thesis. Also, I want to thank Assoc.Prof.Dr. Ahmet Gleç for his participation to thesis defense exam jury and his valuable advices about the thesis.

My special thanks are for Assoc.Prof. Dr. řerife Yalçın for her guidance on development of a new method for determination of calcite and silica contents in the binders of historic mortars, especially for her support in LIBS analyses part of the study. I also thank Res.Assist. Nadir Aras for his helps in LIBS analyses.

I am also very grateful to Dr. Engin Duran for his kind helps and technical support for the statistical evaluation of chemical analyses.

I would also thank Prof.Dr. Ersin Doęer for giving the opportunity to work on the mortars of Aigai, and Assist.Prof.Dr. Zeynep Aktre for her helps in the collaboration with the excavation team of Nysa.

Furthermore, my thanks are for my fellow labmates Kerem řerifaki, řaęlayan Deniz Kaplan and Fulya Murtezaoęlu for their helps, support, and friendship. The times we spent together working in our laboratory are irreplaceable to me.

At last but not the least, although words could not express my appreciation, I owe my dear husband Sercem M. Saęın, who made me to overcome all the difficulties with his encouragement, great care and love. Finally, I would like to express my special thanks to my beloved parents Hasan H. Uęurlu and Rukiye Uęurlu for their endless patience, support and love throughout my life. This thesis is dedicated to these precious people of my life.

## ABSTRACT

### CHARACTERISTICS OF ROMAN MORTARS PRODUCED FROM NATURAL AND ARTIFICIAL POZZOLANS IN AİGAI AND NYSA

The use of lime and natural and artificial pozzolans for mortar production were the important contributions of the Romans to the construction history. In this study, characteristics of Roman lime mortars produced by natural and artificial pozzolans from ancient cities of Aigai and Nysa have been determined in order to understand technology of Roman period lime mortars used in Anatolia. Within this scope, basic physical properties, raw material compositions, microstructural and hydraulic properties, mineralogical and chemical compositions of mortars were investigated by SEM-EDS, XRD, XRF, TGA, FTIR and LIBS analysis. A relatively fast and easy method was proposed for the quantitative determination of  $\text{CaCO}_3$  and  $\text{SiO}_2$  content in the binder compositions by using FTIR, LIBS, SEM-EDS and XRD analyses.

The results indicated that Roman lime mortars either produced by natural or artificial pozzolans were low dense and high porous materials with a high percent of macro pores. Roman lime mortars were mainly produced by using non-hydraulic high calcium lime and pozzolanic aggregates. Lime/aggregate ratios of mortars produced by natural pozzolans were 0.30, and mortars produced by artificial pozzolans were 0.55 respectively. Natural and artificial pozzolans from Aigai and Nysa were found to be produced by using different raw material sources. The method proposed for the quantitative determination of  $\text{CaCO}_3$  and  $\text{SiO}_2$  revealed that FTIR, SEM-EDS and LIBS analysis could be safely used to determine the lime and fine silica content in the binders of historic lime mortars.

Characteristics of lime mortars used in Anatolia were determined to be similar to the mortars used in Central Roman Empire although wall construction techniques of Anatolian architecture were different from the Central Roman Empire. The knowledge produced on the Roman lime mortar characteristics of Anatolian architecture is important for the conservation of ancient sites in Anatolia and the production of new lime mortars to be used in these sites.



## ÖZET

### AİGAI VE NYSA'DA DOĞAL VE SUNİ PUZOLANLAR İLE ÜRETİLEN ROMA HARÇLARININ ÖZELLİKLERİ

Kireç ile doğal ve suni puzolanların harç üretiminde kullanılması Romalıların yapım tarihine getirdikleri önemli katkılardır. Bu çalışmada, Aigai ve Nysa antik kentlerindeki doğal ve suni puzolanlar kullanılarak üretilmiş Roma dönemi harçlarının özellikleri Anadolu'da kullanılmış Roma dönemi kireç harçlarının teknolojilerinin anlaşılması amacıyla belirlenmiştir. Bu amaçla, harçların temel fiziksel özellikleri, hammadde kompozisyonları, mikroyapısal ve hidrolik özellikleri, mineralojik ve kimyasal yapıları SEM-EDS, XRD, XRF, TGA, FTIR ve LIBS analizleri ile belirlenmiştir. Harçların bağlayıcı kısımlarında bulunan kireç ve silikanın ağırlıkça oranlarının belirlenmesi için FTIR, SEM-EDS, LIBS ve XRD yöntemlerinin uygunluğu saptanmıştır.

Analiz sonuçları, doğal veya suni puzolanlar ile üretilmiş Roma dönemi kireç harçlarının düşük yoğunluklu, yüksek gözenekli ve yapılarında yüksek oranda makro gözenekler bulunduran malzemeler olduklarını göstermiştir. Bu harçlar, hidrolik olmayan kireç ve puzolanik agregalar kullanılarak üretilmiştir. Harçların kireç/agrega oranları doğal puzolanlar kullanılarak üretilmiş harçlarda 0.30, suni puzolanlar kullanılarak üretilmiş harçlarda 0.55'dir. Aigai ve Nysa harçlarında kullanılmış puzolanlar farklı hammadde kaynaklarından elde edilmiştir. Harçların bağlayıcı kısımlarını oluşturan kireç ve silika oranlarının belirlenmesi için FTIR, SEM-EDS ve LIBS analizlerinin güvenilir yöntemler oldukları saptanmıştır.

Anadolu'da ve Roma İmparatorluğu'nun merkezindeki duvar yapım teknikleri birbirlerinden farklı olmasına rağmen, her iki bölgedeki kireç harçları benzer özellikler taşımaktadır. Anadolu mimarlığında kullanılmış Roma dönemi kireç harçları üzerine üretilmiş olan bilgi, Anadolu'daki antik kentlerin korunması ve bu kentlerde kullanılacak yeni harçların üretilmesi için önem taşımaktadır.

# TABLE OF CONTENTS

LIST OF FIGURES.....	ix
LIST OF TABLES.....	xiii
CHAPTER 1. INTRODUCTION .....	1
1.1. Roman Lime Mortars .....	2
1.2. Roman Wall Construction Techniques with Lime Mortars .....	10
1.2.1. Wall Construction Techniques in Italian Peninsula during Roman Empire .....	10
1.2.1.1. Opus Incertum.....	11
1.2.1.2. Opus Quasi Reticulatum and Opus Reticulatum.....	12
1.2.1.3. Opus Vittatum .....	13
1.2.1.4. Opus Mixtum .....	15
1.2.1.5. Opus Spicatum .....	16
1.2.1.6. Opus Testaceum .....	18
1.2.2. Wall Construction Techniques in Anatolia during Roman Empire .....	19
1.2.2.1. Walls Comprised of Mortared Rubble Core and Facing.....	20
1.2.2.2. Walls Comprised of Mortared Materials.....	23
1.3. Recent Studies on Roman Lime Mortars .....	26
1.3.1. Basic Physical Properties .....	27
1.3.2. Mechanical Properties of Mortars .....	28
1.3.3. Raw Material Compositions.....	28
1.3.4. Mineralogical Compositions .....	30
1.3.5. Chemical Compositions .....	33
1.3.6. Hydraulic Properties of Mortars.....	35
1.3.7. Pozzolanic Activities of Aggregates .....	35
1.3.8. Microstructural Properties.....	36
1.4. Aim and Scope of the Study .....	38

CHAPTER 2. METHOD .....	40
2.1. Case Areas and Samples .....	40
2.1.1. Aigai .....	42
2.1.2. Nysa.....	48
2.2. Experimental Studies .....	57
2.2.1. Determination of Basic Physical Properties.....	57
2.2.2. Determination of Drying Rates of Mortars .....	58
2.2.3. Determination of Raw Material Compositions .....	59
2.2.4. Quantitative Determination of CaCO <sub>3</sub> and SiO <sub>2</sub> Content in the Binders .....	61
2.2.5. Mineralogical and Chemical Compositions .....	62
2.2.6. Chemical Compositions of Pozzolans.....	63
2.2.7. Pozzolanic Activities of Aggregates .....	63
2.2.8. Hydraulic Properties of Mortars.....	64
2.2.9. Microstructural Properties.....	64
 CHAPTER 3. RESULTS AND DISCUSSIONS .....	 65
3.1. Basic Physical Properties .....	65
3.2. Drying Rates .....	68
3.3. Raw Material Compositions .....	69
3.4. Characteristics of Lime Used in Mortars .....	73
3.5. Characteristics of Pozzolans .....	77
3.5.1. Pozzolanic Activities of Aggregates .....	77
3.5.2. Mineralogical Compositions of Pozzolans.....	78
3.5.3. Chemical Compositions of Pozzolans.....	85
3.5.4. Microstructural Properties of Pozzolans .....	95
3.6. Characteristics of Binders .....	103
3.6.1. Mineralogical and Chemical Compositions of Binders .....	104
3.6.2. Quantitative Determination of CaCO <sub>3</sub> and SiO <sub>2</sub> Content in Binders .....	116
3.6.2.1. FTIR, SEM-EDS, LIBS and XRD Analysis of Standard Mixtures of CaCO <sub>3</sub> and SiO <sub>2</sub> .....	117

3.6.2.2. Determination of CaCO <sub>3</sub> /SiO <sub>2</sub> Ratio in the Binders of Roman Mortar Samples by FTIR, SEM-EDS, LIBS and XRD Analysis.....	122
3.6.2.3. Comparison of the Methods.....	126
3.6.3. Microstructural Properties of Binders.....	127
3.6.4. Hydraulic Properties of Binders.....	131
 CHAPTER 4. CONCLUSIONS .....	 134
 REFERENCES .....	 136
 APPENDICES	
APPENDIX A. BASIC PHYSICAL PROPERTIES OF ROMAN LIME MORTARS .....	142
APPENDIX B. DRYING RATES OF ROMAN LIME MORTARS .....	144
APPENDIX C. LIME/AGGREGATE RATIOS OF ROMAN LIME MORTARS .....	145
APPENDIX D. PARTICLE SIZE DISTRIBUTION OF AGGREGATES .....	147
APPENDIX E. POZZOLANIC ACTIVITIES OF AGGREGATES .....	149
APPENDIX F. STRUCTURAL H <sub>2</sub> O AND CO <sub>2</sub> RATIOS OF ROMAN LIME MORTARS .....	151

## LIST OF FIGURES

<b><u>Figure</u></b>	<b><u>Page</u></b>
Figure 1.1. Lime kiln at Foca.....	3
Figure 1.2. Lime kiln according to Cato.....	4
Figure 1.3. Manufacturing of mortar by using slaked lime .....	8
Figure 1.4. Illustrative drawing of opus incertum wall facing.....	11
Figure 1.5. Illustrative drawing of opus reticulatum wall facing.....	12
Figure 1.6. Opus quasi reticulatum (a) and opus reticulatum (b) .....	13
Figure 1.7. Illustrative drawing of opus vittatum wall facing .....	14
Figure 1.8. Illustrative drawing of opus vittatum mixtum.....	14
Figure 1.9. Illustrative drawing of opus mixtum wall facing .....	15
Figure 1.10. Opus mixtum at Ostia.....	16
Figure 1.11. Illustrative drawing of opus spicatum wall facing .....	17
Figure 1.12. Opus spicatum in the Mansio in Thésée.....	17
Figure 1.13. Illustrative drawing of opus testaceum wall facing.....	18
Figure 1.14. The internal masonry of Colosseum at Rome .....	19
Figure 1.15. Illustrative drawing (a) and photograph (b) (Wall of Baths of Vedius at Ephesus) of mortared rubble faced with small blocks of stone.	21
Figure 1.16. Illustrative drawing of mortared rubble faced with small blocks of stone alternating with courses of brick.....	21
Figure 1.17. Illustrative drawing (a) and photograph (b) (Walls of bouleterion at Nysa) of mortared rubble faced with ashlars.....	22
Figure 1.18. The wall of vomitorium of theatre at Aigai.....	23
Figure 1.19. The walls of agora at Nysa comprised of mortared rubble throughout.....	24
Figure 1.20. The library at Nysa constructed of mortared rubble throughout .....	24
Figure 1.21. Kızıl Avlu at Pergamon constructed by mortared brick throughout .....	25
Figure 1.22. Wall constructed of mortared rubble alternate with horizontal bands of brick in Gymnasium at Pergamon .....	26
Figure 2.1. Locations of Aigai and Nysa .....	41
Figure 2.2. Agora wall of Aigai .....	43
Figure 2.3. Theatre of Aigai.....	44
Figure 2.4. Library of Nysa .....	49

Figure 2.5. Theatre of Nysa .....	50
Figure 3.1. Density values of Roman lime mortars .....	66
Figure 3.2. Porosity values of Roman lime mortars .....	66
Figure 3.3. Drying rates of Roman lime mortars .....	69
Figure 3.4. Lime/aggregate ratios of Roman mortars .....	70
Figure 3.5. Particle size distributions of aggregates of Roman mortars .....	70
Figure 3.6. SEM-EDS images of white lump consisted of calcite crystals within the mortar matrice of N13 at magnifications of 650x (a) and 1000x (b).....	73
Figure 3.7. XRD patterns of lime lumps from Aigai and Nysa .....	74
Figure 3.8. SEM-EDS images of calcite crystals of A6 (a), A12 (b), N17 (c) .....	76
Figure 3.9. Electrical conductivity differences of aggregates of Roman lime mortars .....	77
Figure 3.10. XRD patterns of natural pozzolans from Roman lime mortars of Aigai....	79
Figure 3.11. XRD patterns of natural pozzolans from Roman lime mortars of Nysa ....	80
Figure 3.12. XRD patterns of artificial pozzolans from Roman lime mortars of Aigai .....	81
Figure 3.13. XRD patterns of artificial pozzolans from Roman lime mortars of Nysa (I).....	82
Figure 3.14. XRD patterns of artificial pozzolans from Roman lime mortars of Nysa (II) .....	83
Figure 3.15. CaO (a) and Y (b) contents of natural pozzolans .....	85
Figure 3.16. Ba (a), Sr (b) and CaO (c) contents of artificial pozzolans .....	86
Figure 3.17. The dendrogram graph of CaO.....	90
Figure 3.18. The dendrogram graph of SiO <sub>2</sub> .....	91
Figure 3.19. The dendrogram graph of TiO <sub>2</sub> .....	91
Figure 3.20. The dendrogram graph of Al <sub>2</sub> O <sub>3</sub> .....	92
Figure 3.21. The dendrogram graph of Fe <sub>2</sub> O <sub>3</sub> .....	92
Figure 3.22. The dendrogram graph of MgO.....	93
Figure 3.23. The dendrogram graph of Na <sub>2</sub> O .....	93
Figure 3.24. The dendrogram graph of K <sub>2</sub> O.....	94
Figure 3.25. SEM-EDS images of natural pozzolans used in A1 at magnifications of 500 (a), 1000 (b), 4000 (c), 10000 (d), 20000 (e), 50000 (f), 100000 (g).....	96

Figure 3.26. SEM-EDS images of natural pozzolans used in A2 at magnifications of 500 (a), 1000 (b), 4000 (c), 10000 (d), 20000 (e), 50000 (f), 100000 (g) .....	97
Figure 3.27. SEM-EDS images of natural pozzolans used in N3 at magnifications of 500 (a), 1000 (b), 4000 (c), 10000 (d), 20000 (e), 40000 (f).....	98
Figure 3.28. SEM-EDS images of natural pozzolans used in N7 at magnifications of 500 (a), 1000 (b), 4000 (c), 10000 (d), 20000 (e), 40000 (f).....	99
Figure 3.29. SEM-EDS images of natural pozzolans used in N13 at magnifications of 500 (a), 1000 (b), 4000 (c), 10000 (d), 20000 (e), 40000 (f), 80000 (g), 160000 (h) .....	100
Figure 3.30. SEM-EDS images of natural pozzolans used in N17 at magnifications of 500 (a), 1000 (b), 4000 (c), 10000 (d), 20000 (e).....	101
Figure 3.31. SEM-EDS images of artificial pozzolans used in A5 (a), N1 (b) .....	102
Figure 3.32. SEM-EDS images of artificial pozzolans used in N11 (a), N15(1) (b)....	103
Figure 3.33. XRD patterns of binders produced by natural pozzolans from Aigai .....	105
Figure 3.34. XRD patterns of binders produced by natural pozzolans from Nysa.....	106
Figure 3.35. XRD patterns of binders produced by artificial pozzolans from Aigai....	107
Figure 3.36. XRD patterns of binders produced by artificial pozzolans from Nysa (I) .....	108
Figure 3.37. XRD patterns of binders produced by artificial pozzolans from Nysa (II).....	109
Figure 3.38. FTIR spectra of a standard mixture (CaCO <sub>3</sub> /SiO <sub>2</sub> :1/1).....	117
Figure 3.39. Calibration curve for FTIR analysis results of standard mixtures.....	118
Figure 3.40. Calibration curve for SEM-EDS analysis results of standard mixtures ...	119
Figure 3.41. LIBS spectra of a standard mixture (CaCO <sub>3</sub> /SiO <sub>2</sub> :1/1).....	119
Figure 3.42. Calibration curve for LIBS analysis results of standard mixtures.....	120
Figure 3.43. XRD pattern of a standard mixture (CaCO <sub>3</sub> /SiO <sub>2</sub> :1/1) .....	121
Figure 3.44. Calibration curve for XRD analysis results of standard mixtures.....	121
Figure 3.45. FTIR spectrum of a Roman binder sample (N2).....	122
Figure 3.46. LIBS spectrums of a Roman binder sample (N10) .....	124
Figure 3.47. XRD spectrum of a Roman binder sample (N10) .....	125

Figure 3.48. Weight ratios of CaCO <sub>3</sub> /SiO <sub>2</sub> obtained by FTIR, SEM-EDS, LIBS methods in binders of Roman mortars.....	126
Figure 3.49. SEM images showing strong adhesion between pozzolans and lime in A2 (b) and N16 (b) .....	127
Figure 3.50. SEM images of pozzolan-lime interface at 250x (a) and 1000x (b) (A2) .....	128
Figure 3.51. SEM images of the binder of A9 at magnifications of 1000 (a) and 10000 (b) .....	128
Figure 3.52. SEM images of binder of N13 at magnifications of 1000 (a) and 10000 (b) .....	129
Figure 3.53. SEM images of CSH and CAH formations in A12 (a, b), N13 (c) and N15(1) (d) .....	129
Figure 3.54. SEM images of CSH and CAH formations in Aigai sample (A9) at different magnifications 1000x (a), 2500x (b), 5000x (d), 10000x (d).....	131



# LIST OF TABLES

<b><u>Table</u></b>	<b><u>Page</u></b>
Table 1.1. The main constituents and their proportions in Roman lime mortars according to ancient sources .....	7
Table 2.1. Lime mortars with natural pozzolanic aggregates from Aigai .....	45
Table 2.2. Lime mortars and plasters with artificial pozzolans from Aigai .....	47
Table 2.3. Lime mortars with natural pozzolanic aggregates from Nysa .....	51
Table 2.4. Lime mortars and plasters with artificial pozzolans from Nysa .....	54
Table 3.1. Basic physical properties of Roman lime mortars used for different purposes.....	67
Table 3.2. Basic physical properties of Roman lime mortars determined by previous studies .....	68
Table 3.3. Raw material compositions of Roman lime mortars used for different purposes .....	71
Table 3.4. Raw material compositions of Roman lime mortars determined by previous studies .....	72
Table 3.5. Classification of limes according to hydraulic and cementation indices.....	75
Table 3.6. Chemical compositions and H.I. of lime lumps from Kyme mortars.....	75
Table 3.7. Mineralogical compositions of pozzolanic aggregates of Roman lime mortars determined by previous studies.....	84
Table 3.8. Major chemical compositions of pozzolans determined by XRF (%).....	87
Table 3.9. Major chemical compositions of aggregates (%) determined by previous studies .....	88
Table 3.10. Trace elements compositions of pozzolans determined by XRF (ppm).....	89
Table 3.11. Equality tests of mean/median of clusters .....	95
Table 3.12. Mineralogical compositions of binders of Roman lime mortars determined by previous studies.....	110
Table 3.13. Mineralogical compositions of Roman lime mortars determined by previous studies.....	111
Table 3.14. Major chemical compositions of binders of Roman lime mortars determined by SEM-EDS .....	113

Table 3.15. Major chemical compositions of binders (%) determined by previous studies.....	114
Table 3.16. Major chemical compositions of mortars (%) determined by previous studies.....	115
Table 3.17. CaCO <sub>3</sub> /SiO <sub>2</sub> ratio in the binders of Roman mortar samples by FT-IR, SEM-EDS, XRD and LIBS analysis.....	123
Table 3.18. Elemental compositions of binders of Roman mortars.....	123
Table 3.19. Chemical compositions of CSH and CAH formations .....	130
Table 3.20. Structural H <sub>2</sub> O and CO <sub>2</sub> amounts and CO <sub>2</sub> /H <sub>2</sub> O values of Roman lime mortars.....	132
Table 3.21. CO <sub>2</sub> /Structural H <sub>2</sub> O of Roman lime mortars used for different purposes.....	133
Table 3.22. Structural H <sub>2</sub> O and CO <sub>2</sub> ratios of Roman lime mortars determined by previous studies.....	133

# CHAPTER 1

## INTRODUCTION

Mortars were one of the primary materials of historic structures generally used as binding materials between stones and bricks, as infilling materials of walls, as internal and external finishings for structural elements, as supporting materials for pavements and mosaics and for decorative purposes.

Mud, gypsum and lime were most common binding materials used in mortar production from the beginning of construction history of human until the invention of modern cement nearly 200 years ago.

Mud was probably the oldest binder type used in mortar production. Mud mortars were produced by mixing clay, sand, silt and fibrous materials with water (Pearson 1994, Caron and Lynch 1988). The oldest documented mud mortars dated back to 10.000 years ago were found in Mesopotamia (Davey 1961).

Gypsum ( $\text{CaSO}_4 \cdot 2\text{H}_2\text{O}$ ) seems to be the earliest deliberately manufactured cement for mortars (Davey 1961). It was manufactured by calcining gypsum rock at different temperatures. It probably originated in the Middle East where rich rock gypsum sources were available (Davey 1961). According to Davey and Adam, the first known use of gypsum mortars was in the third millennium in the pyramids at Giza (Egypt) and in the tombs of Saqqara as a lubricant for placement of large stone blocks (Davey 1961, Adam 2005).

Among historic binders, lime ( $\text{Ca}(\text{OH})_2$ ) had been the most common binding material used in historic mortar production. The first known use of lime mortars was in Egypt in 4000 BC (Cowan 1977, Cowper 1998, Vicat 2003). Although lime mortars were used for centuries in the east, the introduction of these mortars to architecture was not before the Hellenistic period (336-30 BC) in the west (Adam 2005). The Greeks used lime only for stuccos, painted renderings and the lining of cisterns instead of using it as a binding agent in the mortars for structural purposes (MacDonald 1965, Adam 2005, Cowper 1998). In the Greek architecture, the walls comprised of large stone blocks were constructed without mortar, rather metal clamps and dowels were used for joints and stone blocks relied on their own weights (Coulton 1980).

Greek lime mortars, which were already famous with their quality, were generally considered as the predecessor of Roman lime mortars (MacDonald 1965). The significant achievement of the Romans was that they had used lime for manufacturing mortars for structural purposes where the Greeks used it mostly for decoration (MacDonald 1965, Adam 2005). The widespread use of lime for mortar production was one of the important contributions of the Romans to architecture. Although the first known use of lime mortars is not certain, Ward-Perkins mentioned it as the first half of the third century BC (Ward-Perkins 1974). The town walls of Cosa dated to 275 BC have been considered as an important example for the early usage of lime mortars in the Roman Period (Ward-Perkins 1974).

## 1.1. Roman Lime Mortars

Romans produced mortars by using lime as a bonding agent and natural and artificial pozzolans as aggregates. The technology of Roman lime mortars, which enabled bonding of rubble masonry, use of concrete in monumental structures and development of vaulted constructions, was one of the most important contributions of the Romans to construction history (MacDonald 1965, Adam 2005, Stierlin 2002).

The development of the technology of Roman lime mortars was an empirical process (Ward-Perkins 1974). For this reason, the word “mortar” we use today does not have a direct equivalent in the Latin language (Ward-Perkins 1974). Rather, it was derived from the word *mortarium* that meant the chamber where lime and sand were mixed together (Ward-Perkins 1974). Vitruvius (90-20 BC) used the word *materia* for mortar in many passages of his *De Architectura* (Ward-Perkins 1974, Grant 1980). In the situations where more certainty was needed such as building contracts found in Puteoli and dated to 106 BC, the ingredients of mortar mixtures were specified as *calx* (lime) and *arena* or *harena* (sand) instead of giving a definite name to the mixture (Ward-Perkins 1974).

The first step of lime manufacturing is the calcination of limestones ( $\text{CaCO}_3$ ) in kilns. The properties of limestones that would be suitable to produce lime for mortar manufacturing were described by Vitruvius in his *De Architectura* (Vitruvius 1960). According to Vitruvius, lime should be absolutely manufactured from white limestones;

and also limes made of less porous limestones were suitable for mortars of structural purposes where limes made of porous limestones could be used in stuccos.

Leon Battista Alberti (1404-1472) stated that ancient architects had preferred to use lime made of hard limestones in arches and lime made of porous stones in plasters in his architectural treatises under the title *De Re Aedificatoria* (Alberti 1986).

In the Roman period, three different processes had been used for the calcination of limestones (Adam 2005). These were burning the limestones:

- In a kiln in which fire is at the bottom (Figure 1.1),
- In a kiln consisted of stacks,
- In the open air which is considered as a primitive technique compared to the others.

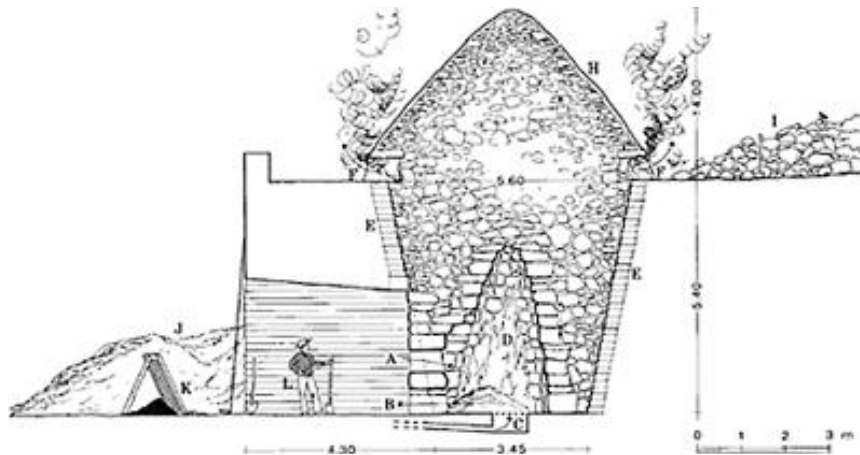


Figure 1.1. Lime kiln at Foca  
(Source: Adam 2005, p.68)

Calcination of limestones and the properties of lime kilns were described in detail by the famous writer Cato (234-149 BC) generally known as Cato the Elder or Cato the Censor in his writings on agriculture, titled *De Agri Cultura* (Adam 2005). According to Cato, a lime kiln should have ten feet width at the bottom, three feet width at the top and twenty feet depth; it could be constructed either of one stokehole or two (Figure 1.2). The fire should be kept constant and the wind should be taken into consideration during calcination. At the end of firing when all the limestones were fully

calcinated, the stones at the bottom would be settled, the stones at the top would be burned, and a less smoky flame would come out.

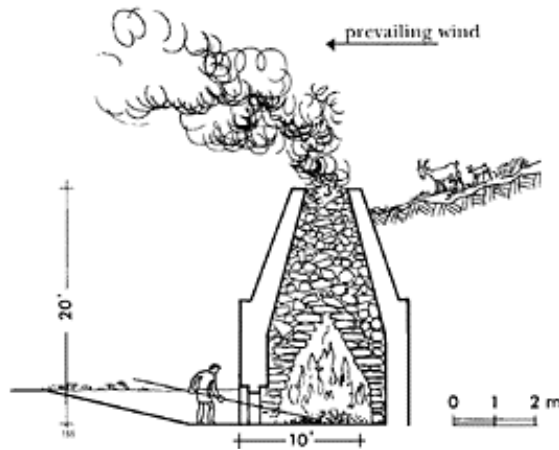


Figure 1.2. Lime kiln according to Cato  
(Source: Adam 2005, p.70)

The stones obtained at the end of the calcination process are called quicklime (CaO). Vitruvius defined quicklime as the form of limestone which has lost its former solidity and strength, and consisted of open pores (Vitruvius 1960).

The last step of lime manufacturing is slaking the quicklime. During slaking, quicklime is hydrated, a strong heat is given and lime (Ca(OH)<sub>2</sub>) is obtained. During slaking, water made its way into the open pores; quicklime began to get hot, and the heat was rejected after it cooled according to Vitruvius (Vitruvius 1960). Alberti defined the ideal slaking process as first adding the water to quicklime lumps very slowly and afterwards keeping them in a shady and moist place (Alberti 1986, p.36):

Vitruvius described a method to determine the slaking degree of lime (Vitruvius 1960). In this method, a hoe should be applied into the slaked lime;

- If the lime stuck to the hoe in bits, that means the lime was not calcined enough.
- If the hoe was dry and clean, that means the lime was dry and not slaked enough.

- If the lime stuck to the hoe like glue, that meant the lime was calcined and slaked well.

In the Roman age, the lime manufacturers sold lime either in the quicklime form or in the slaked lime form (Adam 2005). The advantage of selling in the quicklime form to the manufacturer was the ease of transport (Adam 2005). In these cases, quicklime was slaked at the construction sites. However, if the construction site was not suitable to carry out this process, the lime manufacturer slaked the quicklime in the lime pits which were covered with earth to keep lime for a long time (Adam 2005). Although it was advised to keep lime at least for three years before using it, this advice may have not been taken into consideration in all sites due to its consumption in large amounts (Adam 2005).

The most important contribution of the Romans to the lime mortar technology was the use of pozzolans, which was not a dramatic discovery but a result of centuries of trials and errors (Ward-Perkins 1974, Ward-Perkins 1981). The word pozzolan was derived from the Latin *pulvis puteolanus* meaning “Puteoli powder” and indicating volcanic deposits around Puteoli (modern Pozzuoli) (Ward-Perkins 1974). The characteristics of pozzolans, which bring in hydraulic properties, were first discovered in the second century BC in Puteoli area (Ward-Perkins 1974). Besides, the first known example of lime mortars produced by using natural pozzolans was the waterside building in the harbour of Puteoli in Campania (Ward-Perkins 1981). Vitruvius defined pozzolan as a kind of powder formed as a result of natural causes and found in the neighborhood of Baiae near Mount Vesuvius and recommended its use in lime mortars to obtain hydraulic properties (Vitruvius 1960).

Since there was no theoretical knowledge on pozzolans, various local pozzolan sources had been used for lime mortar manufacturing due to organization and cost matters of construction sites (Ward-Perkins 1974). The problem of using different local pozzolans caused extreme variety in the quality of the local sources due to impurities that eventually made the pozzolan less useful for mortar production (Ward-Perkins 1974). For instance, Vitruvius mentioned that volcanic earth of Tuscany was not capable of producing hydraulic lime mortars (Vitruvius 1960). Later, he explained this situation that soil properties could not be same in all districts and this was about “*nature not man’s pleasure*”. Rather, he insisted that term pozzolan was even unknown in countries across the Adriatic including Anatolia (Vitruvius 1960).

Actually, the problem of using local pozzolan sources that were not always of good quality was solved by the authority of the emperor that provided the centralization of building material production to sell materials of better quality at reasonable prices (Ward-Perkins 1974). From the time of Augustus (27 BC-14 AD), the addition of natural pozzolans, which were derived from the local supplies around Rome, to lime mortars became regular and this type of mortar was used even in ordinary buildings (Ward-Perkins 1981). Fifty years after Augustus, Claudius imported natural pozzolans from Puteoli to his harbours at Ostia (Ward-Perkins 1981). Pantheon, Colosseum, Tournai Cathedral and Domitilla catacombs are some of the significant monumental structures of Romans where lime mortars produced from natural pozzolans were used (Massaza and Pezzuoli 1981, Degryse et al. 2002, Elsen et al. 2004, Sánchez-Moral et al. 2005).

Romans also discovered the use of kiln-fired bricks as artificial pozzolanic materials instead of natural pozzolans in their lime mortars by the first century BC (MacDonald 1965). It was known that the use of bricks in lime mortars was introduced to Roman architecture from the Middle East (Akman et al. 1986). Lime mortars, which were produced by using artificial pozzolans such as crushed brick and tiles, were known as “*cocciopesto*” in Roman times (Massaza and Pezzuoli 1981). *Cocciopesto* mortars were widely used in bath buildings, cisterns, aqueducts etc. due to their hydraulic properties. Vitruvius also stated that fired bricks should be used instead of sand in the first plaster layers of the walls which would be subjected to high humidity (Vitruvius 1960)

The proportions of natural or artificial pozzolans as aggregates to lime in Roman mortars were given by Vitruvius (90-20 BC) in *De Architectura* (Vitruvius 1960), Cato (234-149 BC) in *De Agri Cultura* (Alberti 1986) and Pliny (23-79 AD) in *Naturalis Historia* (Goldsworthy and Min 2009). Vitruvius and Cato recommended the use of lime and aggregates in the proportions of 1/2 and 1/3; whereas Pliny specified the proportion of lime to aggregates as 1/4 (Table 1.1). The higher amounts of aggregates indicated by Pliny might be due to the expensiveness of lime after the Great Fire of Rome (64 AD) (Goldsworthy and Min 2009).



Table 1.1. The main constituents and their proportions in Roman lime mortars according to ancient sources

Lime	Aggregate		The use of mortar	Reference
	Amount	Type		
1 part	3 parts	Pitsand	In the walls of masonry	Vitruvius 1960, p.45 (Book II, Chapter V)
1 part	2 parts	River or sea-sand	In the walls of masonry - if there is no pitsand	Vitruvius 1960, p.45 (Book II, Chapter V)
1 part	2 part	River or sea-sand	<i>Not specified.</i>	Vitruvius 1960, p.45 (Book II, Chapter V)
	1 part	Burnt-brick		
1 part	2 parts	Natural pozzolan	In the walls which are to be underwater (In harbours, breakwaters, shipyards)	Vitruvius 1960, p.162 (Book V, Chapter XII)
1 part	2 parts	Sand	<i>Not specified.</i>	Cato in Alberti 1986, p.45 (Book III, Chapter IV)
1 part	4 parts	Pitsand	On-land construction	Pliny the Elder in Goldsworthy and Min 2009

Although Vitruvius had given proportions for mortars that would be made of any kind of sands, he suggested the use of river or sea-sands only in the situations pitsand (*harenae fossicae* - volcanic ash) could not be found. Vitruvius emphasized that river or sea-sands could cause defects when used in masonry and a wall constructed by using mortars of these kinds of aggregates could not carry vaultings. However, he suggested the use of river sand for stuccos since pitsand would cause cracks during drying due to the great strength of its mixtures, and sea-sand could lead to efflorescence formation due to its salt content. (Vitruvius 1960)

In addition to the properties of lime and aggregates and their proportions in the mixture of the mortars, the amount of water added during manufacturing and the mixing

techniques were the other important factors determining the quality of Roman lime mortars (Adam 2005).

There were two different arguments for explaining the manufacturing processes of Roman lime mortars concerning the use of either slaked lime or quicklime during manufacturing. Vitruvius specified using slaked lime during manufacturing of mortars (Vitruvius 1960). During the manufacturing process, slaked lime that was taken from a slaking pit or a sheltered place and transported with an amphora or a metal bucket was placed into a sort of crater formed of aggregates; and then the water was added gradually and mixing was carried out slowly with a hoe (Figure 1.3) (Adam 2005). A stack of lime paste found unmixed in the middle of pozzolans that were petrified at the moment of eruption of Pompeii in 79 AD was considered as an indicator to verify the use of slaked lime in the manufacturing of mortars by Adam (2005).

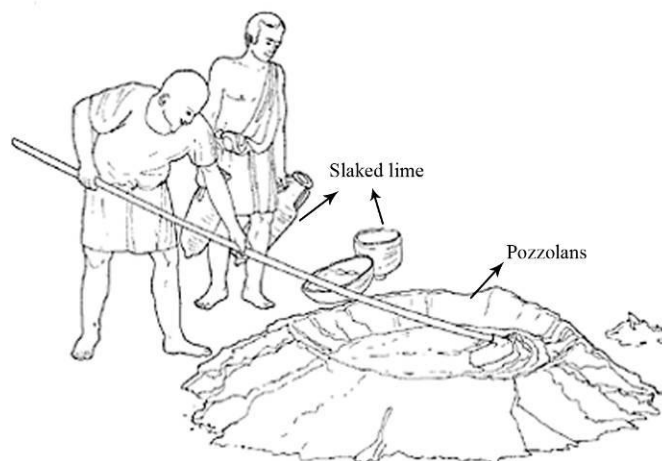


Figure 1.3. Manufacturing of mortar by using slaked lime  
(Source: Adam 2005, p.75)

However, Ward-Perkins and Grant defined the process as mixing quicklime and aggregates first and next hydrating this mixture (Ward-Perkins 1974, Grant 1980). The strength of mortars that were manufactured by this process depended on the chemical reactions between lime and pozzolans induced by the heat given off during the in situ slaking of quicklime (Ward-Perkins 1974, Moropoulou et al. 1996). This process was also known as “hot lime technology” in literature (Moropoulou et al. 1996).

The amount of water used in mixing of mortars depended on the evaporation rate related to the climate of the building was located in and the use of mortar in the building, and varied between 15 to 20 % (Adam 2005). Less water was used in the mortars for the unventilated parts of the structure such as foundations compared to the mortars used for pointings or as plasters (Adam 2005).

Mixing process was carried out until the mixture had a homogenous and uniform appearance that was free from lumps (Adam 2005). Alberti also indicated that mixing should be carried out by stirring often till the smallest particles were incorporated in the mixture (Alberti 1986).

Development of the technology of lime mortars led to the invention of a new material in the Roman period. The new material was Roman concrete (*opus caementicium*) which was composed of lumps of aggregates (*caementa*) of stone, marble or pumice laid in the mortar forming a compact and monolithic building material (Ward-Perkins 1974, Grant 1980, Adam 2005). The role of *caementa* in the concrete was to resist the crushing forces of great weights, to increase the density of the mortar and to reduce the amount of lime to be manufactured (MacDonald 1965). Different kinds of stones were used as *caementa* in the concrete according to their weights and the loads that should be carried. Heavy volcanic stones were used in the foundation walls; where lightweight stones like pumice and tufa were used in the vaults (MacDonald 1965). For instance, five types of *caementa*, each lighter than the one below had been used in the concrete of walls and the dome of Pantheon (MacDonald 1965). Broken bricks, tiles and architectural sculptures, and also the stone pieces of demolished structures were the other materials that could be used as *caementa* in concretes (MacDonald 1965). During the manufacturing process of concrete, the initial step was the production of the lime mortar that was followed by the introduction of *caementa* that consisted of pebbles, stone or broken pieces into the mortar at the time of construction (Adam 2005). Roman concrete was considered as a material that was ideal for casting on a monumental scale and if manufactured correctly could provide continuity from foundations to the vaults (MacDonald 1965).

The first known example of the use of *opus caementicium* was in the Temple of Magna Mater in Palatine and dated to 204 BC (Adam 2005). By the time of Augustus, *opus caementicium* began to be used instead of traditional building materials like stone and timber since it became a cheap and efficient material that could also bear heavier loads (Ward-Perkins 1974, Grant 1980). Economic and structural properties of *opus*

*caementicium* led to the use of new architectural forms like concrete vaulting and the development of new wall construction techniques that consisted of a core and a facing. The cores of the walls were constructed either by *opus caementicium* or by using lime mortared rubble stones. The core and the facing types were the distinctive characteristics of Roman wall constructions which differed according to the regions they were used.

## **1.2. Roman Wall Construction Techniques with Lime Mortars**

Diversities of local practices, traditions, needs, and building material resources resulted in changes in the wall construction techniques of different regions during the Roman Empire which reigned over Europe, Anatolia, Near East and North Africa (Ward-Perkins 1974, Ward-Perkins 1981). In this section, common wall construction techniques in which lime mortars or Roman concrete were used in Italian Peninsula and Anatolia are described and discussed.

### **1.2.1. Wall Construction Techniques in Italian Peninsula during Roman Empire**

The use of lime mortars and concrete by the second century BC led the Romans to use different construction materials and techniques. The use of different types of stones, bricks and tiles, and also Roman concrete provided various opportunities in facings which were generally used in Italian Peninsula which was the centre of the Empire (Adam 2005). The function attributed to the facings were generally to simplify the construction process as well as to provide aesthetics since facing materials grew thinner and became less structural after the inner cores of the walls that were of Roman concrete became able to bear heavier loads (MacDonald 1965, Ward-Perkins 1981).

Roman wall facing techniques are generally classified according to the material (stone and brick) and the bonding type. But it must be remembered that, each type of facing may have been used individually or together with one or more other techniques in a single wall.

The most important facing types used in Italian Peninsula during Roman Empire were:

- Opus incertum
- Opus quasi reticulatum and opus reticulatum
- Opus vittatum
- Opus mixtum
- Opus spicatum
- Opus testaceum

### 1.2.1.1. Opus Incertum

Opus incertum consisted of irregular small stones, which formed the outer skin of *opus caementicium* (Ward-Perkins 1981, Adam 2005) (Figure 1.4).

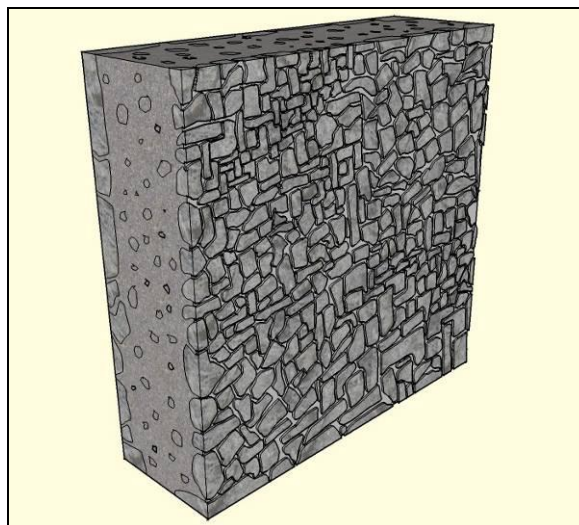


Figure 1.4. Illustrative drawing of opus incertum wall facing  
(Drawing: E. Uğurlu Sağın)

It was considered as “*the first Roman departure from solid work*” by Kirby (Kirby et al. 1990). The greatest development of this type of wall construction was in the second and first centuries BC (Adam 2005). Some of the most important examples of opus incertum on a support of opus caementicium were the acropolis of Ardes, the walls of Cori, the walls of Formia and the walls of Terracina in Italy.

Opus incertum declined in the Sullan Period (85 BC) with some exceptions of rural constructions (Adam 2005). Reticulate constructions replaced opus incertum due to the socio-economic developments resulting in the standardization of stones, systemization of the work of stone-cutters and masons that led to the production of prefabricated elements (Adam 2005).

### 1.2.1.2. Opus Quasi Reticulatum and Opus Reticulatum

Reticulatum facings were comprised of opus caementicium faced with pyramidal stones or terracottas laid with joints inclining 45 degrees to form quite regular patterns on exterior surface of the wall (Kirby et al. 1990, MacDonald 1965) (Figure 1.5).

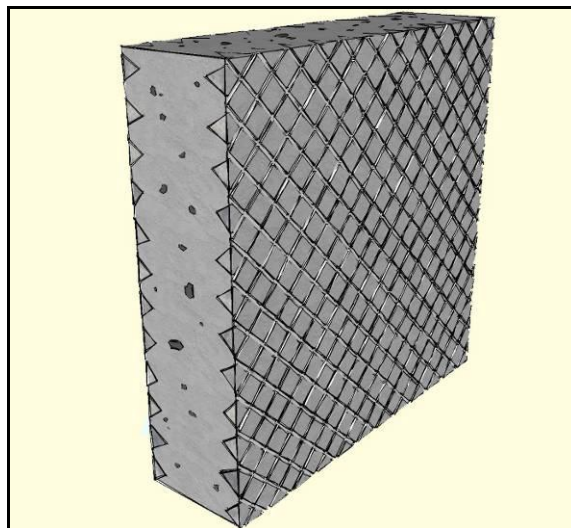


Figure 1.5. Illustrative drawing of opus reticulatum wall facing  
(Drawing: E. Uğurlu Sağın)

Opus quasi reticulatum was the rough phase of the transition from opus incertum to opus reticulatum (Adam 2005) (Figure 1.6 (a)). Small square stones were laid diagonally in this technique. It was used commonly in the last quarter of the second century BC (Adam 2005). The original facing of the basin of Lacus Intarnea, Fountain of the Nymph Iuturna, phase II of the walls of the Temple Magna Mater, Forum Baths of Pompeii, Pompey's Theatre in Rome are some of the examples of the quasi reticulatum construction (MacDonald 1965, Adam 2005).

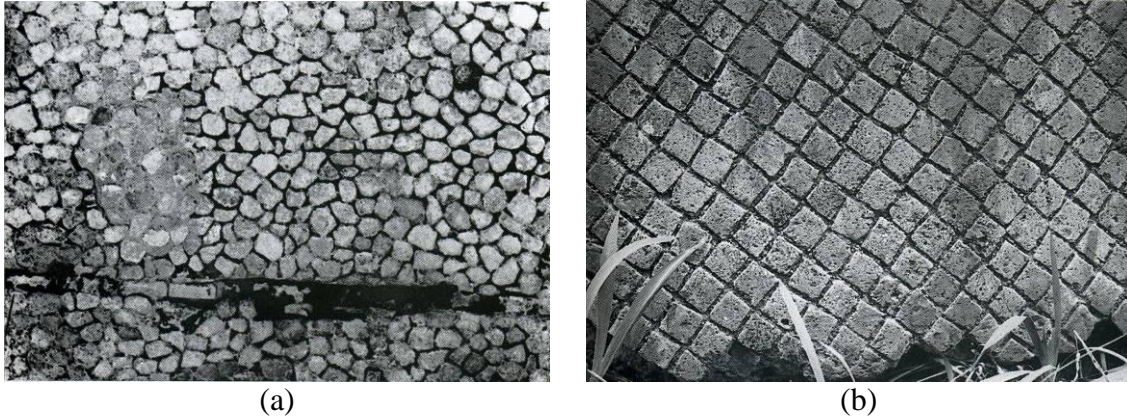


Figure 1.6. Opus quasi reticulatum (a) and opus reticulatum (b)  
 (Source: Ward-Perkins 1974, p.85)

Regular reticulate construction (*opus reticulatum*) (Figure 1.6 (b)) was generally used between the first century BC and first century AD in both public and private monuments in central and central-southern Italy (Adam 2005).

According to Vitruvius *opus incertum* although was not beautiful enough, was stronger than *opus reticulatum* (Vitruvius 1960). Vitruvius also mentioned that the main disadvantage of *reticulatum* constructions was the lack of buttressing of the corners of the wall due to the absence of horizontal courses. Because of the problems in the corners of *reticulatum*, later, *opus vittatum*, comprised of rectangular blocks, began to be used (Adam 2005).

### 1.2.1.3. Opus Vittatum

*Opus vittatum* consisted of rectangular or occasionally square blocks of generally volcanic tufa that were laid in horizontal courses with alternating joints (Adam 2005) (Figure 1.7). The courses of the blocks followed the slope of the ground. The ends of the walls were buttressed with piers, and the corners of the walls and the jambs of the openings were made of stone blocks.

Despite its simplicity, it was hardly seen before the Augustan period (27 BC - 14 AD). The first large works of rectangular stones were not the construction of new buildings but restorations. After the Augustan period, it became a standard wall technique bonded with mortar, and remained until the end of the Roman period (Adam 2005).



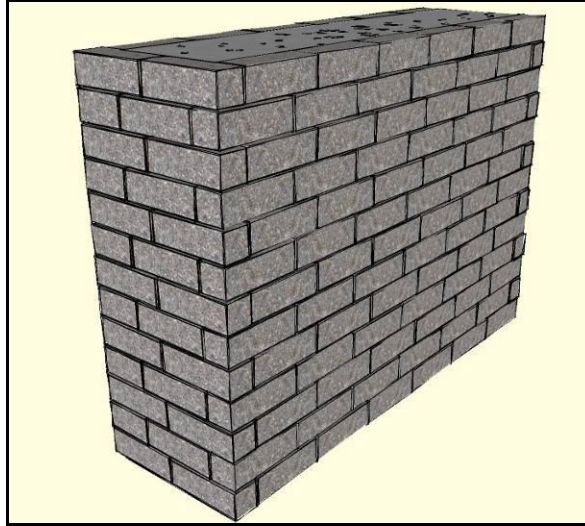


Figure 1.7. Illustrative drawing of opus vittatum wall facing  
(Drawing: E. Uğurlu Sağın)

Opus vittatum was named as opus vittatum mixtum if tufa blocks were intersected by one or more horizontal brick courses (Figure 1.8). Opus vittatum mixtum first appeared during Trajan period (98-117 AD), and spread all around the Empire during Hadrian period (Adam 2005).

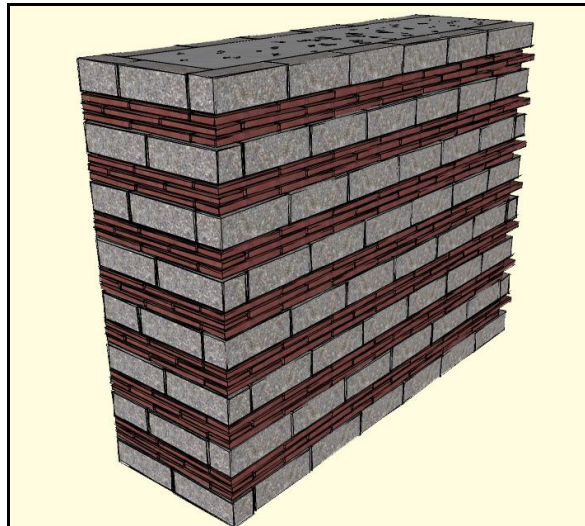


Figure 1.8. Illustrative drawing of opus vittatum mixtum  
(Drawing: E. Uğurlu Sağın)



#### 1.2.1.4. Opus Mixtum

Opus mixtum was generally of opus incertum, opus reticulatum or opus vittatum techniques with brick courses which made true horizontal bonds connecting the two faces of the wall (Adam 2005) (Figure 1.9).

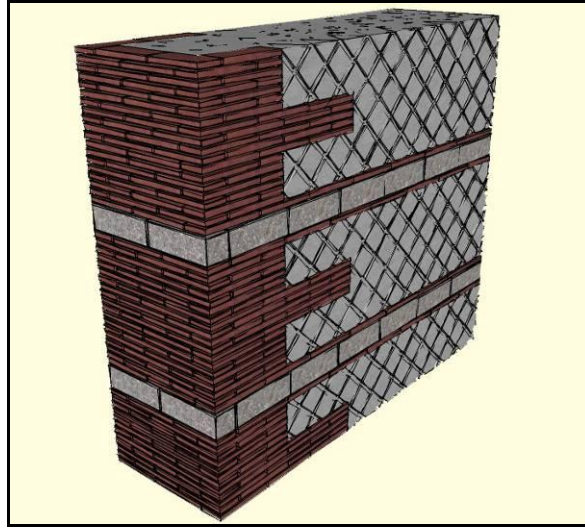
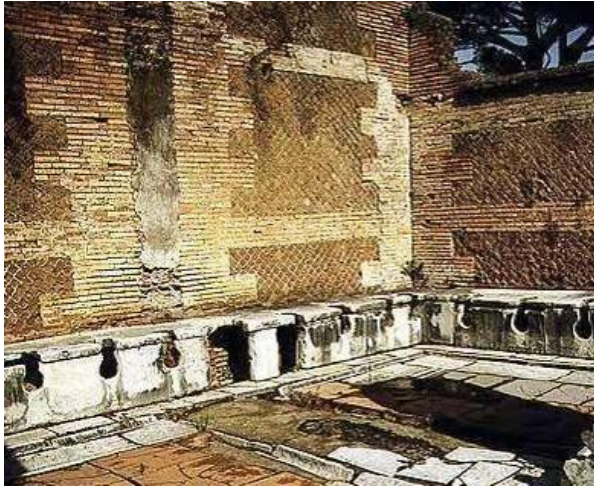


Figure 1.9. Illustrative drawing of opus mixtum wall facing  
(Drawing: E. Uğurlu Sağın)

The width of brick courses varied in different types of *opus mixtum*. In *opus mixtum* walls made with *opus reticulatum* and *opus incertum*, generally five or six courses of brick were used at the corners and/or through the wall surface (Figure 1.9, 1.10). In this system, the reticulate areas were larger than the brick areas (Figure 1.10).



(a)



(b)

Figure 1.10. Opus mixtum at Ostia (Source: (a): Ostia Harbour City of Ancient Rome 2012, (b): The University of Texas at Austin 2012)

Although it is very difficult to make an exact chronology for opus mixtum, it was very popular during the second century AD and did not disappear completely to the end of Roman period (Adam 2005).

### 1.2.1.5. Opus Spicatum

*Opus spicatum* means “ear of wheat” (also called *herring-bone* or *fern-leaf*) due to the arrangement of small stones (Adam 2005). The stones were laid in an angle of about 45 degrees to each other, and each course changing its direction of incline (Figure 1.11). This technique was used in the areas where flat river stones and stones which easily split into small flats were found naturally (Adam 2005).

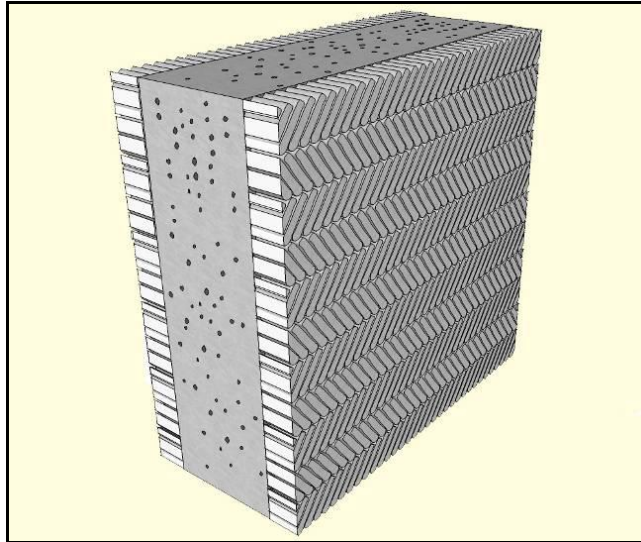


Figure 1.11. Illustrative drawing of opus spicatum wall facing  
(Drawing: E. Uğurlu Sağın)

This technique was generally used for footings, foundations, roadways, in the cores of defensive walls, for filling the gaps and for closing the openings like windows and doors (Adam 2005). The only building that *opus spicatum* used apparently was the Mansio in Thésée (Adam 2005) (Figure 1.12).



Figure 1.12. Opus spicatum in the Mansio in Thésée  
(Source: Montjoye 2012)

### 1.2.1.6. Opus Testaceum

*Opus testaceum* or baked brick facing was one of the most important facing types that gave a very strong visual impression to Roman monuments (Figure 1.13). Baked bricks (*cocti lateres*) came into use due to the standardization of building materials (Adam 2005). In comparison with extraction and dressing of stone blocks, industrial manufacturing of bricks provided an easier and quicker process, accuracy and equality of sizes, greater surface area for support and very close joints (Grant 1980, Adam 2005). Although this type of construction was generally considered as aesthetic, well-planned, time saving and cost effective, it was also very complicated since its several processes required to involve different specialists from the manufacture of bricks to the finished wall or building (MacDonald 1965, Adam 2005).

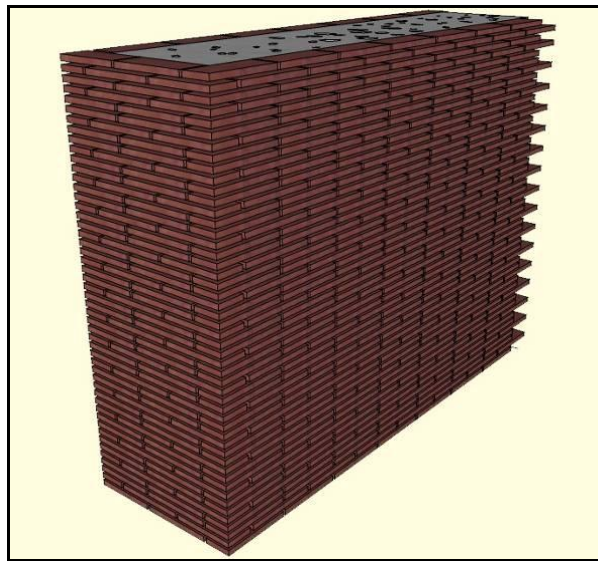


Figure 1.13. Illustrative drawing of opus testaceum wall facing  
(Drawing: E. Uğurlu Sağın)

The first use of brick as facing material was in the reticulate facings in about 80 BC (Grant 1980). The first major construction in which brick appeared was the complex of the Markets of Trajan in the second century AD (Grant 1980, Adam 2005). The internal masonry of Colosseum, the Pantheon, the Baths of Caracalla, the complex on the Palatine, the whole landscape of Ostia, the Tomb of Hadrian, the Domus Aurea were



some of the important examples that opus testaceum was used relating to the city of Rome (Adam 2005) (Figure 1.14).



Figure 1.14. The internal masonry of Colosseum at Rome  
(Photograph: E. Uğurlu Sağın)

### **1.2.2. Wall Construction Techniques in Anatolia during Roman Empire**

Construction techniques used in Anatolian architecture differed from the central Roman architecture even after the reunion under the Roman Empire. Anatolian architecture was defined as “*a Romano-provincial creation of the Augustan age*” (Ward-Perkins 1974, p.159). According to Ward-Perkins, the innovations of the Roman architecture were very slowly accepted by Anatolian architects due to the difference in their historical backgrounds and in the available building material resources (Ward-Perkins 1974, Ward-Perkins 1981).

Anatolia had plentiful sources of building stones, marbles and timber (Ward-Perkins 1974, Ward-Perkins 1981). Marble was the medium of the Anatolian architecture revealing a highly organized commerce that involved production,

prefabrication and export (Ward-Perkins 1974). Brick, which was introduced to Anatolian architecture by the second century AD, was another major material used in its own right especially in the monumental architecture (Ward-Perkins 1974, Ward-Perkins 1981). But, although Anatolia was a rich land of different kinds of building materials, it was not rich enough in terms of volcanic sand resources compared to the Italian Peninsula especially the neighborhood of Baiae near Mount Vesuvius.

Because of all these reasons mentioned above, *opus caementicium* and different types of wall facings frequently used during Roman Period in Italian Peninsula did not have a direct equivalent in Anatolia and also anywhere in the east (Ward-Perkins 1981). Instead of building the walls in a Roman manner of concrete (*opus caementicium*) faced with different types of materials, Anatolian architects preferred to use their own techniques in wall constructions. These techniques can be grouped as walls comprised of mortared rubble core and facing, and walls comprised of mortared materials.

#### **1.2.2.1. Walls Comprised of Mortared Rubble Core and Facing**

In Anatolia, Roman manner of concrete (*opus caementicium*) was translated into the mortared rubble, which consisted of rubble stones horizontally laid in a thick lime mortar (Ward-Perkins 1981). This local interpretation of concrete was used as an inner core in wall constructions and faced with different types of materials. Unlike the wall facings of Italian Peninsula during Roman Empire, materials of Anatolian wall facings generally correspond to the mortared rubble inner core of the wall (Ward-Perkins 1981). Wall facing materials were local stones and brick. Corners and openings like doors and windows were constructed by using large stone blocks (Ward-Perkins 1981).

The most commonly used facing types in Anatolia were (Ward-Perkins 1974, Ward-Perkins 1981):

- Mortared rubble faced with small blocks of stone (Figure 1.15)
- Mortared rubble faced with small blocks of stone alternating with courses of brick (Figure 1.16)
- Mortared rubble faced with ashlar (Figure 1.17)

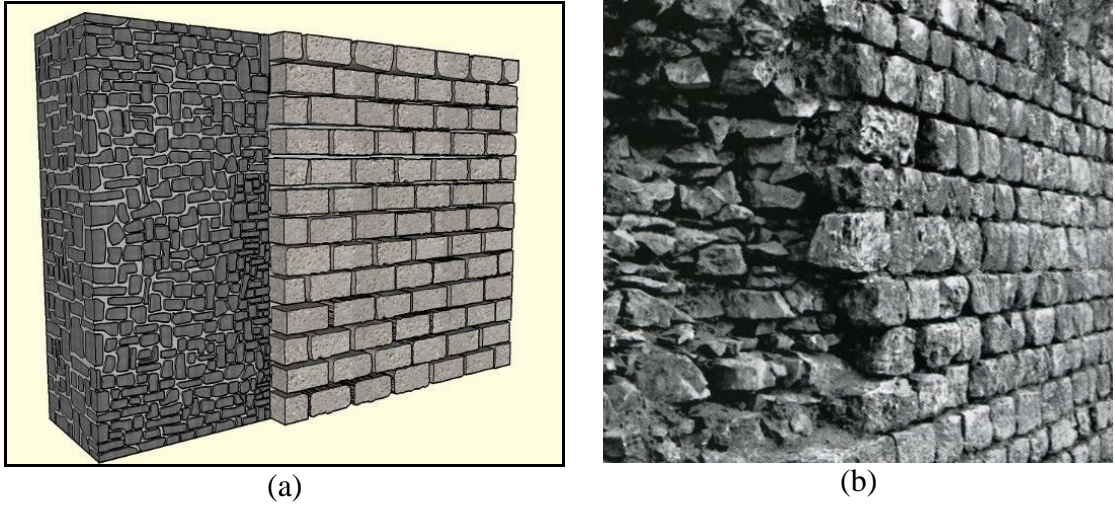


Figure 1.15. Illustrative drawing (a) and photograph (b) (Wall of Baths of Vedius at Ephesus) of mortared rubble faced with small blocks of stone ((a): E. Uğurlu Sağın, (b) Source: Ward-Perkins 1974, p.156)

In the walls comprised of mortared rubble faced with small blocks of stone, the appearance of facing depended on the stone type used. In Ephesus and Pergamon orderly squared blocks of limestones were used as facing materials (Figure 1.15) whereas splintered stones and small river boulders were used in Miletus (Ward-Perkins 1974).

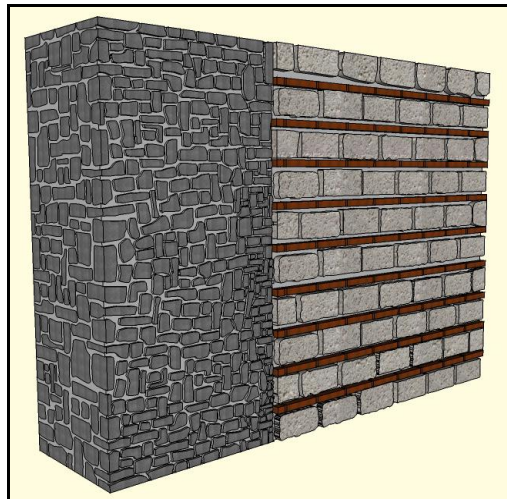


Figure 1.16. Illustrative drawing of mortared rubble faced with small blocks of stone alternating with courses of brick (Drawing: E. Uğurlu Sağın)

In some examples, small blocks of stones were used alternately with courses of brick (Figure 1.16). In appearance, this technique resembled the *opus mixtum* of central Roman Empire (Ward-Perkins 1974). But, the brickwork was not only the part of the facing but also a part of the inner core that gave strength and cohesion and prevented the wall from settlement (Ward-Perkins 1981). The city walls of Nicaea built between 258 and 269 AD was one of the most important examples of this type of wall construction technique in Anatolia (Ward-Perkins 1981).

The third facing type used in Anatolia was the mortared rubble faced with ashlar (Ward-Perkins 1981) (Figure 1.17 and 1.18).

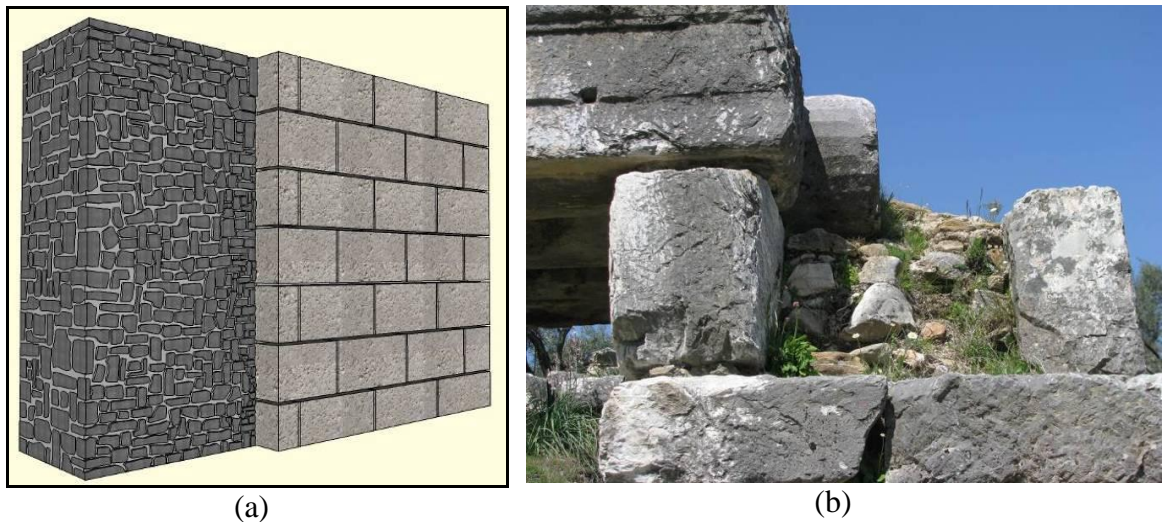


Figure 1.17. Illustrative drawing (a) and photograph (b) (Walls of bouleterion at Nysa) of mortared rubble faced with ashlar (Drawing: E. Uğurlu Sağın)





Figure 1.18. The wall of vomitorium of theatre at Aigai

#### **1.2.2.2. Walls Comprised of Mortared Materials**

Walls, comprised of mortared rubble stones or bricks, were the other widespread type of wall constructions used in Anatolian architecture of Roman period. This type of masonry was generally observed in three different ways. These are (Ward-Perkins 1981):

- Mortared rubble throughout
- Mortared brick throughout
- Mortared rubble alternate with horizontal bands of brick

Walls comprised of mortared rubble were used not only as an inner core of walls faced with different materials but also as a wall type of their own right in a great number of cities (Figure 1.19 and 1.20).



Figure 1.19. The walls of agora at Nysa comprised of mortared rubble throughout



Figure 1.20. The library at Nysa constructed of mortared rubble throughout



The use of brick was considered as an emergence of a substitute material for Roman concrete in Anatolian architecture since it was freely used both for the construction of the walls and the vaults (Ward-Perkins 1974, Ward-Perkins 1981). Actually, sun dried bricks were used in Anatolia likewise in Egypt and Syria since classical times (Ward-Perkins 1981). However, the buildings constructed of sun dried bricks rarely remained except for the very dry climates of Near East due to the destructible structure of the bricks (Ward-Perkins 1974, Ward-Perkins 1981). Fired bricks were introduced to Anatolian architecture from the central Roman Empire probably early in the second century AD, and their first use was in the upper storey of Library at Ephesus (Ward-Perkins 1981). Fired bricks were used mostly as mortared brick throughout in wall constructions. The most important monuments constructed by using walls comprised of mortared bricks throughout were the Kızıl Avlu or Serapeum and Temple of Asklepios Soter at Pergamon, and the Harbourside Baths at Ephesus (Ward-Perkins 1981) (Figure 1.21).



Figure 1.21. Kızıl Avlu at Pergamon constructed by mortared brick throughout (Source: Radt 2002, p.198)

Bricks were also used in horizontal bands alternate with wider bands of mortared rubble in Roman period walls in Anatolia (Ward-Perkins 1981) (Figure 1.22). The first appearance of this technique in Anatolia was during the second century AD (Ward-Perkins 1981).



Figure 1.22. Wall constructed of mortared rubble alternate with horizontal bands of brick in Gymnasium at Pergamon

### 1.3. Recent Studies on Roman Lime Mortars

Determination of Roman lime mortar characteristics became an important subject in the second half of the 20<sup>th</sup> century. The studies on Roman lime mortars were mostly published in international journals. Most of the studies on the characterization of Roman period lime mortars were focused on monuments located in Italy which denoted central Roman Empire, especially the city of Rome (Benedetti et al. 2004, Sánchez-Moral et al. 2005, Silva et al. 2005, Mirieollo et al. 2010, Jackson et al. 2009, Jackson et al. 2010, Jackson et al. 2011). Colosseum (Silva et al. 2005), Theatre of Marcellus (Jackson et al. 2011), Forum and Markets of Trajan, Baths of Caracalla (Jackson et al. 2009, Jackson et al. 2010) were some of the most important Roman monuments that lime mortar characteristics were determined. Following Italy, other countries that Roman period lime mortar characteristics investigated were Spain (Genestar et al. 2006,

Franquelo et al. 2008, Pavia and Caro 2008, Robador et al. 2010), Turkey (Güleç and Tulun 1997, Degryse et al. 2002, Özkaya and Böke 2009, Miriello et al. 2011), Portugal (Velosa et al. 2007), Greece (Zamba et al. 2007), Tunisia (Farci et al. 2005) and Slovenia (Kramar et al. 2011). Within the scope of the studies carried out in Turkey, lime mortar characteristics of ancient cities of Sagalassos (Degryse et al. 2002) and Kyme (Miriello et al. 2011); the Serapis Temple in Pergamon (Özkaya and Böke 2009) and Roman baths in Ankara (Güleç and Tulun 1997) were determined.

The general aim of the studies was to determine the characteristics of Roman lime mortars in order to provide information both on historic mortar technology and on the sites that mortar samples were taken. Besides this, some of the studies were also aimed to define the characteristics of suitable repair mortars (Degryse et al. 2002, Velosa et al. 2007, Özkaya and Böke 2009); and to investigate the possible raw material sources for the manufacturing of mortars (Franquelo et al. 2008, Jackson et al. 2010).

Studies mainly determined physical properties, raw material compositions, chemical and mineralogical compositions, hydraulic and microstructural properties and petrography of the selected Roman period lime mortars for their characterization. The results of these studies are given as below.

### **1.3.1. Basic Physical Properties**

Basic physical properties of Roman lime mortars were generally described according to their density and porosity percentage values (Farci et al. 2005, Sánchez-Moral et al. 2005, Jackson et al. 2009, Özkaya and Böke 2009, Jackson et al. 2011, Kramar et al. 2011, Miriello et al. 2011). Density values of mortars produced by natural pozzolanic aggregates were found 1.5 g/cm<sup>3</sup> by Özkaya and Böke (2009), between 1.430-1.785 g/cm<sup>3</sup> by Jackson et al. (2009), and 1.804 g/cm<sup>3</sup> by Jackson et al. (2011). Density values of mortars produced by artificial pozzolanic aggregates were found between 2.47-2.78 g/cm<sup>3</sup> by Kramar et al. (2011), and between 1.5-1.7 g/cm<sup>3</sup> by Farci et al. (2005).

Özkaya and Böke (2009) determined the porosity value of mortars produced by natural pozzolanic aggregates as 36 %, whereas Sánchez-Moral et al. (2005) identified it between 39-42 % for the same type of mortars. Porosity values of mortars produced by artificial pozzolanic aggregates were found to be lower than those produced by

natural pozzolanic aggregates by Farci et al. (2005) and Kramar et al. (2011). The porosity values of this type of mortars ranged between 23.9-49.7 % according to Kramar et al. (2011), and 24.2-44.3 % according to Farci et al. (2005).

Also, some of the studies analyzed pore sizes of mortars (Farci et al. 2005, Sánchez-Moral et al. 2005, Kramar et al. 2011). The results of these studies revealed that the pore sizes were  $< 100 \mu\text{m}$  for the mortars produced by natural pozzolanic aggregates (Sánchez-Moral et al. 2005); between 59.8-503.9 nm (Kramar et al. 2011) and  $< 0.01\text{-}30 \mu\text{m}$  (Farci et al. 2005) for the mortars produced by artificial pozzolanic aggregates.

### **1.3.2. Mechanical Properties of Mortars**

Özkaya and Böke (2009) and Jackson et al. (2009) investigated the mechanical properties of Roman lime mortars produced by natural pozzolans.

Özkaya and Böke defined the mechanical properties of mortars by their compressive strength and modulus of elasticity values. Compressive strengths of mortars were found as 6.6 MPa, and modulus of elasticity were determined as 630.6 MPa, respectively.

Jackson et al. described the mechanical properties through tensile failures which were determined by point load tests; and tensile strengths which were determined by Brazilian tests. Tests results revealed that tensile failures of lime mortars were 3.79 MPa, whereas tensile strengths ranged between 0.7 and 0.9 MPa.

### **1.3.3. Raw Material Compositions**

Raw material compositions of Roman mortars were described by defining lime/aggregate ratios (Degryse et al. 2002, Benedetti et al. 2004, Sánchez-Moral et al. 2005, Genestar et al. 2006, Franquelo et al. 2008, Özkaya and Böke 2009, Robador et al. 2010) or binder/aggregate ratios (Velosa et al. 2007, Miriello et al. 2010, Kramar et al. 2011, Miriello et al. 2011), and the particle size distribution of aggregates (Degryse et al. 2002, Benedetti et al. 2004, Sánchez-Moral et al. 2005, Özkaya and Böke 2009, Robador et al. 2010).

The most common techniques used for the determination of raw material compositions are dissolving by hydrochloric acid (HCl) (Benedetti et al. 2004, Velosa et al. 2007, Özkaya and Böke 2009, Robador et al. 2010), optical microscopy on thin sections (Degryse et al. 2002, Miriello et al. 2010, Miriello et al. 2011), polarizing microscopy on thin sections (Sánchez-Moral et al. 2005, Kramar et al. 2011), and mechanical sieving (Genestar et al. 2006).

Lime/aggregate ratios of Roman mortars produced by using natural pozzolanic aggregates were found as 1/4 by Özkaya and Böke (2009); and between 0.5/1-1.1/1 by Sánchez-Moral et al.(2005). Genestar et al. (2006) specified lime/aggregate ratios between 2-5 for mortars produced by siliceous aggregates, and between 0.5-2.5 for mortars produced by brick aggregates. Degryse et al. (2002) found weight percents of lime and aggregates as 45 % - 55 % for mortars of natural pozzolanic aggregates, 65 % - 35 % for brick aggregates and 40 % - 20 % - 20 % for mortars comprised of both types of pozzolans. Benedetti et al. (2004) also determined the weight percents of lime between 30-65 %, and brick aggregates between 35-70 %. Franquelo et al. (2008) and Robador et al. (2010) investigated the lime mortars comprised of brick aggregates and sand. Franquelo et al. (2008) determined their ratios as 1 (lime) / 1.5-1.8 (brick) / 1 (sand); and Robador et al. (2010) determined the weight percents of lime, brick aggregates and sand as 24.2-25.5 % (lime), 19-24.3 % (brick), 46.1 % (sand).

The rest of studies concerning the raw material compositions of Roman period lime mortars emphasized the binding properties of the parts of mortars size < 1/16 mm and identified the raw material compositions upon the binder and aggregate percents (Velosa et al. 2007, Miriello et al. 2010, Kramar et al. 2011, Miriello et al. 2011). Miriello et al. (2010) determined the weight percent of binder parts between 30-51 % and aggregate parts between 35-52 %; and Miriello et al. (2011) determined the binder and aggregate percents as 67-83 % and 15-30 % of the mortars produced by using natural pozzolanic aggregates. For the mortars comprised of brick aggregates weight percents of binder parts were found between 25-44 % by Miriello et al. (2010); between 35-65 % by Kramar et al. (2011); and between 30-20 % by Velosa et al. (2007). Brick aggregate parts of these mortars were in the range of 42 - 61 % (Miriello et al. 2010); 65-35 % (Kramar et al. 2011), and 70-80 % (Velosa et al. 2007).

Particle size distributions of aggregates were also considered as a part of the raw material compositions. Özkaya and Böke (2009) and Velosa et al. (2007) mentioned that the aggregates > 1000 µm constituted the largest fraction of aggregates in the

mortars of natural pozzolanic aggregates. Sánchez-Moral et al. (2005) indicated that the natural pozzolanic aggregates sized between 0.5-2 mm and 100-300  $\mu\text{m}$  generated the largest fraction among the total of the aggregates. Kramar et al. (2011) stated that aggregate sizes were between 0.02-1.49 mm for lime mortars comprised of brick aggregates. Both of these studies did not specify the percentage values of the largest fraction of aggregates.

Degryse et al. (2002) determined that the aggregates of 4-4.74 mm as 3.87 %, 2-4 mm as 30.58 %, 1-2 mm as 25.61 %, 500  $\mu\text{m}$ -1mm as 14.09 %, 250-500  $\mu\text{m}$  as 11.42 %, 125-20  $\mu\text{m}$  as 8.82 %, 63-125  $\mu\text{m}$  5.64 % both for mortars composed of natural pozzolanic and brick aggregates. Benedetti et al. (2004) stated that brick aggregates < 0.1 mm constituted the fraction of 30 %, and between 0.1-0.5 mm constituted the fraction of 35 %. Benedetti et al. (2004) also mentioned that aggregates greater than 0.5 mm. were only a few among the total of the aggregates. According to Robador et al. (2010), the percentage of aggregates sizes of 1-2 mm was 24.16 %, 0.595-1mm was 13.97 %, 0.420-0.595 mm 32.13 % and 0.320-0.420 mm was 13.52 %. Miriello et al. (2010, 2011) defined the aggregate sized of lime mortars through the mean aggregate sizes and maximum aggregate sizes. Mean aggregate sizes of mortars composed of natural pozzolanic aggregates were found between 0.47-1.25 mm (Miriello et al. 2010) and between 0.7-1.4 mm (Miriello et al. 2011). Also, mean aggregate sizes of brick aggregates were found in the range of 2.64-8.54 mm by Miriello et al. (2010). Maximum aggregate sizes were between 1.92-15 mm (Miriello et al. 2010) and 5.2-6.3 mm (Miriello et al. 2011) for natural pozzolanic aggregates; and between 18-27 mm) for brick aggregates (Miriello et al. 2010).

### **1.3.4. Mineralogical Compositions**

Mineralogical composition analyses were carried out on mortars and aggregates used in their production (Benedetti et al. 2004, Franquelo et al. 2008, Robador et al. 2010, Miriello et al. 2011); binder parts of mortars (size < 63  $\mu\text{m}$ ) and their aggregates (Degryse et al. 2002, Robador et al. 2010, Jackson et al. 2011, Kramar et al. 2011); only mortars (Güleç and Tulun 1997, Sánchez-Moral et al. 2005, Velosa et al. 2007, Miriello et al. 2010); only binders (Jackson et al. 2009); or only aggregates (Farci et al. 2005,



Zamba et al. 2007, Özkaya and Böke 2009, Jackson et al. 2010). However, mineralogical compositions of lime lumps were not mentioned in any of the studies.

Most of the studies preferred to use X-ray diffractometer (XRD) for the determination of mineralogical compositions with the exception of some studies using SEM-EDS (Miriello et al. 2011), optical and polarizing microscopy (Degryse et al. 2002, Miriello et al. 2011) and petrographic analyses (Jackson et al. 2010).

Miriello et al. (2011) determined that lime mortars in Kyme (Turkey), which were comprised of natural pozzolanic aggregates, were composed of mainly calcite, anorthite, quartz, goethite, muscovite, vaterite, chlorite, albite; and the natural pozzolanic aggregates of these mortars consisted of quartz, plagioclase, muscovite, calcite, biotite, heulandite and opaque minerals.

Benedetti et al. (2004) found that lime mortars of natural pozzolanic aggregates consisted of calcite, sanidine, aragonite, graphite and amorphous materials; whereas lime mortars of brick aggregates consisted of calcite, quartz, muscovite, dolomite, hematite, periclase, diopside, analcime and labradorite. Mineralogical compositions of the natural pozzolans used in these mortars were composed of quartz, diopside, sanidine, dolomite, biotite; and brick aggregates were composed of quartz, diopside, sanidine, dolomite, biotite, hematite, serandite and calcite.

Mineralogical compositions of brick aggregates and also the lime mortars produced by using these aggregates were investigated by Franquelo et al. (2008). According to Franquelo et al. (2008), brick aggregates were composed of quartz, anorthite, hematite, mica, calcite, muscovite; and lime mortars were consisted of quartz, calcite, mica and anorthite.

Güleç and Tulun (1997) determined that lime mortars produced by brick aggregates were composed of mainly quartz, calcite, albite, and small amounts of muscovite and vermiculite by polarizing microscopy.

According to Miriello et al. (2010) lime mortars of natural pozzolans were comprised of calcite, anorthite, analcime, leucite, sanidine, augite, phlogopite, albite, sillimanite, goethite, cowlesite, wollastonite, zircon, ludwigite and also CSH phases (hillebrandite, okenite, tobermorite, xonotlite); and lime mortars of brick aggregates contained calcite, quartz, albite, tobermorite, montmorillonite, andradite, augite, phlogopite, sanidine, nepheline, dypingite, plagioclase.

Sánchez-Moral et al. (2005) determined the mineralogical compositions of lime mortars produced by natural pozzolanic aggregates as mainly calcite, phyllosilicate, analcime and augite; and traces of feldspar and quartz.

Velosa et al. (2007) identified that the mineralogical compositions of mortars produced by brick aggregates were composed of quartz, calcite, feldspar, and phyllosilicates; and traces of dolomite, magnesite, and pyrite.

Mineralogical composition of the binder parts of mortars produced by natural pozzolanic aggregates were composed of calcite, analcime, leucite, diopside, vaterite and strätlingite; and natural pozzolanic aggregates were consisted of analcime, leucite, diopside, hematite and calcite according to Jackson et al. (2011). Strätlingite which was defined as a calcium-aluminate cement hydrate was also specified by Jackson et al. (2009). Calcite, diopside, sanidine, leucite, analcime, and clay minerals were the other minerals determined by Jackson et al. (2009).

Degryse et al. (2002) defined the mineralogical compositions of binders comprised of natural pozzolans as sanidine, anorthite and also amorphous glass phases; and the pozzolans as plagioclase, alkali-feldspar, augite, diopside, biotite and amphiboles.

Binders of mortars produced by brick aggregates were composed of calcite, dolomite, quartz and muscovite; whereas the brick aggregates were composed of dolomite, calcite, quartz and muscovite according to Kramar et al. (2011).

Robador et al. (2010) also determined the mineralogical compositions of brick aggregates as quartz, calcite, anorthite, hematite; and binders of lime mortars manufactured by these aggregates were composed of quartz, anorthite, mica, hematite.

Mineralogical compositions of natural pozzolanic aggregates were found to be composed of quartz, sanidine, analcime, biotite, ignimbrite, feldspar by Jackson et al. (2010); albite, K-feldspar, quartz, amorphous minerals by Özkaya and Böke (2009); and quartz and calcite by Zamba et al. (2007). Farci et al. (2005) determined the mineralogical compositions of brick aggregates as calcite, quartz, feldspar, gehlenite, sanidine, plagioclase, biotite.

### 1.3.5. Chemical Compositions

Chemical compositions are one of the most important features that most of the studies determined to characterize the Roman lime mortars. In the scope of chemical composition analyses, major chemical compositions of mortars (Sánchez-Moral et al. 2005, Velosa et al. 2007, Miriello et al. 2010, Robador et al. 2010, Miriello et al. 2011), binders (Jackson et al. 2009, Jackson et al. 2010, Miriello et al. 2010, Jackson et al. 2011, Kramar et al. 2011, Miriello et al. 2011), aggregates (Jackson et al. 2009, Kramar et al. 2011, Miriello et al. 2010, Miriello et al. 2011), lime lumps (Miriello et al. 2011); and also trace element compositions of mortars (Sánchez-Moral et al. 2005, Miriello et al. 2010, Miriello et al. 2011) were determined.

The most commonly used technique for the determination of chemical compositions is X-ray fluorescence (XRF) (Velosa et al. 2007, Jackson et al. 2009, Miriello et al. 2010, Robador et al. 2010, Miriello et al. 2011). Other techniques used for this purpose were scanning electron microscope coupled with X-ray energy dispersive system (SEM-EDS) (Jackson et al. 2010, Miriello et al. 2010, Miriello et al. 2011); inductively coupled plasma mass spectrometry (Sánchez-Moral et al. 2005, Jackson et al. 2011); inductively coupled plasma atomic emission spectroscopy (ICP-OES) (Kramar et al. 2011); atomic absorption spectroscopy (AAS) (Sánchez-Moral et al. 2005); and electron microprobe analysis (EMPA) (Sánchez-Moral et al. 2005).

Mortars produced by using natural pozzolanic aggregates were composed of higher amounts of SiO<sub>2</sub> (27.6-45.1 %), CaO (12.2-30.7 %); moderate amounts of Al<sub>2</sub>O<sub>3</sub> (6.8-14.7 %), Fe<sub>2</sub>O<sub>3</sub> (1.7-7.4 %), MgO (1.7-8.4 %); and low amounts of Na<sub>2</sub>O<sub>3</sub> (0.3-3.5), K<sub>2</sub>O (1.2-5.0 %), TiO<sub>2</sub> (0.3-0.9 %), P<sub>2</sub>O<sub>5</sub> (0.2-0.5 %), MnO (0.07-0.1 %) (Sánchez-Moral et al. 2005, Miriello et al. 2010, Miriello et al. 2011).

Similarly, mortars which were comprised of brick aggregates used as artificial pozzolans consisted of SiO<sub>2</sub> (28.4-57.9 %), CaO (13.0-24.7 %), Al<sub>2</sub>O<sub>3</sub> (2.6-14.6 %), Fe<sub>2</sub>O<sub>3</sub> (2.3-7.2 %), MgO (1.5-5.2 %), Na<sub>2</sub>O<sub>3</sub> (0.1-1.3 %), K<sub>2</sub>O (0.6-2.4 %), TiO<sub>2</sub> (0.004-0.8 %), P<sub>2</sub>O<sub>5</sub> (0.2-0.3 %), MnO (0.02-0.2 %) (Velosa et al. 2007, Miriello et al. 2010, Robador et al. 2010).

Trace element compositions of mortars were investigated by Sánchez-Moral et al. (2005), Jackson et al. (2009), Miriello et al. (2010, 2011), and Kramar et al. (2011). Trace elements determined in the compositions of mortars consisted of natural

pozzolanic aggregates were Nb, Zr, Y, Sr, Rb, Ni, Cr, V, La, Ce, Co, Ba, Cu, Zn and Pb. Trace elements compositions of lime mortars produced by brick aggregates were found as Nb, Zr, Y, Sr, Rb, Ni, Cr, V, La, Ce, Co and Ba by Miriello et al. (2010).

Binders of the mortars produced by natural pozzolans were composed of high amounts of SiO<sub>2</sub> (3.8-50.8 %), CaO (14.3-90.6 %); moderate amounts of Al<sub>2</sub>O<sub>3</sub> (1.2-14.7 %), MgO (1.8-13.1 %); and low amounts of Na<sub>2</sub>O<sub>3</sub> (0.5-1.2 %), K<sub>2</sub>O (0.3-3.7 %), TiO<sub>2</sub> (0.3-0.9 %), P<sub>2</sub>O<sub>5</sub> (0.3-1.2 %), MnO (0.1-0.4 %) (Jackson et al. 2009, Jackson et al. 2010, Jackson et al. 2011, Miriello et al. 2011).

Binders consisted of brick aggregates were also composed of SiO<sub>2</sub> (0.4-14.3 %), CaO (29.5-90.6 %), Al<sub>2</sub>O<sub>3</sub> (0.2-4.6 %), MgO (1.9-6.3 %), Na<sub>2</sub>O<sub>3</sub> (0.02-0.9 %), K<sub>2</sub>O (0.05-0.7 %), TiO<sub>2</sub> (0.02-0.3 %), P<sub>2</sub>O<sub>5</sub> (0.1-0.7 %) (Miriello et al. 2010, Kramar et al. 2011).

Major chemical compositions of natural pozzolanic aggregates were consisted of SiO<sub>2</sub> (42.9-84.8 %), CaO (0.3-12.8 %), Al<sub>2</sub>O<sub>3</sub> (6.0-24.2 %), MgO (0.6-26.1 %), Na<sub>2</sub>O<sub>3</sub> (0.4-13.4 %), K<sub>2</sub>O (1.0-17.6 %), MnO (0.2-0.7 %), P<sub>2</sub>O<sub>5</sub> (0.1-0.8 %), TiO<sub>2</sub> (0.3-1.1 %) (Jackson et al. 2009, Miriello et al. 2010, Miriello et al. 2011).

Major chemical composition of brick aggregates were determined by Kramar et al. (2011). The composition was as 0.21-2.70 % SiO<sub>2</sub>, 28.97-43.00 % CaO, 0.10-3.24 % Al<sub>2</sub>O<sub>3</sub>, 4.33-12.87 % MgO, 0.023-0.043 % Na<sub>2</sub>O<sub>3</sub>, 0.039-0.258 % K<sub>2</sub>O, 0.012-0.033 % MnO, 0.055-0.442 % P<sub>2</sub>O<sub>5</sub>, 0.001-0.023 % TiO<sub>2</sub>.

None of the studies determined trace element compositions of aggregates although variances in trace element compositions are accepted as peculiar characteristics to the source of materials and evaluated for this purpose in some archeometric studies (Mommensen 2001, Cardiano et al. 2004).

The chemical composition of lime lumps representing the lime part used in the mortar was determined by only Miriello et al. (2011). According to Miriello et al. (2011), chemical composition of the lime lump was composed of mainly CaO (84.1-94.1 %), small amounts of SiO<sub>2</sub> (1.3-7.6 %), and minor amounts of other minerals (Al<sub>2</sub>O<sub>3</sub>, MgO, Na<sub>2</sub>O<sub>3</sub>, K<sub>2</sub>O, MnO, P<sub>2</sub>O<sub>5</sub>, TiO<sub>2</sub>).

### **1.3.6. Hydraulic Properties of Mortars**

Hydraulic properties of Roman lime mortars are described by only a limited number of studies (Silva et al. 2005, Genestar et al. 2006, Pavia and Caro 2008, Özkaya and Böke 2009, Miriello et al. 2011).

Silva et al. (2005), Genestar et al. (2006) and Özkaya and Böke (2009) determined hydraulic properties of mortars according to the weight loss between 200-600 °C due to the loss of structurally bound water (H<sub>2</sub>O) of hydraulic products and the weight loss between 600-900 °C due to the loss of CO<sub>2</sub> released during the decomposition of calcium carbonate. If the ratio of CO<sub>2</sub>/H<sub>2</sub>O is below 10, the mortar is accepted hydraulic (Bakolas et al. 1998, Moropoulou et al. 2000). This ratio was found between 0.287-2.11 by Silva et al. (2005), 2.95 by Özkaya and Böke (2009), and between 4.3-7.5 by Genestar et al. (2006). These results revealed that investigated Roman lime mortars used in Roman Colosseum and cistern (Silva et al. 2005), in Serapis Temple (Özkaya and Böke 2009) and in the Roman city of Pollentia (Genestar et al. 2006) were hydraulic.

Miriello et al. (2011) described hydraulic properties of mortars through the determination of their hydraulicity indices (H.I.). Hydraulicity indices of mortars from Kyme (Turkey) were found between 0.11 and 0.23 indicating that they had hydraulic properties.

Pavia and Caro (2008) only mentioned that investigated mortars were hydraulic but did not explain the technique they used.

### **1.3.7. Pozzolanic Activities of Aggregates**

Pozzolanic activity of aggregates is the least emphasized characteristic in the studies. This feature was investigated only by Özkaya and Böke (2009). In this study, XRD, SEM-EDS analyses and electrical conductivity measurements before and after the addition of pozzolan powders into calcium hydroxide solution (Luxan et al. 1989) were used to estimate the pozzolanic activities. Amorphous minerals were determined on the XRD patterns by the broad peak between 20-30 °2Theta. Also, SEM-EDS images revealed the glassy phases of silica. Electrical conductivity measurements showed high differences (7 µS/cm) before and after the addition of pozzolan powders to the saturated

calcium hydroxide solution. The results of these three methods indicated that aggregates used in the lime mortars of Serapis Temple were pozzolanic.

### **1.3.8. Microstructural Properties**

Microstructural properties analyses were generally intended for pozzolans and lime, products of reaction between lime and pozzolans, and mortar matrices in general (Degryse et al. 2002, Farci et al. 2005, Sánchez-Moral et al. 2005, Silva et al. 2005, Velosa et al. 2007, Zamba et al. 2007, Pavía and Caro 2008, Jackson et al. 2009, Özkaya and Böke 2009, Robador et al. 2010, Jackson et al. 2011, Kramar et al. 2011, Miriello et al. 2011). The most common technique for the determination of microstructural properties was SEM-EDS (Farci et al. 2005, Silva et al. 2005, Zamba et al. 2007, Jackson et al. 2009, Özkaya and Böke 2009, Robador et al. 2010, Jackson et al. 2011, Kramar et al. 2011, Miriello et al. 2011). ESEM (Sánchez-Moral et al. 2005), petrographic analysis (Degryse et al. 2002, Sánchez-Moral et al. 2005, Pavía and Caro 2008) and optical microscopy (Velosa et al. 2007) were the other techniques used for microstructural properties.

#### **Mortar matrices:**

Microstructural analyses of Roman period mortars from Serapis Temple carried out by Özkaya and Böke (2009) indicated that these mortars were stiff, hard and compact due to the adhesion between aggregates and lime.

Miriello et al. (2011) insisted that traces of reused mortar fragments probably from the old walls had been used as aggregate materials in the production of mortars used in archaeological site of Kyme (Turkey).

#### **Pozzolans used as aggregates:**

Microstructural properties analyses of natural pozzolanic aggregates were generally on determination of their shapes (Özkaya and Böke 2009) or their crystal structures (Degryse et al. 2002, Miriello et al. 2011)

The shapes of natural pozzolanic aggregates used in the mortars from Serapis Temple were described as semi-rounded, easily granulated and very porous enabling the adherence to lime (Özkaya and Böke 2009). Natural pozzolanic aggregates of mortars from Sagalassos (Turkey) were found to be composed of submicroscopic crystals and a glass phase (Degryse et al. 2002). Also, traces of metamorphic rocks mainly phyllades

were observed within the structure of some natural pozzolanic aggregates of mortars from Kyme (Turkey) (Miriello et al. 2011).

Microstructural properties of brick particles used as artificial pozzolanic aggregates were described by their pore structure (Farci et al. 2005) and their shapes (Velosa et al. 2007). Farci et al. (2005) stated that brick aggregates had a tight granular structure which made the brick less permeable to water. The microstructure of brick aggregates were determined as of low roundness and medium sphericity, and found dispersed through the mortar matrix; whereas the coarse grains were revealed a very low mixing and homogeneity within the rest of the raw materials as a result of microscopic analyses by Velosa et al. (2007).

### **Lime lumps:**

Microstructural properties of lime used in the production of Roman lime mortars were determined by the investigation of lime lumps found within the mortars (Sánchez-Moral et al. 2005, Silva et al. 2005, Velosa et al. 2007, Zamba et al. 2007, Robador et al. 2010).

Lime binder parts of the mortars from La Rioja (Spain) were defined as fine grained and essentially free from fractures indicating a low shrinkage (Pavía and Caro 2008). High specific surface area and low shrinkage were interpreted as the soft-burn of raw limestone.

Zamba et al. (2007) defined lime lumps as solely composed of neoformed euhedral calcite crystal assemblages, mostly in rhombohedral form, and rare sub-microscopic quartz fragments. Zamba et al. suggested that original micritic calcite crystals were transformed into sparry calcite as a result of aging.

Silva et al. (2005) studied the microstructural properties of lime mortars from Roman Colosseum and cistern, and calcite crystals found within the mortars. In this study, it was found that the spaces between aggregates were filled by large calcite crystals with an etched morphology. The crystals were covered by small (500-100  $\mu\text{m}$ ) prismatic particles composed of Si and had a characteristic morphology with channels that was considered as secondary skeletons of diatoms.

Robador et al. (2010) investigated the carbonate particles found in the pores of brick aggregates. Hydromorphic calcite crystals, which formed by recrystallisation of calcium carbonate, were determined within the pores. Different formations composed of Si, Al and Ca representing the reaction between lime and silicate compounds were also observed inside the pores of aggregates.

Calcite crystals were also determined by Velosa et al. (2007) inside the pores of brick aggregates within the Roman mortars from Conímbriga. Calcite crystals were also detected within the discontinuities between aggregates and mortar matrix in this study. Sánchez-Moral et al. (2005) also determined calcite crystals inside fissures of mortars by ESEM and polarizing microscopy.

**Products of reaction between lime and pozzolans:**

Gel-like formations composed of calcium, silicon and aluminum which might indicate the hydraulic products were determined within the mortar matrices of Serapis Temple (Özkaya and Böke 2009).

Reaction and strong adhesion between binder and aggregates, and homogeneity of the mortars were also indicated by Pavía and Caro (2008).

Kramar et al. (2011) observed two types of reaction rims around brick aggregate fragments of the mortars from the bath complex of the Roman villa rustica near Mošnje (Slovenia). The first type of reaction rim was the calcium carbonate rims of a thickness about 20  $\mu\text{m}$  around individual brick grains due to the higher mobility of Ca compared to Si, and might represent the weakened areas of mortars. The second type of rims indicated the pozzolanic reaction between brick aggregates and lime, had a thickness of about  $\mu\text{m}$  and composed of Al, Ca and Mg.

The crystals found inside the pores and covering the calcite crystals were identified as rod-like mineral assemblages that formed thin to thick networks which were mainly composed of CaO-SiO<sub>2</sub> and Al<sub>2</sub>O<sub>3</sub>, Fe<sub>2</sub>O<sub>3</sub>, MgO and K<sub>2</sub>O possibly indicating CSH (Zamba et al. 2007).

Likewise, Jackson et al. (2009) and Jackson et al. (2011) determined blade-like strätlingite crystals composed of calcium aluminate hydrate (C<sub>2</sub>ASH<sub>8</sub>) which gave high compressive strength to modern cements within the matrices of Roman lime mortars from Markets of Trajan (Rome) and Theatre of Marcellus (Rome).

#### **1.4. Aim and Scope of the Study**

Technology of Roman mortars, which were produced by using lime and natural and artificial pozzolans, reflect an important achievement resulted in new architectural forms and construction techniques. Recent researches are carried out mostly on the determination of the characteristics of Roman lime mortars used in the imperial



buildings in Italian Peninsula denoting Central Roman Empire whereas there are a few studies on the characteristics of Roman lime mortars used in Anatolia.

In this study, characteristics of Roman lime mortars produced by natural and artificial pozzolans have been determined in order to understand technology of Roman period lime mortars used in Anatolia. In the scope of this study, the ancient cities of Aigai (Manisa) and Nysa (Aydın) were selected for the case areas. The reason for the selection of Aigai and Nysa is that they were two of the eastern provincial cities of Roman Empire located in a close district. Lime mortars produced by using natural and artificial pozzolans were collected from all the accessible Roman period buildings in these cities. Furthermore, necessary legal permissions were taken to collect samples.

Physical properties, raw material compositions, hydraulic properties of mortars; chemical and mineralogical compositions of lime, natural and artificial pozzolans, and binders which are the fine mortar matrices are determined by using standard test methods, XRF, XRD, SEM-EDS, FTIR and TGA analyses. Binders composed of small grain sized silica and carbonated lime have been considered as the main part that give hydraulic character and high strength to the mortar. Hence, this study also aimed to develop a relatively fast and easy method for quantitative determination of  $\text{CaCO}_3$  and  $\text{SiO}_2$  in the binder compositions by using FTIR, LIBS, SEM-EDS and XRD analyses.

## **CHAPTER 2**

### **METHOD**

This is a case study focusing on the characteristics of Roman lime mortars used in the ancient cities of Aigai and Nysa. Data collection was carried out through experiments in which standard test methods, scanning electron microscope (SEM) coupled with energy dispersive spectroscopy (EDS), X-ray diffraction (XRD), X-ray fluorescence (XRF), thermogravimetric analysis (TGA) and Fourier transformed infrared spectroscopy (FTIR) were used. Results of XRF analyses were interpreted through hierarchical clustering and statistical test methods. Furthermore, a new method was developed for the quantitative determination of  $\text{CaCO}_3$  and  $\text{SiO}_2$  content in the binder parts of the mortars by using SEM-EDS, FTIR, XRD and laser induced breakdown spectroscopy (LIBS).

#### **2.1. Case Areas and Samples**

The ancient cities of Aigai and Nysa were selected as the case areas to investigate the characteristics of Roman period lime mortars produced from natural and artificial pozzolans (Figure 2.1).

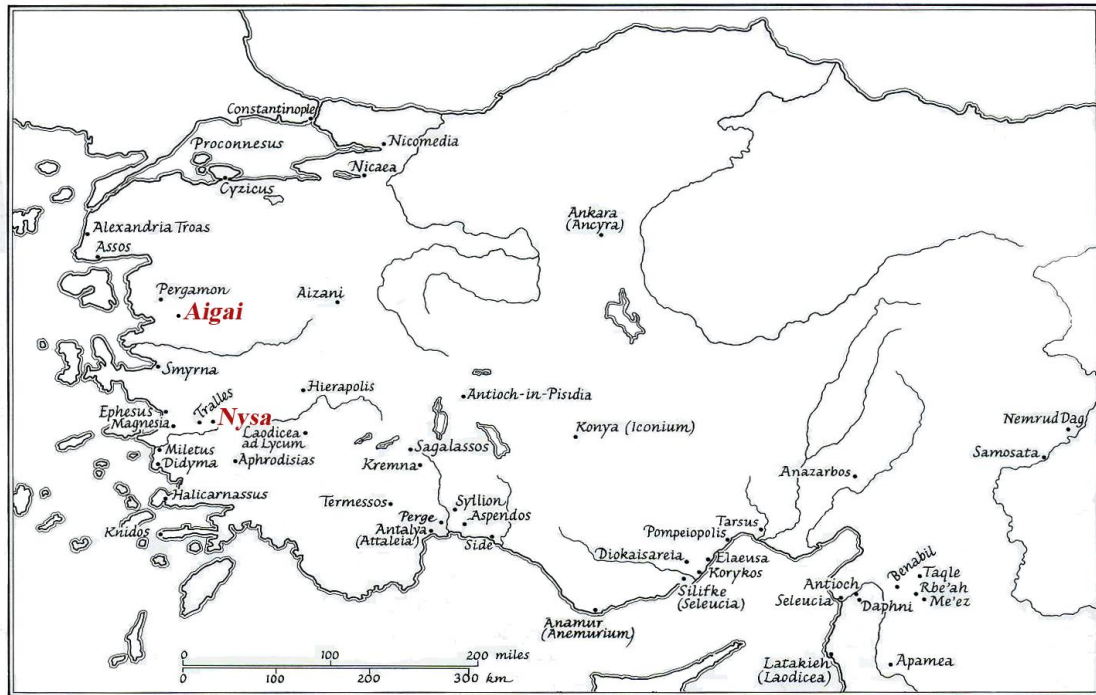


Figure 2.1. Locations of Aigai and Nysa  
(Source: Ward-Perkins 1981)

Thirty-three mortar samples were collected accessible Roman period buildings under the supervision of archeologists in charge of the excavations. During sampling, mortars were collected in the sizes suitable for the analyses, without harming the original material characteristics of buildings.

Collected mortar samples were used in the rubble core of the walls (four samples), in walls comprised of mortared rubble (ten samples) or mortared ashlar (two samples) throughout, in arches and vaults (five samples), as supporting for coverings and mosaics (six samples), and as plasters (six samples).

Depending on the macroscopic investigations, mortar samples were classified into two categories according to the types of their aggregates. These groups were lime mortars produced with natural pozzolans and lime mortars produced with artificial (crushed bricks) pozzolans.

Samples were labeled with a letter showing the site they were taken from (A:Aigai, N:Nysa) and a number for the convenience of tables and graphs of the results of analyses and the statistical programme used for interpretation of results.

### 2.1.1. Aigai

Aigai was located almost on the top of Mount Gün, near Köselier Village in Manisa. The city was first mentioned as Aigai by historian Herodotus, as Aegae by geographer Strabo and as Aegaeae by natural philosopher Plinius (Strabon 2005).

Aigai was mentioned as a member of Aeolian cities with Cyme, Larissa, Neonteichos, Temnos, Killa, Notium, Aigirossa, Pitane, Myrina, Gryneia and Smyrna by Herodotus and Strabo (Strabon 2005). Aeolis was defined as the coastal region lying between Troia on the north, Ionia on the south and Lydia on the east that had been founded by Aeolians whom migrated from Greece after 1100 BC (Strabon 2005).

The history of Aigai does not go back earlier than seventh century BC depending on the present findings in the site (Doğer 2007). Aigai was always a free and independent member of Aeolis. It never played a political role within the Aeolian league led by Cyme, since it was drawn into mountains and did not have a special position in terms of trade and industry networks. Together with its neighbor Temnos, Aigai was always isolated from the wars and fluctuations in the region including the Persian raids for centuries. Until the third century BC, Aigai was only a small fortress-city. The importance of Aigai for Aeolis was derived from creating an interior outpost due to its location. It was developed in the Hellenistic period and gained public buildings like agora and bouleuterion in this period. The city had been dominated by the kingdom of Pergamon from 218 BC until the last king of Pergamon left Aeolis to Rome in 133 BC. Aigai resembled the city of Pergamon in planning, terracing and settlement because of the close relations it established with the kingdom. Catastrophic earthquake that occurred in 17 AD had been very destructive for Aigai. After this earthquake, the city was restored with the help of the emperor Tiberius. The name of Aigai was lastly encountered in the bishop lists dated to 5<sup>th</sup> century AD and in the travel book of Hierokles. Aigai was abandoned together with its neighbor Temnos after the Arabic raids in seventh century AD. The last settlements in the city were the Iron Gate and a small Byzantine fortress dated to 12<sup>th</sup> and 13<sup>th</sup> centuries located in a limited area behind the Iron Gate. The location of Aigai was determined by W.M Ramsay in 1881 as a result of the travel he had done with M.Baltazzi of Ali Agha and M. Reinech (Ramsay 1881).

The first studies in Aigai are the detailed surface researches carried out in 1885-1886 by German archaeologists who began to conduct excavations in Pergamon (Umar 2002). The results of these researches were published in the book “Altertümer von Aigai” in 1889 (Umar 2002). Since 2004, a team supervised by Prof.Dr. Ersin Doğer (Ege University) is carrying out the archaeological excavations in Aigai.

Bouleterion, agora building (Figure 2.2), macellum, theatre (Figure 2.3), baths, and cisterns were the most important buildings of the site.



Figure 2.2. Agora wall of Aigai






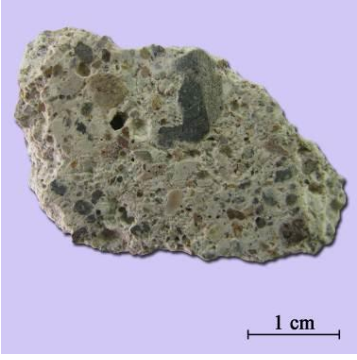




Figure 2.3. Theatre of Aigai

In Aigai, ten mortar samples were collected from stage building and vomitorium of theatre, terrace wall of agora, terrace wall of stadium, baths, bouleterion and macellum. Seven samples were the lime mortars produced with natural pozzolans (Table 2.1), and three samples were the lime mortars produced with artificial pozzolans (Table 2.2).

Lime mortars produced from natural pozzolans were used in the walls comprised of ashlar (stage building of theatre, stadium), rubble core of the walls faced with ashlar (terrace wall of agora, vomitorium of theatre), vault constructed of stones (bath) and under stone covering of floor (macellum) (Table 2.1). Lime mortars produced from artificial pozzolans were used in the rubble core of the wall faced with ashlar (bath); as plaster (bouleterion), and as paving layer on the superstructure (bath) (Table 2.2).



Table 2.1. Lime mortars with natural pozzolanic aggregates from Aigai

	Location of Sample	Sample	Definition
A1			Mortar from the rear wall comprised of ashlars  <i>Stage building of theatre</i>
A2			Mortar from the rubble core of terrace wall faced with ashlars  <i>Terrace wall of Agora</i>
A3			Mortar from the rubble core of wall faced with ashlars  <i>Vomitorium of theatre</i>
A6			Mortar from the vault constructed of stones  <i>South bath</i>

(cont. on next page)

Table 2.1 (cont.)


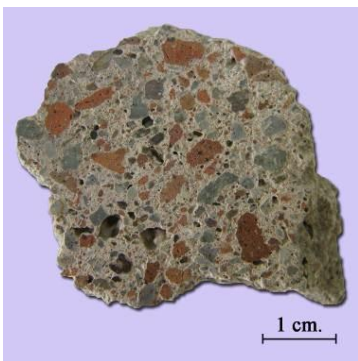





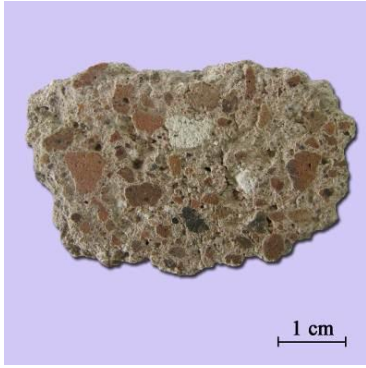



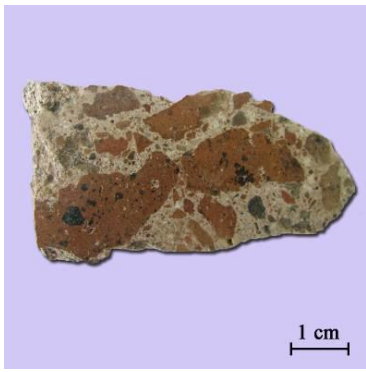
	Location of Sample	Sample	Definition
A7			Mortar from the terrace wall comprised of ashlars  <i>Stadium</i>
A9			Mortar used under stone covering of floor  <i>Macellum</i>
A12			Mortar from the rubble core of wall faced with ashlars  <i>Building</i>



Table 2.2. Lime mortars and plasters with artificial pozzolans from Aigai

	Location of Sample	Sample	Definition
A5			Plaster from the wall <i>Bouleterion</i>
A10			Mortar from the rubble core of wall faced with ashlar <i>North bath</i>
A11			Mortar used as paving over the super structure <i>South bath</i>

### 2.1.2. Nysa

Nysa was located on the south side of Aydın Mountains, 3 km. to the northwest of Sultanhisar district of Aydın. It was one of the most important cities of Caria which also comprised Mylasa, Iassos, Euromos, Heraclia, Priene, Miletos, Didyma, Hierapolis, Labraunda and Laodiceia.

The information about the history of Nysa is mainly obtained from the geographer Strabo and the historian Stephanus of Byzantium. Strabo the Greek geographer who was born in 63 BC in Amasia and died after 21 AD studied rhetoric and grammar under Aristodemos in Nysa (Bean 1989). Strabo said that three brothers from Sparta named Athymbrus, Athymbradus and Hydrelus founded three cities in their own names, and then united these cities under a single city Nysa of which Athymbrus was considered as the founder (Bean 1989, İdil 1999). Because of this, the city was first known as Athymbra and then Antiocheia (Bean 1989, İdil 1999). On the other hand, according to Stephanus who lived in sixth century AD, the Carian Nysa was founded by Antiochos I of Syria, son of Seleukos, in the first half of the third century BC and named after his wife (Bean 1989, Akurgal 2001). Strabo described Nysa as a kind of double city divided by a stream and joined by a bridge (Strabon 2005).

Although the individual history of Nysa is not very clear, it was known that Nysa as a civil city, gained the privilege of being a city that right of asylum was requested from after it was captured by Antiochos III (223-187 BC). The development of the city was especially in the Roman Imperial Era (İdil 1999). During Byzantine period, Nysa was captured by Seljuks in the 12<sup>th</sup> century for a short period of time and afterwards it began to be dominated by the Byzantines again (İdil 1999). Nysa gradually lost its importance after its invasion by Tamerlane in 1402 (İdil 1999). In the first half of 19<sup>th</sup> century, various research visits were held to Nysa. First archaeological researches in Nysa were carried out in 1907 and 1909 by German archaeologists led by Dr. Pringsheim. Their excavations were delimited by agora, theatre, bouleterion and stadium buildings. It was also known that a Greek team carried out some excavations at the site in 1921. In the years following 1960, some excavations were carried out in bouleterion by İzmir Archaeological Museum. Since 1990, an archaeological team

supervised by Prof.Dr. Vedat İdil (Ankara University) carried out the excavations in Nysa.

The most significant buildings of Nysa were the library (Figure 2.4), gymnasium, stadium, roman bridge, theatre (Figure 2.5), tunnel, bouleterion and agora. Library of Nysa built in the second century AD was two-storeyed structure and considered as the best preserved library building in Anatolia, next to the Celcius Library of Ephesus (Akurgal 2001) (Figure 2.4). The theatre was also a well preserved building of the site and famous with its frises on the stage section.



Figure 2.4. Library of Nysa






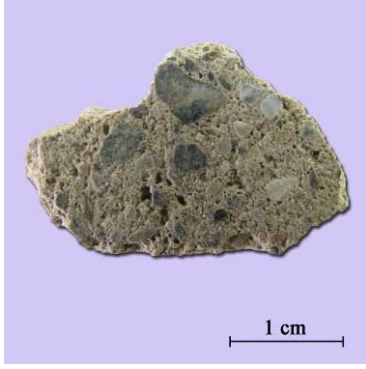




Figure 2.5. Theatre of Nisa

Twenty-three mortar samples from bath, temple, podium of theatre, cistern, water basin and bridge were collected from Nisa. Ten samples were the lime mortars produced with natural pozzolans (Table 2.3), and thirteen samples were the lime mortars produced with artificial pozzolans (Table 2.4).

Lime mortars produced with natural pozzolans were used in the walls comprised of mortared rubble throughout (temple, library, water basin, bridge cistern), vault constructed of stones, and arches constructed of stones or bricks (bath) (Table 2.3). Lime mortars produced with artificial pozzolans were used in the walls comprised of mortared rubble throughout (library, pool of the temple), in arches constructed of stones (cistern); as supporting for marble coverings (bath, water basin) and mosaics (library), as paving layer (theatre) and also as plaster (library, water basin, cistern) (Table 2.4).






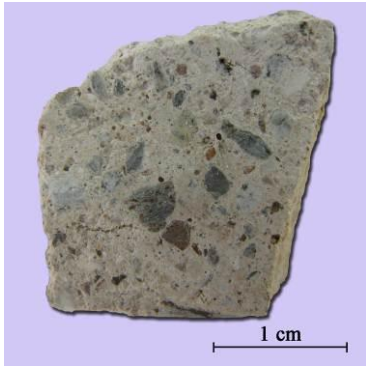


Table 2.3. Lime mortars with natural pozzolanic aggregates from Nysa

	Location of Sample	Sample	Definition
N3			Mortar from the wall comprised of mortared rubble throughout <i>Temple</i>
N4			Mortar from the east wall comprised of mortared rubble throughout <i>Library</i>
N7			Mortar from the west wall comprised of mortared rubble throughout <i>Library</i>
N10			Mortar from the vault constructed of stones <i>Building (located on the west side of library)</i>

(cont. on next page)

Table 2.3. (cont.)

	Location of Sample	Sample	Definition
N12			Mortar from the arch constructed of bricks <i>Bath</i>
N13			Mortar from the arch constructed of stones <i>Bath</i>
N16			Mortar from the wall comprised of mortared rubble throughout <i>Water basin</i>

(cont. on next page)



Table 2.3. (cont.)


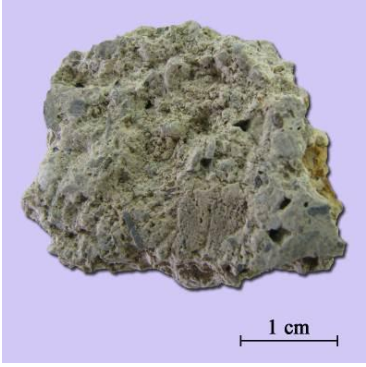



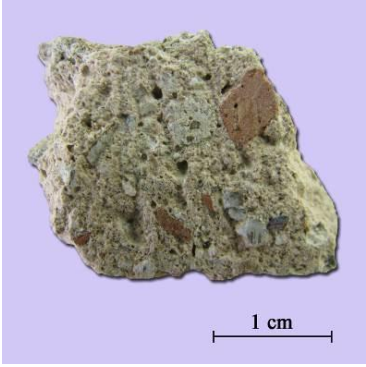

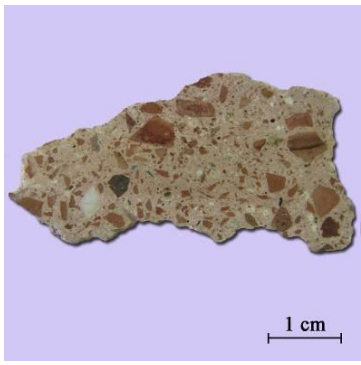

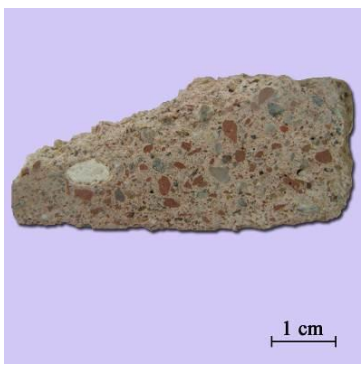

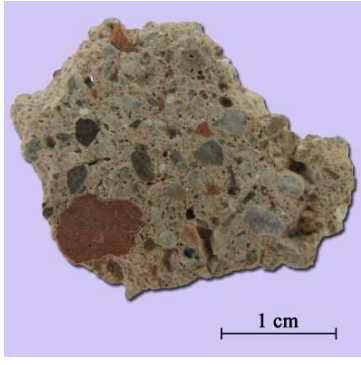

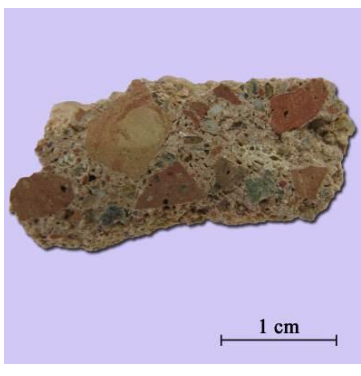
	Location of Sample	Sample	Definition
N17			Mortar from the footing comprised of mortared rubble throughout <i>Bridge</i>
N21			Mortar from the wall comprised of mortared rubble throughout <i>Bridge</i>
N23			Mortar from the wall comprised of mortared rubble throughout <i>Cistern</i>




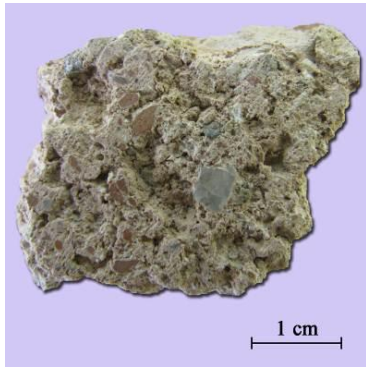




Table 2.4. Lime mortars and plasters with artificial pozzolans from Nysa

	Location of Sample	Sample	Definition
N1			Mortar used as paving on the podium <i>Theatre</i>
N2			Mortar from the wall comprised of mortared rubble throughout <i>Pool of the temple</i>
N5			Mortar from the wall comprised of mortared rubble throughout <i>Library</i>
N6			Mortar used as supporting for mosaics <i>Library</i>

(cont. on next page)


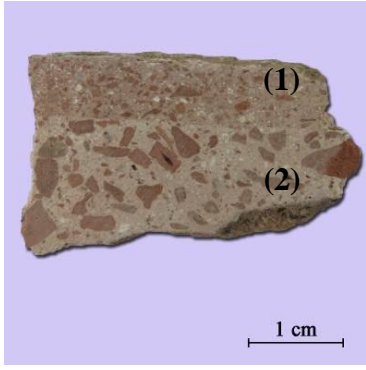



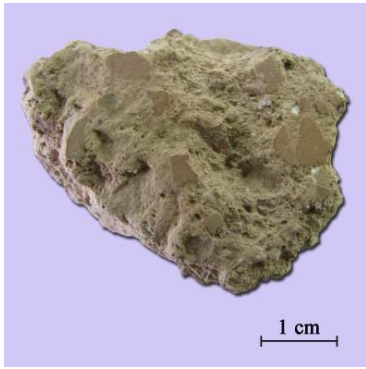




Table 2.4. (cont.)

	Location of Sample	Sample	Definition
N8			Plaster covering the wall surface <i>Library</i>
N9			Plaster covering the inner vault surface <i>Building (located on the west side of library)</i>
N11			Mortar from the west wall comprised of mortared rubble throughout <i>Library</i>
N14			Mortar used as supporting for the marble covering on the outer wall <i>Bath</i>

(cont. on next page)

Table 2.4. (cont.)

	Location of Sample	Sample	Definition
N15(1) – N15(2)			Plaster layers ((1) fine plaster, (2) rough plaster) covering the inner surface of the wall  <i>Water basin</i>
N20			Mortar used as supporting for the marble covering on the outer wall  <i>Water basin</i>
N22			Mortar from the arch constructed of stones  <i>Cistern</i>
N24			Plaster covering the inner surface of the wall  <i>Cistern</i>

## 2.2. Experimental Studies

Experimental studies covered determination of the following properties:

- Basic physical properties (density, porosity)
- Drying rates of mortars
- Raw material compositions (lime/aggregate ratios and particle size distribution of aggregates)
- Quantitative determination of CaCO<sub>3</sub> and SiO<sub>2</sub> content in the binders
- Mineralogical and chemical compositions of binders, aggregates, lime lumps
- Microstructural properties of binders, aggregates, lime lumps
- Hydraulic properties of mortars
- Pozzolanic activities of aggregates

### 2.2.1. Determination of Basic Physical Properties

Bulk density and porosity values describe the basic physical properties of material. Basic physical properties were determined by standard test methods (RILEM 1980). Density is the ratio of the mass to its bulk volume and is expressed in grams per cubic centimeters (g/cm<sup>3</sup>). Porosity is the ratio of the pore volume to the bulk volume of the sample, and is usually expressed in percent (%).

Measurement of density and porosity was carried out on two specimens of each sample. First, samples were dried in an oven at low temperatures (40°C) for at least 24 hours. Then they were weighed by a precision balance (AND HF-3000G) to determine their dry weights ( $M_{dry}$ ). Subsequently, they were entirely saturated with distilled water in a vacuum oven (Lab-Line 3608-6CE Vacuum Oven). The saturated weights ( $M_{sat}$ ) and the Archimedes weights ( $M_{arch}$ ) were determined with hydrostatic weighing in distilled water by using the precision balance. Bulk densities (D) and porosities (P) of samples were calculated by using the formulas given below:

$$D \text{ (g/cm}^3\text{)} = M_{dry} / (M_{sat} - M_{arch}) \quad (2.1)$$

$$P \text{ (%) } = [(M_{sat} - M_{dry}) / (M_{sat} - M_{arch})] \times 100 \quad (2.2)$$

where;

D : Density ( $\text{g/cm}^3$ )       $M_{\text{dry}}$  : Dry weight (g)       $M_{\text{sat}} - M_{\text{dry}} = \text{Pore volume (g)}$   
P : Porosity (%)       $M_{\text{sat}}$  : Saturated weight (g)       $M_{\text{sat}} - M_{\text{arch}} = \text{Bulk volume (g)}$   
 $M_{\text{arch}}$  : Archimedes weight (g)

### 2.2.2. Determination of Drying Rates of Mortars

Two specimens of mortars of approximately 50-60 g. and 30x30x30 mm. with prismatic shapes were used to determine the drying rates. Drying rates of 12 mortar samples could be determined since the dimensions of the rest of mortars were not enough to carry out this experiment.

Samples were dried in an oven at 50 °C for 48 hours to constant weight. Then, they were saturated with distilled water in a vacuum oven (Lab-Line 3608-6CE Vacuum Oven) for 24 hours. Their dry ( $M_{\text{dry}}$ ) and saturated weights ( $M_{\text{sat}}$ ) were measured by a precision balance (AND HF-3000G). After measuring their saturated weights, they were left for drying at room conditions that have approximately 27° and 45 % relative humidity. The weight losses of samples were followed by weight measurements ( $M_{\text{wet}}$ ) at certain time intervals of 15-30-60 minutes, 2-3-4 hours and 2-3 days subsequently.

The drying rate is indicated as the density of vapor flow rate (g) evaporated from the surface of the sample and it is calculated as a function of average moisture content (M) for each time span versus surface area of the sample by using the following formula (RILEM 1980):

$$g \text{ (kg / m}^2 \cdot \text{s)} = M / (A \times t) \quad (2.3)$$

where;

g : Density of flow rate

M : Moisture content of the sample (kg) at the time t

A : Total surface of the area of the prismatic test specimen ( $\text{m}^2$ )

t : Time span (second)



M (moisture content of the sample) is calculated by using dry, wet and saturated weights of samples:

$$M = (M_{\text{wet}} - M_{\text{dry}}) / (M_{\text{sat}} - M_{\text{dry}}) \quad (2.4)$$

where;

$M_{\text{sat}}$  : Saturated weight (kg)

$M_{\text{dry}}$  : Dry weight (kg)

$M_{\text{wet}}$  : Wet weight (kg) at a certain time

### 2.2.3. Determination of Raw Material Compositions

Raw material composition analyses were carried out in order to determine lime-aggregate ratios and the particle size distributions of the aggregates. The amount of lime and aggregate used in the preparation of the mortars were determined after the dissolution of carbonated lime in dilute hydrochloric acid (Jedrzejewska 1981). Determination of the particle size distributions of the aggregates were carried out by sieve analyses.

Two specimens from each sample were dried in an oven and weighed ( $M_{\text{sam}}$ ) by a precision balance. Then the dried samples were left in a dilute hydrochloric acid (%5) solution until the carbonated lime dissolved entirely. Insoluble part was filtered, washed with distilled water, dried in an oven and weighed by a precision balance ( $M_{\text{agg}}$ ). Ratios of acid soluble and insoluble parts were calculated by the following formulas:

$$\text{Insoluble \%} = [(M_{\text{sam}} - M_{\text{agg}}) / (M_{\text{sam}})] \times 100 \quad (2.5)$$

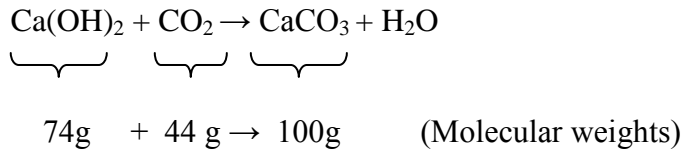
$$\text{Acid Soluble \%} = 100 - \text{Insoluble \%} \quad (2.6)$$

where;

$M_{\text{sam}}$  = Dry weight of the sample (g)

$M_{\text{agg}}$  = Dry weight of the aggregates (g)

Acid soluble ratio does not give the exact lime ratio, since it is calculated with the dissolved carbonated lime ( $\text{CaCO}_3$ ). The lime ratio must be calculated according to the lime ( $\text{Ca(OH)}_2$ ) which had been used during the production process of mortars.



Lime transforms into carbonated lime when it reacts with carbon dioxide ( $\text{CO}_2$ ) in the atmosphere. According to the molecular weights as shown in the equation above, 100 gram carbonated lime derives from 74 gram lime. Therefore, lime/aggregate ratio was calculated as following:

$$\text{Aggregate \%} = (100 \times \text{Insoluble}) / [((\text{Acid Soluble \%} \times \text{M.W.}_{\text{Ca(OH)}_2}) / \text{M.W.}_{\text{CaCO}_3}) + \text{Insoluble \%}] \quad (2.7)$$

$$\text{Lime \%} = 100 - \text{Aggregate \%} \quad (2.8)$$

where;

$\text{M.W.}_{\text{CaCO}_3}$  = Molecular weight of  $\text{CaCO}_3$  which is 100.

$\text{M.W.}_{\text{Ca(OH)}_2}$  = Molecular weight of  $\text{Ca(OH)}_2$  which is 74.

Determination of particle size distributions of aggregates was carried out by sieving them through a series of sieves (Retsch mark) having the sieve sizes of 53  $\mu\text{m}$ , 125  $\mu\text{m}$ , 250  $\mu\text{m}$ , 500  $\mu\text{m}$ , 1180  $\mu\text{m}$  by using an analytical sieve shaker (Retsch AS200). Particles remained on each sieve surface were weighed by a precision balance and their percentages were calculated.

#### **2.2.4. Quantitative Determination of CaCO<sub>3</sub> and SiO<sub>2</sub> Content in the Binders**

Fine mortar matrices (< 63 μm) composed of small grain sized silica and carbonated lime called “binder” was considered as the main part that gave high strength to mortars (Bakolas et al. 1995, Middendorf et al. 2005). Mineralogical compositions of binders constituted of many studies to define the mortar characteristics (Bakolas et al. 1995, Barba et al. 2009, Miriello et al. 2011). In this study, a relatively fast and easy method for the quantitative determination of CaCO<sub>3</sub> and SiO<sub>2</sub> content in binder compositions is proposed by using FTIR, LIBS, SEM-EDS and XRD analyses.

For this purpose, a series of standard mixtures of CaCO<sub>3</sub> (Carlo Erba 327059 ) and SiO<sub>2</sub> (Sigma-Aldrich S5631) were prepared in ten combinations of varying weight ratios from 0.5 to 5.0, to generate calibration curves for FTIR, SEM-EDS, XRD and LIBS analysis. These ratios are nearly equivalent to CaCO<sub>3</sub>/SiO<sub>2</sub> ratios that are usually found within the compositions of the binders of the historic mortars (Jackson et al. 2009, Miriello et al. 2010, Miriello et al. 2011). The samples were prepared by gently mixing the stoichiometric proportions of two components in an agate mortar.

The methods proposed by FTIR, LIBS, SEM-EDS, XRD analysis were applied on eight mortar samples produced by using natural pozzolans (A1, A2, A3, A7, N4, N10, N12, N13). For the XRD, FTIR, SEM-EDS and LIBS analyses, mortar matrices, which are free from coarse grained aggregates, were gently ground into powder form and then sieved to obtain a less than 1/16 mm diameter fraction (Miriello 2010, Miriello 2011). XRD, SEM-EDS, FTIR and LIBS analysis were then carried out for the prepared binder samples to find out the weight ratios of CaCO<sub>3</sub> to SiO<sub>2</sub> by using calibration equations obtained from standard mixture analyses.

For FTIR analysis, a few milligram of standard mixtures and the powdered binders of the Roman mortar samples were dispersed in about 80 milligram of spectral grade potassium bromide (KBr) and pressed into pellets under 10 tons/cm<sup>2</sup> pressure. Spectral measurements were carried out on a Spectrum BX II FTIR spectrometer (Perkin Elmer) that was operated in the absorbance mode. Spectra were normally acquired with the use of 4 cm<sup>-1</sup> resolution yielding IR traces over the range of 400 to 4000 cm<sup>-1</sup>. All data were corrected for pure KBr spectrum. Three measurements were taken for each sample. The average of the three measurements was used for preparing the calibration curve. The area of the absorbance peaks of CaCO<sub>3</sub> at 1432 cm<sup>-1</sup> and

SiO<sub>2</sub> at 1100 cm<sup>-1</sup> were used to plot calibration curves against their standard weight ratios. The areas of the same peaks were also calculated for the binders to determine CaCO<sub>3</sub>/ SiO<sub>2</sub> content by using the calibration curve.

SEM-EDS analyses were carried out on pellets prepared by pressing powder samples under 10 tons/cm<sup>2</sup> pressures. Philips XL 30S FEG Scanning Electron Microscope (SEM) coupled with X-Ray Energy Dispersive System (EDS) was used. Analyses were carried out on three different 0.63 mm<sup>2</sup> areas of the pellets. The average of the three results was used for preparing the calibration curve and the calculations of the weight ratios of CaCO<sub>3</sub> to SiO<sub>2</sub> in the binders of the mortar samples.

The elemental compositions of the standard mixtures and the binders of the mortars samples were determined by LIBS. For this analysis, pressed powder pellets were used. LIBS analyses were performed by measuring the spectral line intensities of the neutral calcium and silicon emitted from the plasma produced by a Q-switched Nd:YAG laser. Each data is produced by the addition of ten consecutive single laser pulses. Plasma emission was detected by an echelle type spectrograph (200-850 nm spectral range) equipped with an ICCD detector.

XRD patterns of the standard mixtures and the powdered binders of the Roman mortars were obtained by using a Philips X-Pert Pro X-ray Diffractometer. The instrument was operated with CuK $\alpha$  radiation with Ni filter adjusted to 40 kV and 40mA in the range of 2-60° with a scan speed of 1.6° per minute. The Rietveld method was used to quantify the CaCO<sub>3</sub> and SiO<sub>2</sub> content in the standard mixtures and in the binders of the mortar samples by using X'Pert High Score Plus analysis software. The weight ratios of CaCO<sub>3</sub> to SiO<sub>2</sub> found by Rietveld method were used to generate a calibration curve.

### **2.2.5. Mineralogical and Chemical Compositions**

Mineralogical compositions of binders, pozzolans used as aggregates and lime lumps were determined by X-ray diffraction (XRD). XRD analyses were carried out by using a Philips X-Pert Pro X-ray Diffractometer. The instrument was operated with CuK $\alpha$  radiation with Ni filter adjusted to 40 kV and 40mA in the range of 2-60° with a scan speed of 1.6° per minute. The analyses were performed on finely ground samples



less than 53  $\mu\text{m}$ . The Philips X'Pert Graphics and Identity software program was used to identify the mineral phases in each X-ray diffraction spectrum.

Chemical compositions of binders and lime lumps were determined by Scanning Electron Microscope (SEM) coupled with X-Ray Energy Dispersive System (EDS). SEM-EDS analyses were performed by a Philips XL 30S FEG on pellets of binders prepared by pressing powder samples under 10 tons/cm<sup>2</sup> pressures. Results were taken from three different areas of samples and the averages of results were used to determine the chemical compositions. SEM-EDS analyses of lime lumps were performed on broken surfaces of mortar samples.

### **2.2.6. Chemical Compositions of Pozzolans**

Major, minor and trace element compositions of pozzolans were assessed by X-ray fluorescence spectroscopy (XRF). XRF analyses were carried out by a Spectro IQ II on melt tablets of powdered samples < 53  $\mu\text{m}$  diluted with lithium tetraborat.

Results of XRF analyses of were evaluated through hierarchical clustering which is a useful methodology that helps distinguishing the samples which have similar characteristics from those which instead have far different values. Hierarchical clustering was implemented for oxides (CaO, SiO<sub>2</sub>, TiO<sub>2</sub>, Al<sub>2</sub>O<sub>3</sub>, Fe<sub>2</sub>O<sub>3</sub>, MgO, Na<sub>2</sub>O, K<sub>2</sub>O) constituting major chemical compositions of pozzolans in order to determine whether or not these oxides can generate a cluster of samples with similar values. For this purpose, a distance measure using “Average Linkage Method” and the “Euclidean distance” were employed by using Stata Data Analysis and Statistical Software.

T-test, Anova, Kruskal Wallis and Mann-Whitney tests were implemented to the results obtained as a result of hierarchical clustering in order to control results from an inferential point of view by using EViews 4.1 Software. The reason for using several tests to control the results was to check the robustness of the results.

### **2.2.7. Pozzolanic Activities of Aggregates**

Pozzolanic activities of aggregates were determined by following the reaction between lime and aggregates. The differences in electrical conductivities (mS/cm) before and after the addition of fine aggregates (less than 53  $\mu\text{m}$ ) into saturated calcium

hydroxide solution with a ratio of 1g./40 ml. were measured (Luxán et al. 1989) after two minutes. Electrical conductivity differences more than 2 mS/cm reveal good pozzolanicity (Luxán et al. 1989).

### **2.2.8. Hydraulic Properties of Mortars**

Hydraulic properties of mortars were established by determination of the percentages of the weight losses of binders between 200-600 °C and 600-900 °C by using Shimadzu TGA-21. Weight losses between 200 and 600 °C were mainly due to the loss of chemically bound water of hydraulic products, and weight losses between 600 and 900 °C were due to the loss of carbon dioxide (CO<sub>2</sub>) released during the decomposition of carbonated lime (Bakolas et al. 1998, Moropoulou et al. 2000). The mortars can be accepted as hydraulic when the ratio of CO<sub>2</sub>/ chemically bound water was lower than 10 (Bakolas et al. 1998, Moropoulou et al. 2000).

### **2.2.9. Microstructural Properties**

The morphologies and microstructures were determined by using Philips XL-30-SFEG Scanning Electron Microscope (SEM) coupled with X-Ray Energy Dispersive System (EDS). SEM-EDS analyses were mainly based on the investigation of microstructural properties of pozzolans, characteristics of pozzolan-binder interfaces and general microstructure of mortars. The analyses were performed on powder samples of pozzolans, and broken and polished surfaces of mortar samples by using secondary electron (SE), backscattered electron (BSE) modes at different magnifications.

## CHAPTER 3

### RESULTS AND DISCUSSIONS

Basic physical properties, raw material compositions, mineralogical and chemical compositions, microstructural and hydraulic properties of Roman lime mortars of Aigai and Nysa; and mineralogical and chemical compositions, microstructural properties and pozzolanic activities of natural and artificial pozzolans used as aggregates in these mortars were determined by standard test methods, XRF, XRD, SEM-EDS and TGA analyses. XRF analyses of pozzolans used as aggregates were evaluated through hierarchical clustering analyses and statistical tests. Also, a new method was developed for the quantitative determination of carbonated lime ( $\text{CaCO}_3$ ) and silica ( $\text{SiO}_2$ ) content in the binder parts of the mortars by using SEM-EDS, FTIR, XRD and LIBS. This chapter presents the results and the discussions of the analyses.

#### 3.1. Basic Physical Properties

Basic physical properties of mortars could be described by density and porosity values. Density values of mortars produced by using natural pozzolans were in the range of 1.40-1.74  $\text{g/cm}^3$  for Aigai samples and 1.39-1.91  $\text{g/cm}^3$  for Nysa samples (Figure 3.1, Appendix A). Density values of mortars produced by artificial pozzolans were between 1.44-1.63  $\text{g/cm}^3$  in Aigai and 1.10-1.77  $\text{g/cm}^3$  in Nysa (Figure 3.1, Appendix A). Density values of both types of mortars from Aigai were almost similar to each other where density values of mortars with natural pozzolans were higher than mortars with artificial pozzolans in Nysa samples.

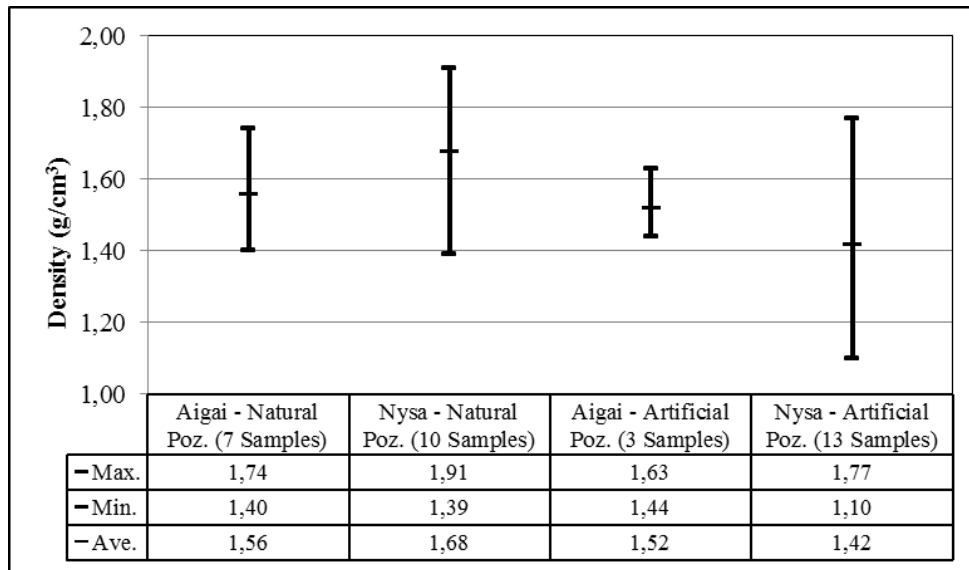


Figure 3.1. Density values of Roman lime mortars

Porosity values of mortars with natural pozzolans were between 28.84-41.96 % in Aigai, and between 24.97-44.55 % in Nysa by volume respectively (Figure 3.2, Appendix A). Porosity values of mortars consisted of artificial pozzolans ranged between 33.50-42.33 % for Aigai, and between 25.59-55.55 % for Nysa by volume respectively (Figure 3.2, Appendix A). According to the results, lime mortars produced from artificial pozzolans used in Nysa were found as more porous than the other types of mortars.

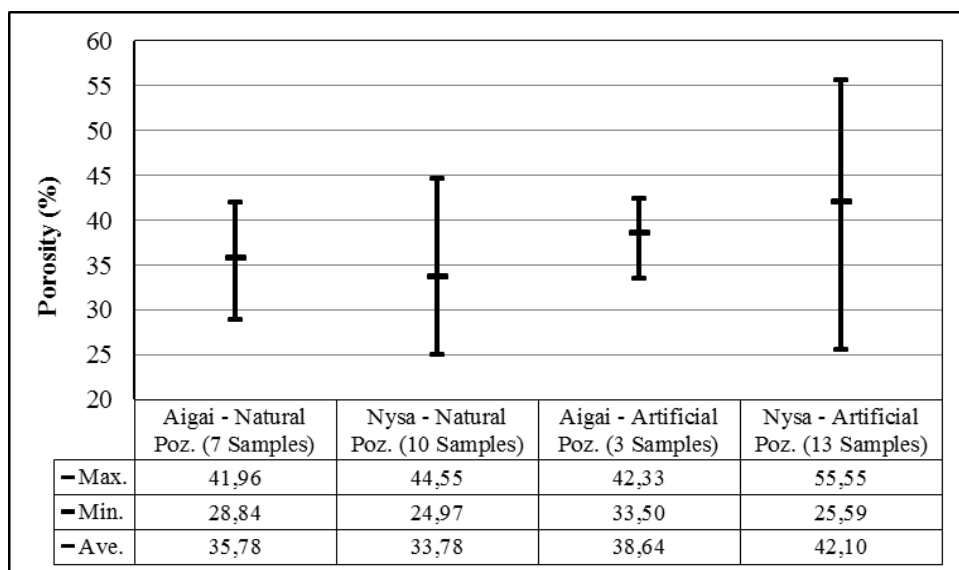


Figure 3.2 Porosity values of Roman lime mortars

Evaluation of basic physical properties of mortars according to their different uses in the structure revealed that mortars used in the construction of walls comprised of rubble stones or ashlar throughout were slightly more dense and low porous compared to the other mortar types (Table 3.1). Density values of mortars used for the rubble cores of the walls and also for arches and vaults were similar to each other; and a few lower than those used for walls comprised of mortared rubble or ashlar throughout (Table 3.1). Plasters used on inner and outer surfaces of walls, and mortars used as supporting for coverings and mosaics had lower density and higher porosity values than all of the other mortar types (Table 3.1). This could be explained by the use of higher amounts of lime in the plasters compared to the mortars.

Table 3.1. Basic physical properties of Roman lime mortars used for different purposes

<b>Use of Mortar</b>	<b>Density (g/cm<sup>3</sup>)</b>	<b>Porosity (% by vol.)</b>
Rubble core of the wall (A2, A3, A10, A12)	1.41 - 1.72	31.05 - 40.29
Wall - Mortared rubble throughout (N2, N3, N4, N5, N7, N11, N16, N17, N21, N23)	1.39 - 1.84	24.79 - 44.55
Wall - Mortared ashlar throughout (A1, A7)	1.58 - 1.74	28.84 - 36.12
Arch, Vault (A6, N10, N12, N13, N22)	1.10 - 1.91	24.97 - 55.55
Supporting for coverings, mosaics (A9, A11, N1, N6, N14, N20)	1.23 - 1.63	33.50 - 50.84
Plaster (A5, N8, N9, N15(1), N15(2), N24)	1.23 - 1.44	39.90 - 49.18

Density and porosity values of Roman lime mortars from Aigai and Nysa were almost in the same ranges with lime mortars used in several Roman period buildings located in Bergama (Turkey) (Özkaya and Böke 2009), Rome (Italy) (Sánchez-Moral et al. 2005, Jackson et al. 2009, Jackson et al. 2011), Slovenia (Kramar et al. 2011) and Tunisia (Farci et al. 2005) (Table 3.2). This observation revealed that Roman lime mortars used in different regions were manufactured by using similar raw materials with similar preparation techniques; thus affecting the density and porosity values to be similar to each other.

Table 3.2. Basic physical properties of Roman lime mortars determined by previous studies

<b>Roman Building/Site (Reference)</b>	<b>Aggregate Type of Mortar</b>	<b>Density (g/cm<sup>3</sup>)</b>	<b>Porosity (%)</b>
Saint Callistus and Domitilla catacombs - Rome (Italy) <i>(Sánchez-Moral et al.2005)</i>	Natural poz.	-	39 – 42
The Markets of Trajan - Rome (Italy) <i>(Jackson et al. 2009)</i>	Natural poz.	1.43 – 1.79	-
Serapis Temple - Bergama (Turkey) <i>(Özkaya and Böke 2009)</i>	Natural poz.	1.5	36
The Theatre of Marcellus - Rome (Italy) <i>(Jackson et al. 2011)</i>	Natural poz.	1.80	-
Cisterns - Uthina (Tunisia) <i>(Farci et al. 2005)</i>	Artificial poz.	1.5 - 1.7	24.2 - 44.3
Roman villa - Mošnje (Slovenia) <i>(Kramar et al. 2011)</i>	Artificial poz.	2.47 - 2.78	23.9 - 49.7

### 3.2. Drying Rates

The drying rates of mortars are described by the density of vapor flow rate (g) evaporated from the surface of the sample for specific time spans. Results of the analyses performed on 12 mortar samples reveal that, ~50 % adsorbed water inside the pores evaporated within 30 minutes (Figure 3.3, Appendix B). This may indicate that macro pores have a high percent in the total porosity of mortars which allowed evaporation to be faster. The higher percent of macro pores ( $r > 2.5 \mu\text{m}$ ) also led the Roman lime mortars to be less susceptible to freeze-thaw and salt crystallization cycles (Carretero et al. 2002, Cultrone et al. 2004). Further investigation for the determination of exact pore distribution of Roman lime mortars could be carried out by using Mercury Intrusion Porosimetry.

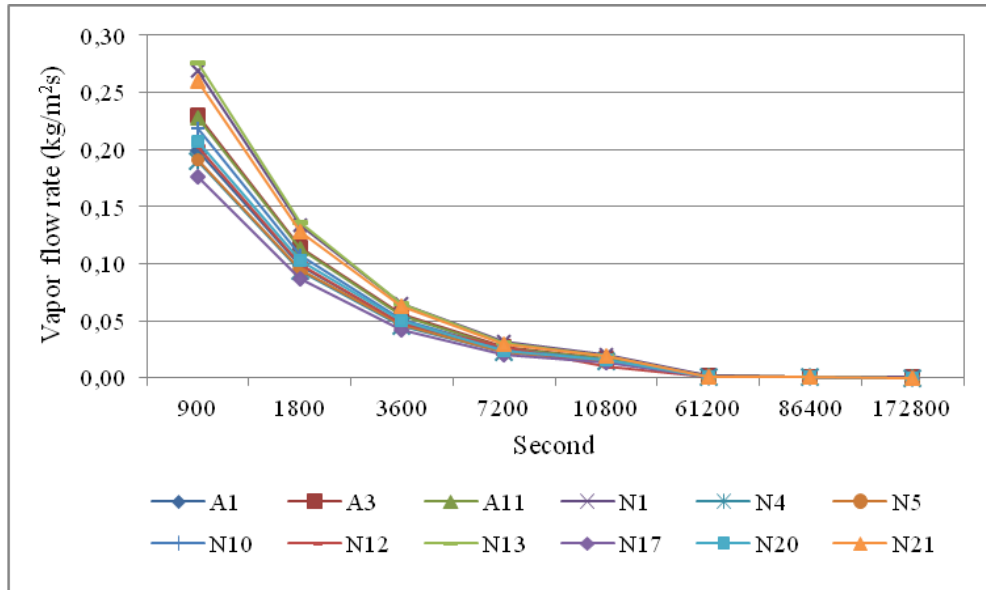


Figure 3.3. Drying rates of Roman lime mortars

### 3.3. Raw Material Compositions

Raw material compositions of lime mortars were defined by lime/aggregate ratios and particle size distribution of aggregates. Lime/aggregate ratios of mortars produced by natural pozzolans were found between 0.19-0.36 in Aigai mortars, and between 0.22-0.64 in Nysa mortars (Figure 3.4, Appendix C). Mortars produced by artificial pozzolans had lime/aggregate ratios in the range of 0.21-1.19 in Aigai mortars and 0.24-0.89 in Nysa mortars (Figure 3.4, Appendix C). These results revealed that lime/aggregate ratios of mortars produced by using natural pozzolans were lower than mortars produced by artificial pozzolans. This could be explained by the dissolution of acid soluble calcareous aggregates as a result of the method used for the determination of raw material compositions depended on the dissolution of carbonate particles in dilute acid.

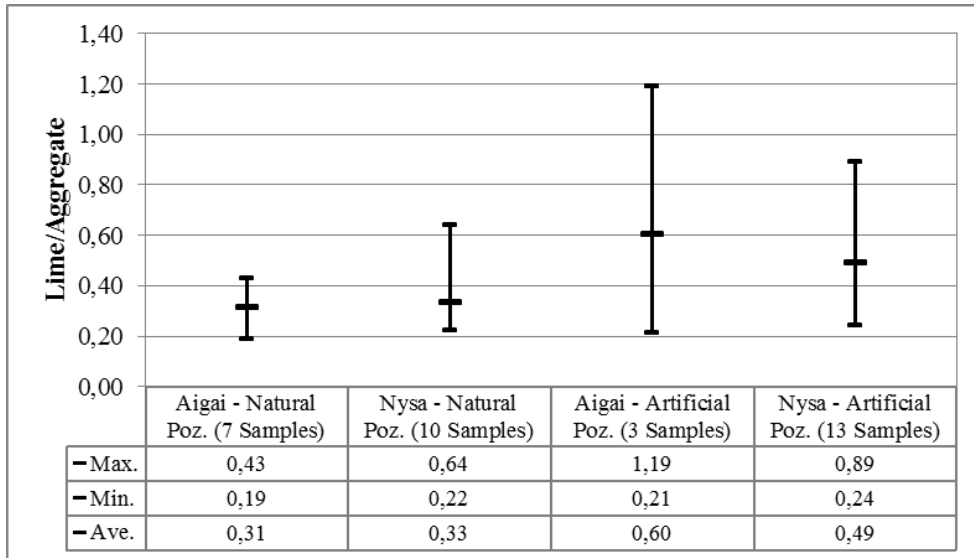


Figure 3.4. Lime/aggregate ratios of Roman mortars

Aggregates which had particle sizes greater than 1180  $\mu\text{m}$  constituted the major fraction that ranged between 11.2-65.1 % of total aggregates in all mortar samples (Figure 3.5, Appendix D).

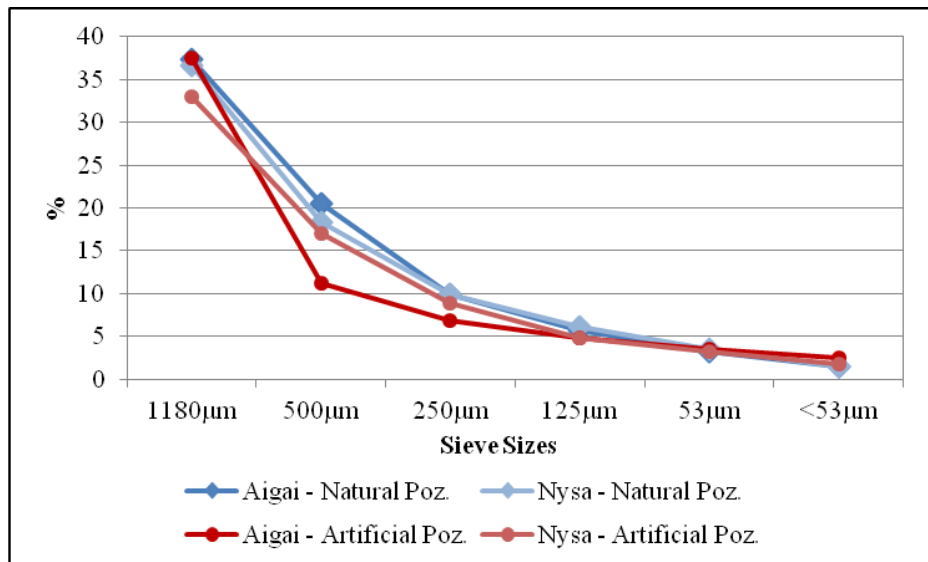


Figure 3.5. Particle size distributions of aggregates of Roman mortars

Raw material compositions of mortars were found almost similar to each other when compared according to their uses within the structure although there were slight differences between them. Lime/aggregate ratio values of mortars used for wall



constructions, arches and vaults and supporting for coverings and mosaics were very close to each other, but lower than plasters (Table 3.3, Appendix C). The fraction of aggregates with particle sizes greater than 1180  $\mu\text{m}$  was identified to be highest in the mortars used as supporting for coverings and mosaics (Table 3.3, Appendix D).

Table 3.3. Raw material compositions of Roman lime mortars used for different purposes

<b>Use of Mortar</b>	<b>Lime/Aggregate Ratio</b>	<b>Aggregates &gt;1180 <math>\mu\text{m}</math>. (% wt.)</b>
Rubble core of the wall (A2, A3, A10, A12)	0.19 - 0.33	18.5 - 45.1
Wall - Mortared rubble throughout (N2, N3, N4, N5, N7, N11, N16, N17, N21, N23)	0.22 - 0.64	13.3 - 41.0
Wall - Mortared ashlar throughout (A1, A7)	0.26 - 0.28	27.9 - 44.6
Arch, Vault (A6, N10, N12, N13, N22)	0.24 - 0.49	11.2 - 45.5
Supporting for coverings, mosaics (A9, A11, N1, N6, N14, N20)	0.21 - 0.62	30.4 - 65.1
Plaster (A5, N8, N9, N15(1), N15(2), N24)	0.41 - 0.89	18.6 - 42.9

Lime/aggregate ratios of Roman lime mortars produced by natural or artificial pozzolans from Aigai and Nysa were similar to the lime/aggregate ratio values of lime mortars from different Roman period buildings in Turkey (Degryse et al. 2002, Özkaya and Böke 2009), Italy (Benedetti et al. 2004, Sánchez-Moral et al. 2005), and Spain (Benedetti et al. 2004, Franquelo et al. 2008, Robador et al. 2010) (Table 3.4). These values also resembled the lime/aggregate ratios given in the historic sources written in the Roman period (Table 1.1). Aggregates with sizes greater than 1180  $\mu\text{m}$  were also determined as the largest fraction by the recent studies (Degryse et al. 2002, Benedetti et al. 2004, Sánchez-Moral et al. 2005, Özkaya and Böke 2009, Robador et al. 2010) (Table 3.4). These results revealed that the use of raw materials in the production of Roman lime mortars were nearly same in different locations of Central Roman Empire and its provinces including Spain and Anatolia.

Table 3.4. Raw material compositions of Roman lime mortars determined by previous studies

Roman Building/Site (Reference)	Aggregate Type of Mortar	Lime/Aggregate	Particle Size Distributions of Aggregates	
Saint Callistus and Domitilla catacombs - Rome (Italy) ( <i>Sánchez-Moral et al. 2005</i> )	Natural poz.	0.5/1 - 1.1/1	The largest fraction	0.5 - 2 mm 100 - 300 $\mu\text{m}$
Serapis Temple - Bergama (Turkey) ( <i>Özkaya and Böke 2009</i> )	Natural poz.	1/4	The largest fraction	> 1180 $\mu\text{m}$
Sagalassos - Turkey ( <i>Degryse et al. 2002</i> )	Natural poz.	45 % / 55 %	< 4.74 mm: 3.87 % < 4 mm :30.58 % < 2 mm: 25.61 % < 1 mm: 14.09 % < 500 $\mu\text{m}$ : 11.42 % < 250 $\mu\text{m}$ : 8.82 % < 125 $\mu\text{m}$ : 5.64 % < 63 $\mu\text{m}$ : -	
	Artificial poz.	65 % / 35 %		
	Natural poz.+ Artificial poz.	40 % / 20 % / 20 %		
Roman Villa in Sorrento of Pollio Felice - (Naples) (Italy) ( <i>Benedetti et al. 2004</i> )	Artificial poz.	30-65 % / 35-70 %	< 0.1 mm: 30 % 0.1 – 0.5 mm: 35 % > 0.5 mm: Few	
The Forum and residences of Pollentia - Mallorca (Spain) ( <i>Genestar et al. 2006</i> )	Natural poz.	2 - 5	-	
	Artificial poz.	0.5 - 2.5	-	
Mithraeum House - Spain ( <i>Robador et al. 2010</i> )	Artificial poz	24.2-25.5 % (lime) / 19-24.3 % (brick) / 46.1 % (sand)	1 - 2 mm: 24.16 % 0.595 - 1mm: 13.97 % 0.420 - 0.595 mm: 32.13 % 0.320 - 0.420: 13.52 %	
Mithraeum House - Spain ( <i>Franquelo et al. 2008</i> )	Artificial poz.+sand	1 (lime) / 1.5-1.8 (brick) / 1 (sand)	-	

### 3.4. Characteristics of Lime Used in Mortars

Small, white, round and soft fragments found in the mortars called as “lime lump” were accepted to be representing the lime used in the production of mortars, and having the same chemical composition with the raw material (Bakolas et al. 1995, Bruni et al. 1997, Barba et al. 2009).

Lime lumps (Figure 3.6) were observed in mortar samples as a result of a poor labor and mixing used in their production. Mineralogical and chemical compositions and microstructural properties of lime lumps (*A1*, *A6*, *A12*, *N13*, *N17*) were determined by XRD and SEM-EDS analysis in order to identify the characteristics of lime used in the production of Roman lime mortars.

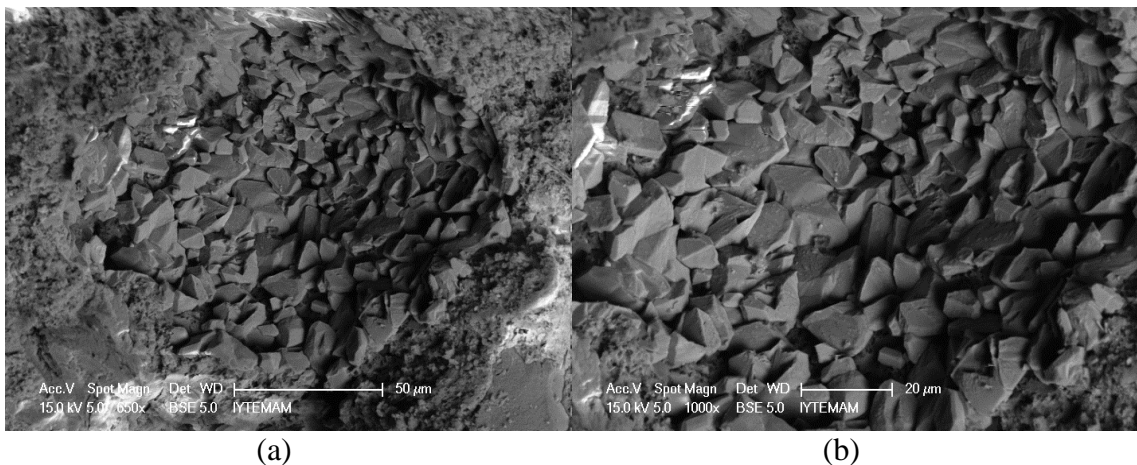


Figure 3.6 SEM-EDS images of white lump consisted of calcite crystals within the mortar matrix of N13 at magnifications of 650x (a) and 1000x (b)

In the XRD patterns of lime lumps from Aigai and Nysa, only sharp calcite peaks derived from carbonated lime were detected (Figure 3.7).

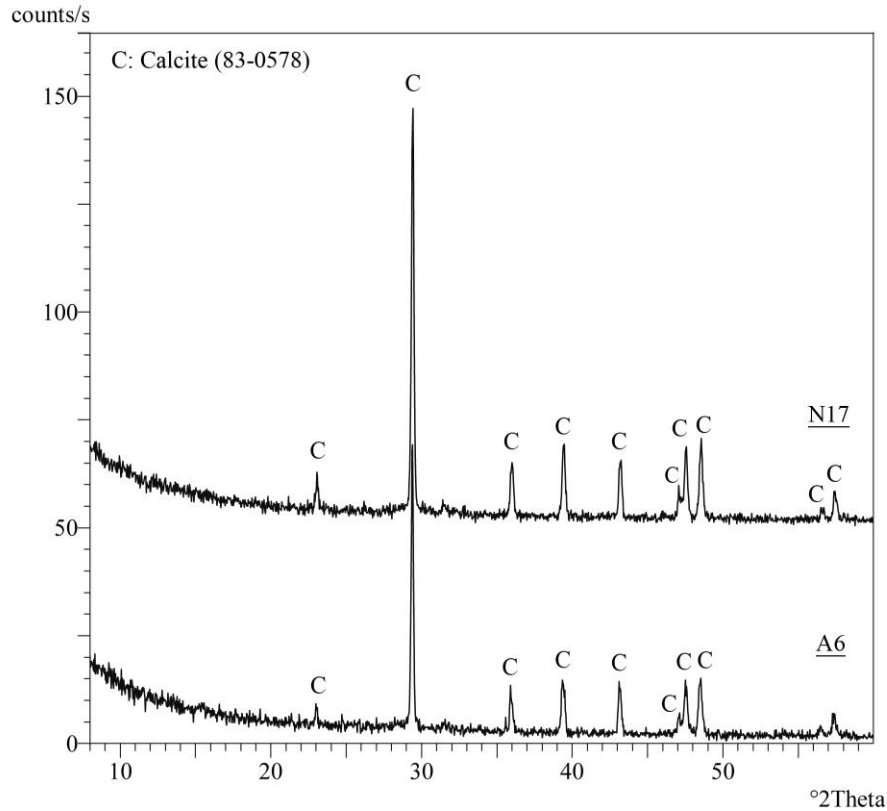


Figure 3.7. XRD patterns of lime lumps from Aigai and Nysa

SEM-EDS analysis revealed that lime lumps from binders of Aigai were composed of mainly CaO (91.0-100 %); and traces of SiO<sub>2</sub> (0.0-5.8 %), Na<sub>2</sub>O (0.0-3.0%), Al<sub>2</sub>O<sub>3</sub> (0.0-1.6 %), MgO (0-0.9 %) and P<sub>2</sub>O<sub>5</sub> (0.0-0.9 %). Similarly, lime lumps from binders of Nysa were composed of mainly CaO (89.0-91.8 %); and traces of SiO<sub>2</sub> (5.1-7.6 %), Na<sub>2</sub>O (0.0-0.3 %), Al<sub>2</sub>O<sub>3</sub> (0.7-3.0 %) and MgO (0-1.6 %).

Chemical compositions of lime lumps can be used to calculate their hydraulic (H.I.) and cementation indices (C.I.) in order to determine their hydraulic properties according to Boynton formula ((3.1), (3.2)) (Boynton 1980, Vicat 2003).

$$\text{H.I.} = (\% \text{Al}_2\text{O}_3 + \% \text{Fe}_2\text{O}_3 + \% \text{SiO}_2) / (\% \text{CaO} + \% \text{MgO}) \quad (3.1)$$

$$\text{C.I.} = (2.8 \% \text{SiO}_2 + 1.1 \% \text{Al}_2\text{O}_3 + 0.7 \% \text{Fe}_2\text{O}_3) / (\% \text{CaO} + 1.4 \% \text{MgO}) \quad (3.2)$$

Limes can be classified according to their hydraulic and cementation indices (Vicat 2003). The lower indices values showed less hydraulic character of lime (Table 3.5) (Vicat 2003).

Table 3.5. Classification of limes according to hydraulic and cementation indices

<b>Lime</b>	<b>Hydraulic Index</b>	<b>Cementation Index</b>
Non-hydraulic	< 0.1	< 0.3
Weakly hydraulic	0.1 - 0.2	0.3 - 0.5
Moderately hydraulic	0.2 - 0.4	0.5 - 0.7
Highly hydraulic	> 0.4	0.7 - 1.1

Hydraulic indices and cementation indices of lime lumps from binders of Aigai mortars were between 0.0-0.09 and 0.0-0.2. For lime lumps from binders of Nysa, hydraulic indices were between 0.06-0.1, and cementation indices were between 0.16-0.23. These results indicated that lime lumps of mortars from Aigai and Nysa could be classified as non-hydraulic.

Chemical compositions and hydraulic and cementation indices values of lime lumps of Roman lime mortars from Aigai and Nysa were found to be similar to the lime lumps used in the mortars of Kyme (Turkey) which were also non-hydraulic (Miriello et al. 2011) (Table 3.6).

Table 3.6. Chemical compositions and H.I. of lime lumps from Kyme mortars

<b>Chemical Composition (%)</b>										<b>H.I.</b>
<b>SiO<sub>2</sub></b>	<b>TiO<sub>2</sub></b>	<b>Al<sub>2</sub>O<sub>3</sub></b>	<b>Fe<sub>2</sub>O<sub>3</sub></b>	<b>MnO</b>	<b>MgO</b>	<b>CaO</b>	<b>Na<sub>2</sub>O</b>	<b>K<sub>2</sub>O</b>	<b>P<sub>2</sub>O<sub>5</sub></b>	
1.25-7.57	n.d.-0.23	1.03-3.05	n.d.-0.81	n.d.-0.32	0.67-2.41	84.07-94.07	0.11-1.97	n.d.-0.46	0.85-1.63	0.11-0.23

SEM-EDS images indicated that lime lumps were composed of micritic calcite crystals with sizes smaller than 5 µm (Figure 3.8). Small sized micritic calcite crystals may be formed as a result of long aging of lime putty which improved the plasticity and carbonation rate of lime (Rodriguez-Navarro et al. 1998). It may also show that lime

used in the Roman mortars was manufactured from porous limestones with firing temperatures around 900 °C (Moropoulou et al. 2001).

Results of XRD and SEM-EDS analyses of lime lumps revealed that non-hydraulic and high calcium lime comprised of small portlandite ( $\text{Ca}(\text{OH})_2$ ) crystals were used during the production of Roman lime mortars

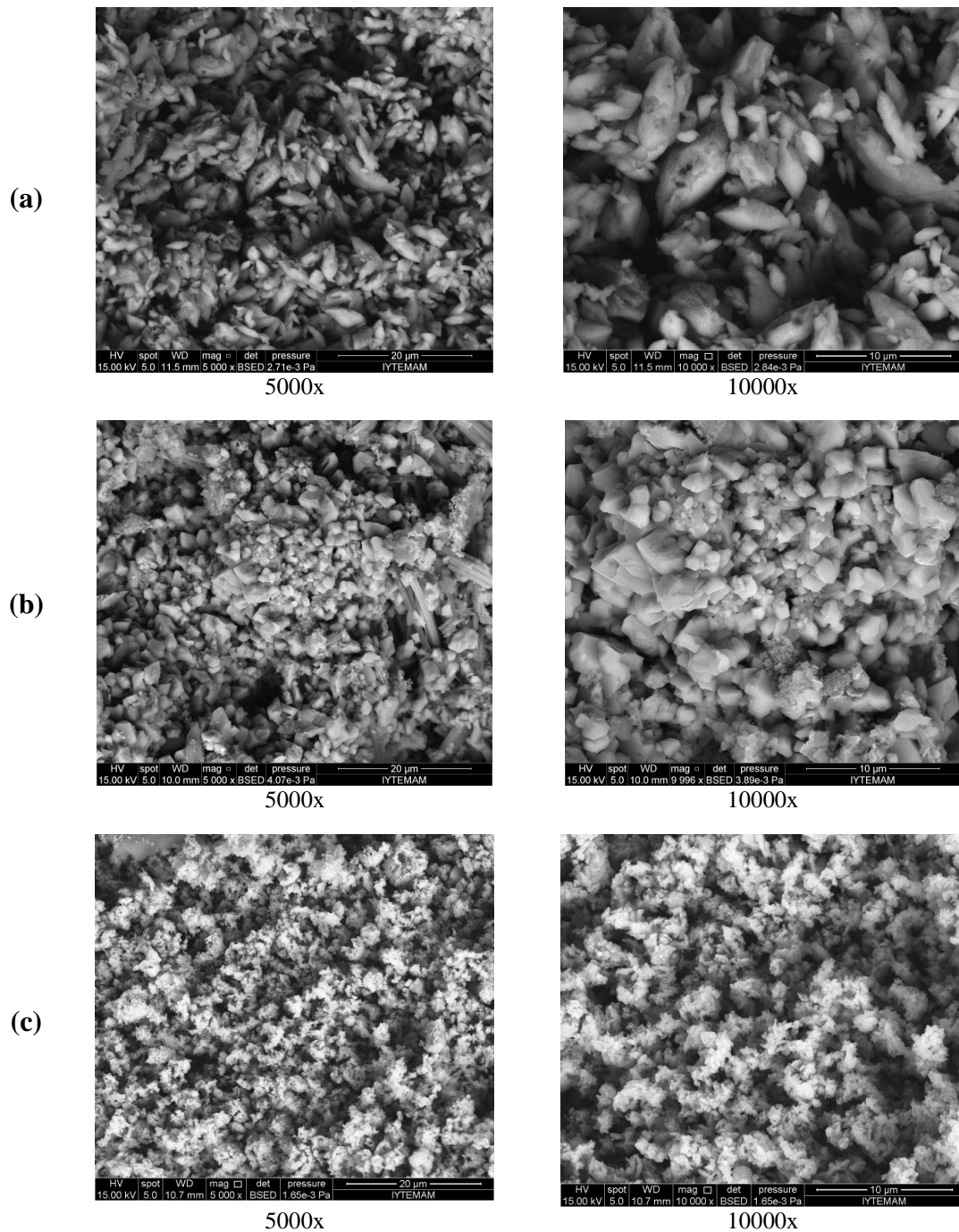


Figure 3.8. SEM-EDS images of calcite crystals of A6 (a), A12 (b), N17 (c)

### 3.5. Characteristics of Pozzolans

Pozzolanicity, mineralogical and chemical compositions and microstructural properties of fine pozzolanic aggregates (< 53  $\mu\text{m}$ ) were determined by electrical conductivity measurements, XRD, XRF and SEM-EDS analyses. Results of XRF analyses were evaluated by using statistical analyses.

#### 3.5.1. Pozzolanic Activities of Aggregates

Pozzolanicity of aggregates were investigated by measuring the electrical conductivity differences before and after the addition of fine aggregates (< 53  $\mu\text{m}$ ) into saturated calcium hydroxide solution. The electrical conductivity differences higher than 2 mS/cm revealed good pozzolanicity in this technique (Luxán et al. 1989).

Electrical conductivity differences of natural pozzolans were between 5.11-7.85 mS/cm in the lime mortars from Aigai, and between 3.25-6.02 mS/cm in the lime mortars from Nysa (Figure 3.9, Appendix E). Similarly, lime mortars produced by artificial pozzolans exhibited electrical conductivity differences between 3.50-6.69 mS/cm in Aigai samples, 3.25-8.09 mS/cm in Nysa samples (Figure 3.9, Appendix E). These results revealed that all pozzolans used as aggregate in the Roman lime mortars from Aigai and Nysa could be regarded as highly energetic.

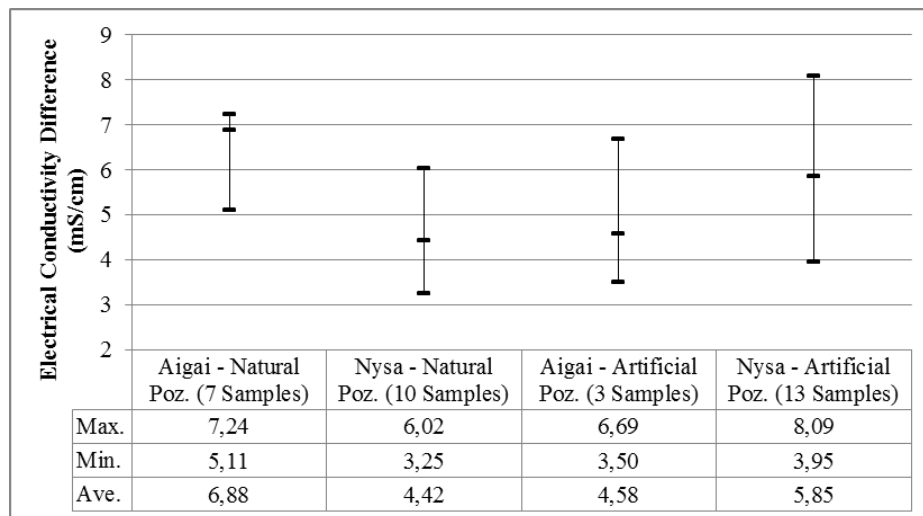


Figure 3.9. Electrical conductivity differences of aggregates of Roman lime mortars



### 3.5.2. Mineralogical Compositions of Pozzolans

Mineralogical compositions of pozzolans used as aggregates in the Roman lime mortars were determined by XRD analyses. XRD analysis revealed that natural pozzolans used in the mortars from Aigai were composed of quartz ( $\text{SiO}_2$ ), albite ( $\text{Na}(\text{AlSi}_3\text{O}_8)$ ), anorthite ( $\text{CaAl}_2\text{Si}_2\text{O}_8$ ) and muscovite ( $\text{KAl}_2(\text{Si}_3\text{Al})\text{O}_{10}(\text{OH},\text{F})_2$ ) (Figure 3.10). XRD patterns of natural pozzolans from lime mortars of Nysa indicated mainly quartz, albite, anorthite and muscovite minerals (Figure 3.11). Also, on XRD patterns of some samples (N3, N4, N12, N21) traces of phillipsite mineral were detected (Figure 3.11).

The peaks of pozzolanic minerals such as amorphous silicates with a diffuse band between  $20\text{-}30^\circ 2\theta$  were slightly observed on the XRD patterns of Aigai samples (Figure 3.10) but not detected on the XRD patterns of Nysa samples (Figure 3.11). This indicated higher amounts of amorphous silicates in Aigai pozzolans which could also be observed by their pozzolanicity values (Figure 3.9)

XRD analysis showed that artificial pozzolanic aggregates of lime mortars from Aigai were mainly composed of albite, anorthite and quartz (Figure 3.12). In addition to these minerals, muscovite was also identified on the XRD patterns of artificial pozzolanic aggregates of lime mortars from Nysa (Figure 3.13, 3.14).

XRD analyses were also used to predict the firing temperatures of artificial pozzolanic aggregates like crushed bricks and tiles. High firing temperatures exceeding  $900^\circ\text{C}$  results in damage in their amorphous structure and leads the formation of high temperature mineral phases like mullite and cristoballite (Cardiano et al. 2004). The absence of mullite and cristoballite minerals in the mineralogical compositions of the natural pozzolanic aggregates shows that the firing temperature did not exceed  $900^\circ\text{C}$ .

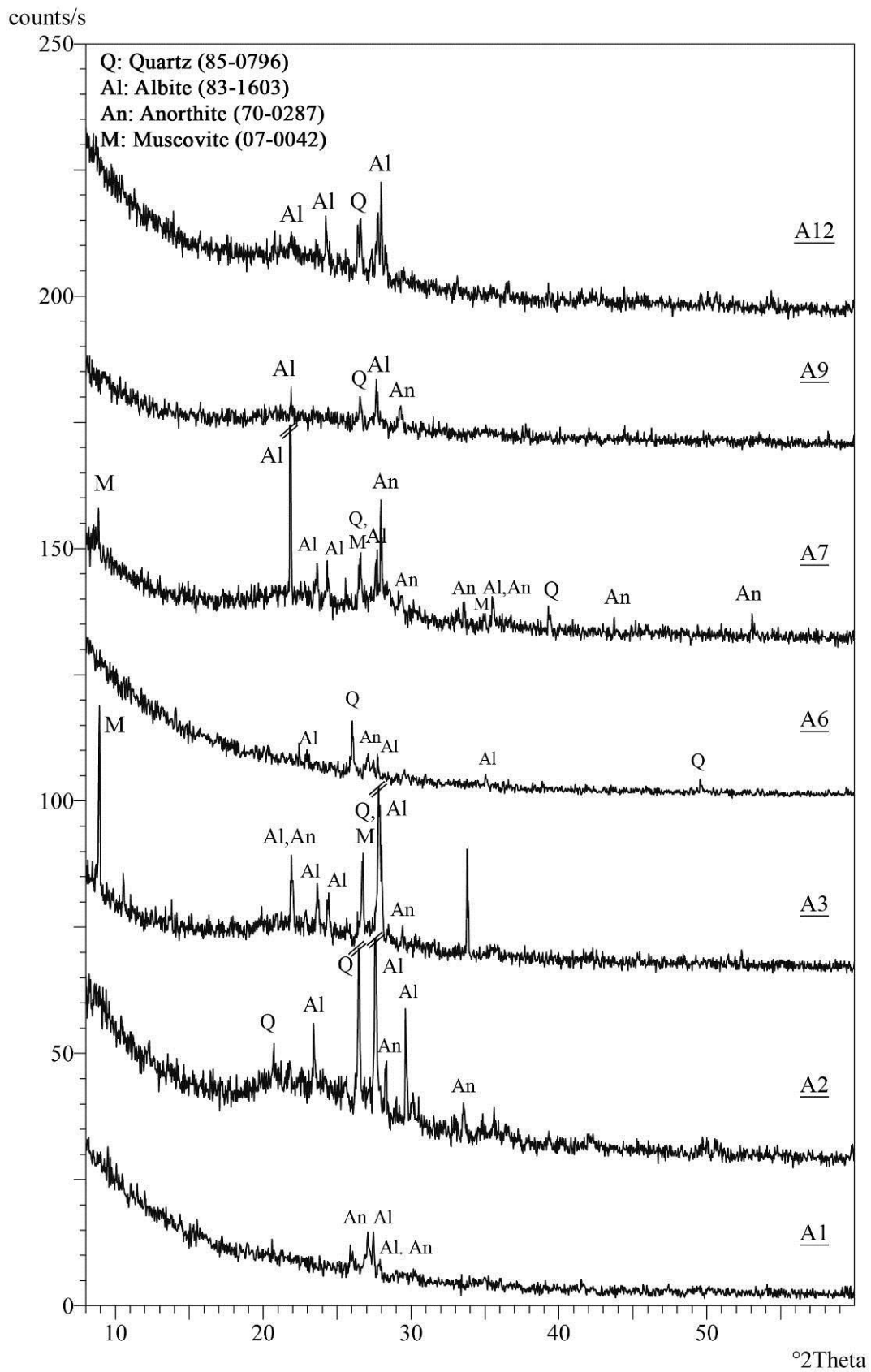


Figure 3.10. XRD patterns of natural pozzolans from Roman lime mortars of Aigai

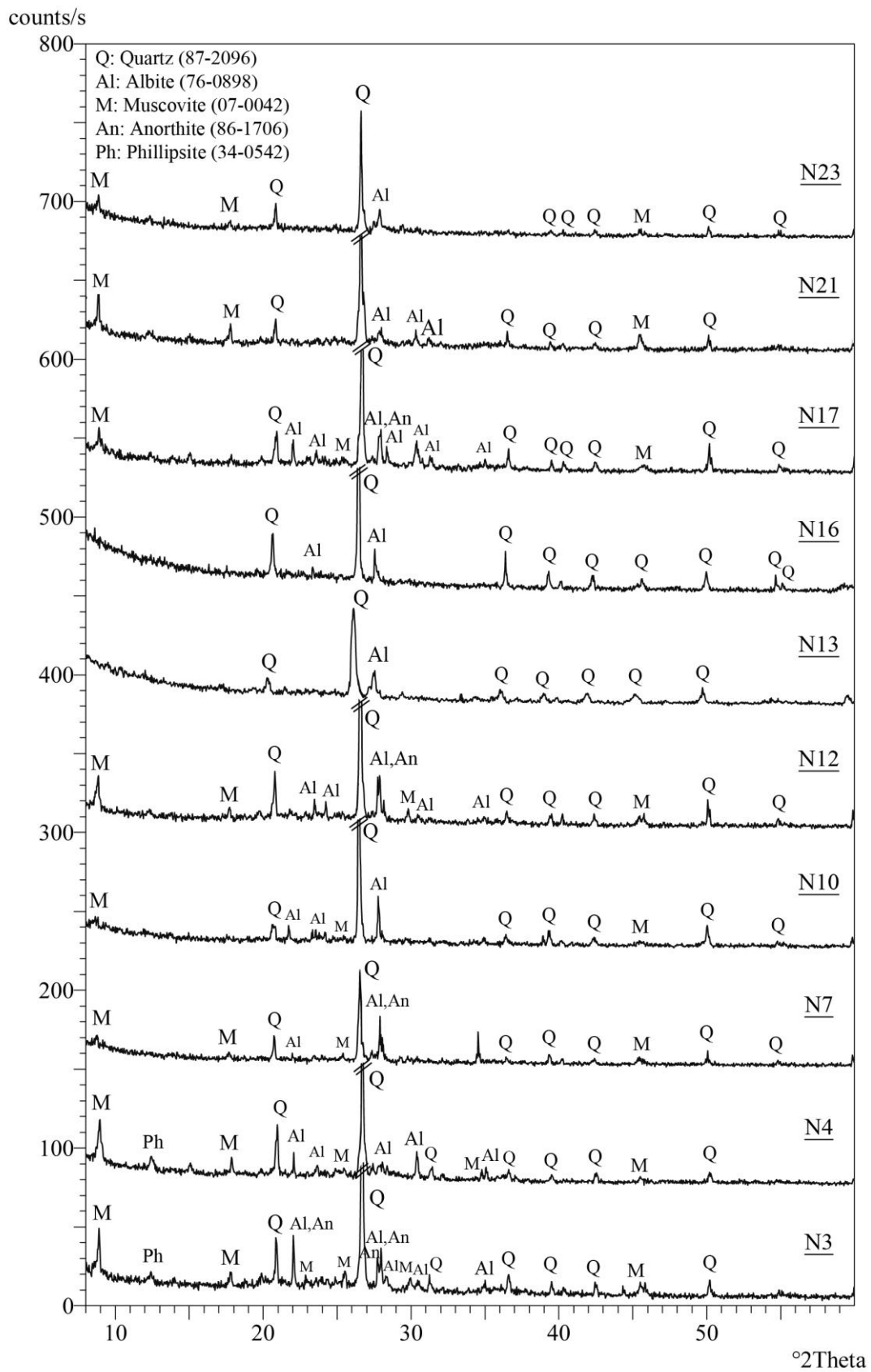


Figure 3.11. XRD patterns of natural pozzolans from Roman lime mortars of Nysa

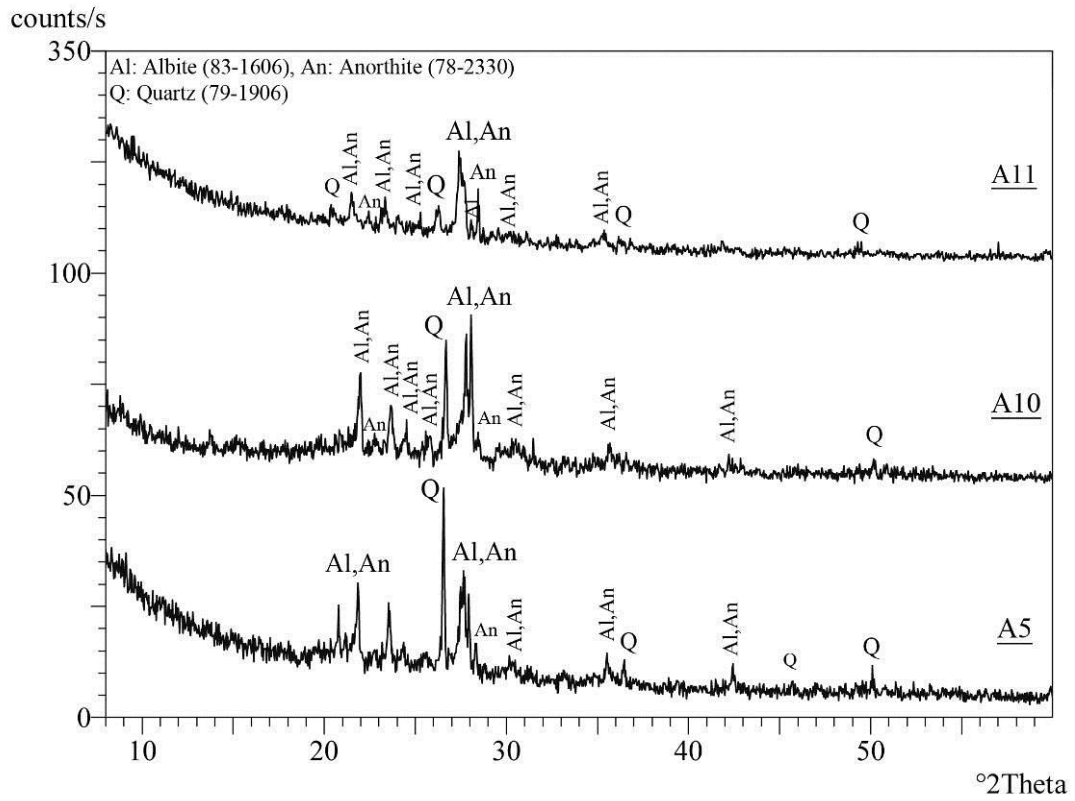


Figure 3.12. XRD patterns of artificial pozzolans from Roman lime mortars of Aigai

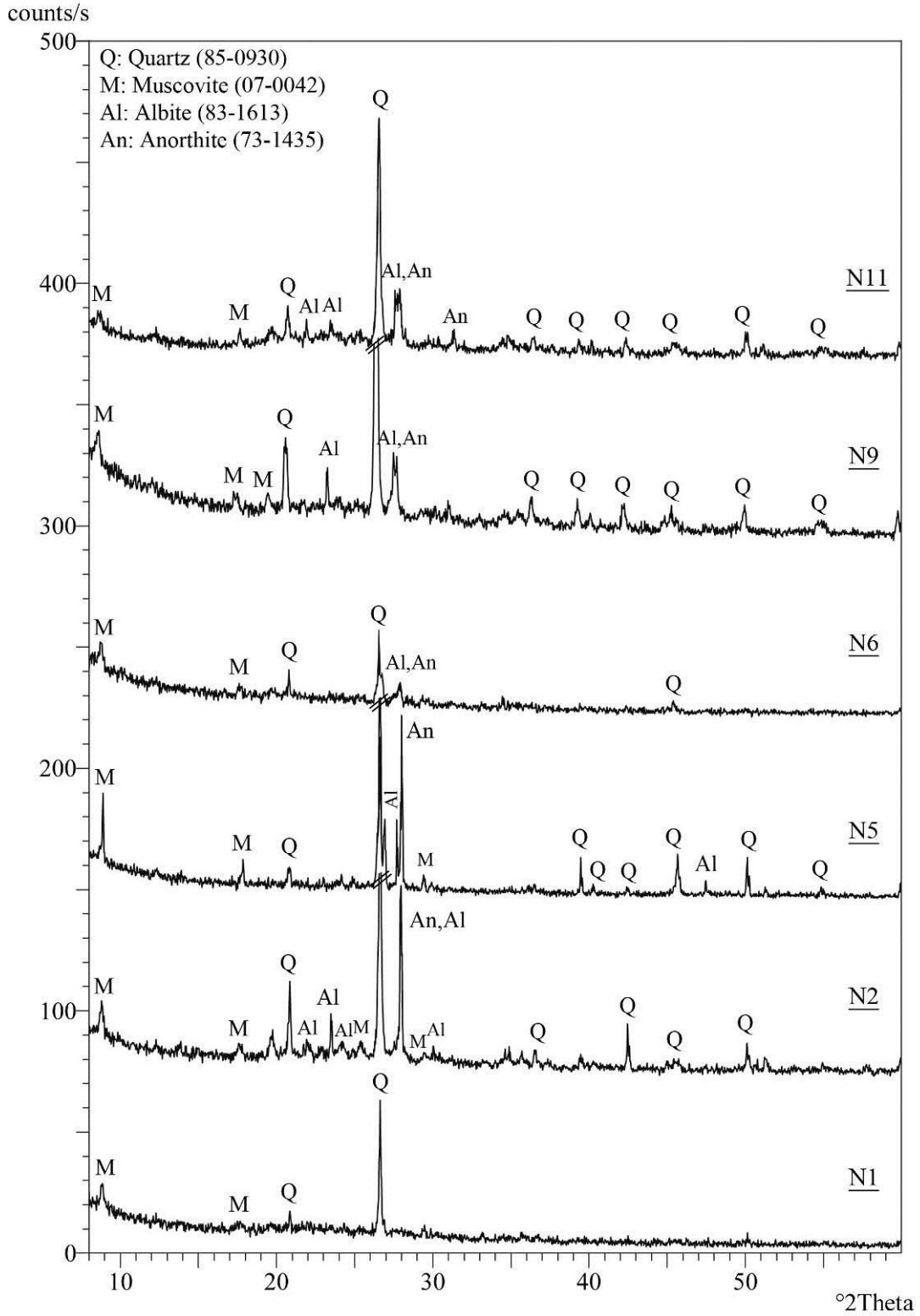


Figure 3.13. XRD patterns of artificial pozzolans from Roman lime mortars of Nysa (I)

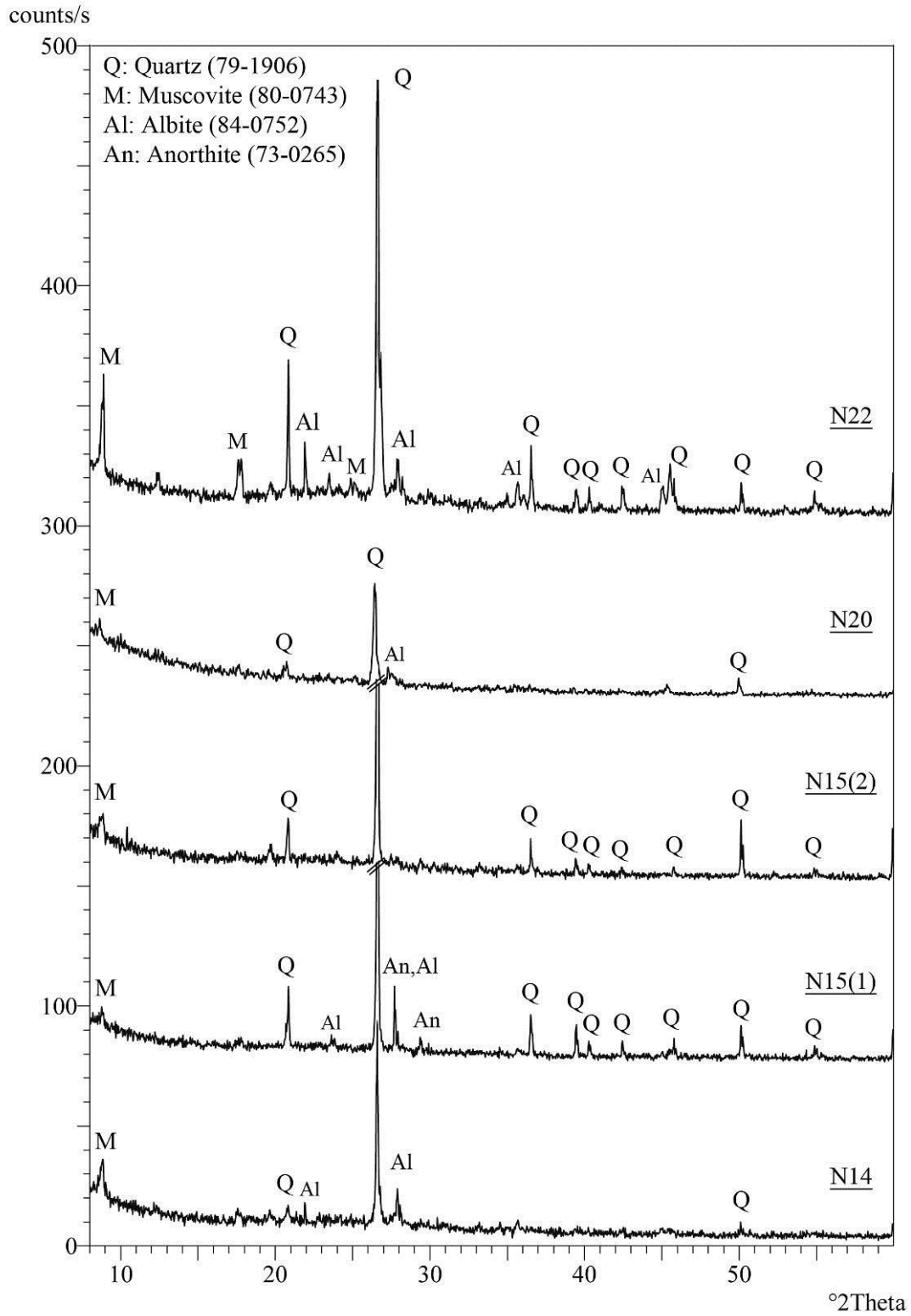


Figure 3.14. XRD patterns of artificial pozzolans from Roman lime mortars of Nysa (II)

Mineralogical compositions of natural and artificial pozzolanic aggregates used in the mortars of Aigai and Nysa showed similarities with the mineralogical compositions of pozzolans used in different regions (Table 3.7). The small differences between the mineralogical compositions may be due to the use of local material sources.

Table 3.7. Mineralogical compositions of pozzolanic aggregates of Roman lime mortars determined by previous studies

<b>Roman Building/Site (Reference)</b>	<b>Agg. Type of Mortar</b>	<b>Method</b>	<b>Minerals</b>
Sagalassos - Turkey ( <i>Degryse et al. 2002</i> )	Natural poz.	Optical microscopy	Plagioclase, alkali-feldspar, augite, diopside, biotite, amphiboles
Roman Villa of Pollio - Italy ( <i>Benedetti et al. 2004</i> )	Natural poz.	XRD	Quartz, diopside, sanidine, dolomite, biotite
Saithidai's Heroon Podium - Greece ( <i>Zamba et al. 2007</i> )	Natural poz.	XRD	Quartz, calcite
Serapis Temple - Turkey ( <i>Özkaya and Böke 2009</i> )	Natural poz.	XRD	Albite, K-feldspar, quartz, amorphous minerals
Rome - Italy ( <i>Jackson et al. 2010</i> )	Natural poz.	Petrographic analysis	Quartz, sanidine, analcime, biotite, ignimbrite, feldspar
Kyme - Turkey ( <i>Miriello et al. 2011</i> )	Natural poz.	Polarized microscopy	Quartz, plagioclase, muscovite, calcite, biotite, opaque minerals
The Theatre of Marcellus - Rome (Italy) ( <i>Jackson et al. 2011</i> )	Natural poz.	XRD	Analcime, leucite, diopside, hematite, calcite
Roman Villa of Pollio - Italy ( <i>Benedetti et al. 2004</i> )	Artificial poz.	XRD	Quartz, diopside, sanidine, dolomite, biotite, hematite, serandite, calcite
Cisterns - Uthina (Tunisia) ( <i>Farci et al. 2005</i> )	Artificial poz.	XRD	Calcite, quartz, feldspar, gehlenite, sanidine, plagioclase, biotite
Mithraeum House - Spain ( <i>Franquelo et al. 2008</i> )	Artificial poz.	XRD	Quartz, anorthite, hematite, mica, calcite, muscovite
Roman villa - Mošnje (Slovenia) ( <i>Kramar et al. 2011</i> )	Artificial poz.	XRD	Dolomite, calcite, quartz, muscovite
Mithraeum House - Spain ( <i>Robador et al. 2010</i> )	Artificial poz.	XRD	Quartz, anorthite, mica, hematite



### 3.5.3. Chemical Compositions of Pozzolans

Major and trace element compositions of pozzolans used as aggregates in the Roman lime mortars were determined by XRF analyses.

The results of the analyses revealed that natural pozzolans were mainly composed of high amounts of SiO<sub>2</sub> (39.95-75.58 %), moderate amounts of Al<sub>2</sub>O<sub>3</sub> (5.01-14.71 %), Fe<sub>2</sub>O<sub>3</sub> (2.20-5.95 %), and low amounts of MgO (1.00-2.58 %), CaO (0.34-2.76 %), Na<sub>2</sub>O (0.53-1.94 %), K<sub>2</sub>O (0.28-2.15 %) and TiO<sub>2</sub> (0.48-1.29 %) (Table 3.8). Likewise, high amounts of SiO<sub>2</sub> (54.71-79.39 %), moderate amounts of Al<sub>2</sub>O<sub>3</sub> (7.06-16.09 %), Fe<sub>2</sub>O<sub>3</sub> (2.29-7.53 %), and low amounts of MgO (0.40-2.94 %), CaO (0.43-3.27 %), Na<sub>2</sub>O (0.40-2.23%), K<sub>2</sub>O (0.90-2.85 %) and TiO<sub>2</sub> (0.68-1.31 %) constituted the major element compositions of artificial pozzolans (Table 3.8). These results were almost in the same ranges with the major chemical compositions of pozzolanic aggregates used in lime mortars from various Roman period buildings (Jackson et al. 2009, Miriello et al. 2010, Kramar et al. 2011, Miriello et al. 2011) (Table 3.9). Trace elements detected in the compositions of pozzolans were P, S, Cr, Ga, Sr, Y, Zr, Mo, Cd, Ba (Table 3.10).

Chemical compositions analyses revealed that calcium oxide (CaO) and rare earth element yttrium (Y) were distinctive for grouping natural pozzolans used in Aigai and Nysa mortars (Figure 3.15). CaO content of Aigai pozzolans were higher than Nysa pozzolans; whereas Y was higher in pozzolans of Nysa.

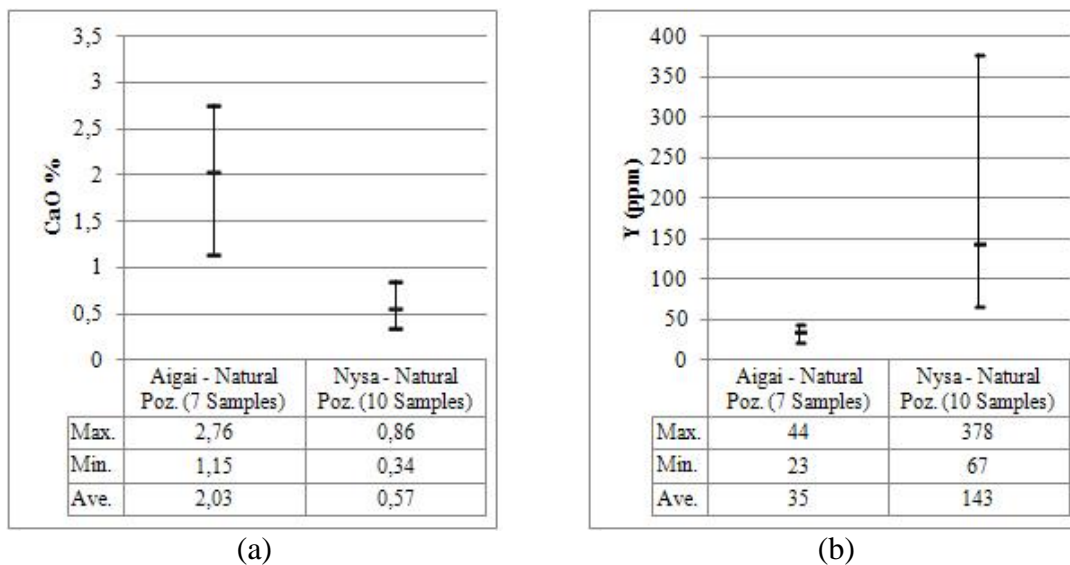
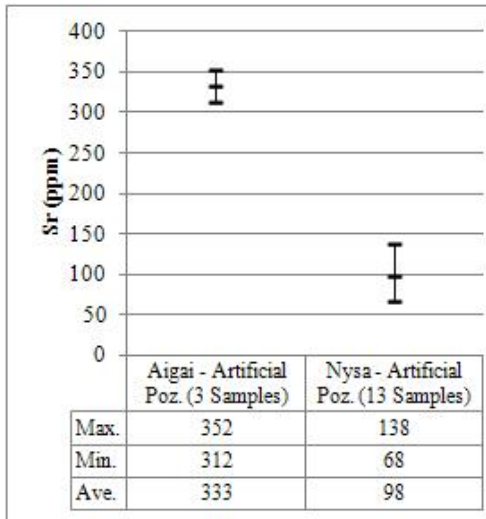
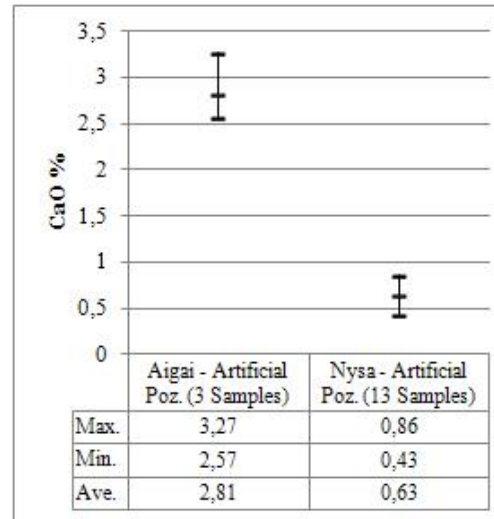


Figure 3.15. CaO (a) and Y (b) contents of natural pozzolans

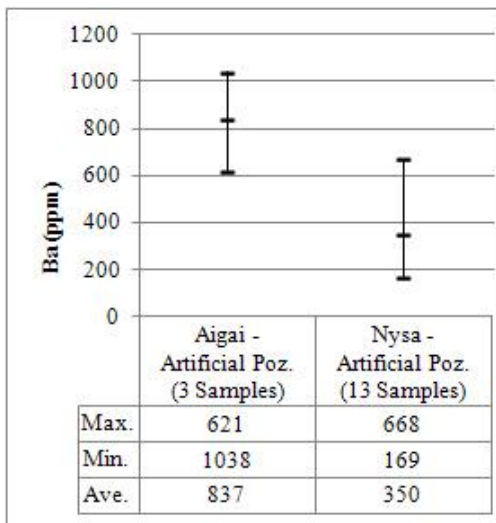
Artificial pozzolans can be differentiated by their alkaline earth metal contents (Ba, Sr, Ca). Artificial pozzolans used in Aigai mortars had higher calcium (CaO), barium (Ba) and strontium (Sr) values compared to Nysa mortars (Figure 3.16).



(a)



(b)



(c)

Figure 3.16. Ba (a), Sr (b) and CaO (c) contents of artificial pozzolans

Table 3.8. Major chemical compositions of pozzolans determined by XRF (%)

<b>Sample Type</b>	<b>SiO<sub>2</sub></b>	<b>TiO<sub>2</sub></b>	<b>Al<sub>2</sub>O<sub>3</sub></b>	<b>Fe<sub>2</sub>O<sub>3</sub></b>	<b>MgO</b>	<b>CaO</b>	<b>Na<sub>2</sub>O</b>	<b>K<sub>2</sub>O</b>
Natural pozzolans of lime mortars from Aigai (A1, A2, A3, A6, A7, A9, A12)	39.95 - 74.69	0.48 - 0.92	5.81 - 11.17	2.29 - 4.74	1.45 - 2.58	1.15 - 2.76	0.53 - 1.93	0.28 - 1.15
	65.62 (ave.)	0.70 (ave.)	8.41 (ave.)	3.51 (ave.)	1.94 (ave.)	2.03 (ave.)	1.19 (ave.)	0.70 (ave.)
Natural pozzolans of lime mortars from Nysa (N3, N4, N7, N10, N12, N13, N16, N17, N21, N23)	67.20 - 75.58	0.70 - 1.29	5.01 - 14.71	2.20 - 5.95	1.00 - 2.53	0.34 - 0.86	0.63 - 1.94	0.58 - 2.15
	72.04 (ave.)	0.91 (ave.)	11.16 (ave.)	3.07 (ave.)	1.95 (ave.)	0.57 (ave.)	1.40 (ave.)	1.54 (ave.)
Artificial pozzolans of lime mortars from Aigai (A5, A10, A11)	54.71 - 70.38	0.68 - 1.02	12.55 - 15.16	4.16 - 5.45	2.14 - 2.62	2.57 - 3.27	0.72 - 2.23	0.91 - 2.85
	61.99 (ave.)	0.90 (ave.)	13.69 (ave.)	5.00 (ave.)	2.31 (ave.)	2.81 (ave.)	1.69 (ave.)	1.46 (ave.)
Artificial pozzolans of lime mortars from Nysa (N1, N2, N5, N6, N8, N9, N11, N14, N15(1), N15(2), N20, N22, N24)	59.12 - 79.39	0.71 - 1.31	7.06 - 16.09	2.29 - 7.53	0.40 - 2.94	0.43 - 0.86	0.40 - 1.80	0.90 - 2.35
	68.84 (ave.)	0.91 (ave.)	11.76 (ave.)	4.75 (ave.)	2.73 (ave.)	0.63 (ave.)	1.48 (ave.)	1.74 (ave.)

Table 3.9. Major chemical compositions of aggregates (%) determined by previous studies

<b>Roman Building/ Site (Reference)</b>	<b>Agg. Type of Mortar</b>	<b>Method</b>	<b>SiO<sub>2</sub></b>	<b>TiO<sub>2</sub></b>	<b>Al<sub>2</sub>O<sub>3</sub></b>	<b>Fe<sub>2</sub>O<sub>3</sub></b>	<b>MnO</b>	<b>MgO</b>	<b>CaO</b>	<b>Na<sub>2</sub>O</b>	<b>K<sub>2</sub>O</b>	<b>P<sub>2</sub>O<sub>5</sub></b>
The Markets of Trajan - Rome ( <i>Jackson et al. 2009</i> )	Natural poz.	XRF	42.9-51.69	0.87-1.14	11.81-21.40	9.41-11.17	0.16-0.22	1.48-5.13	1.88-10.68	n.d.-1.32	2.68-6.95	0.26-0.75
Houses in Pompeii - Italy ( <i>Miriello et al. 2010</i> )	Natural poz.	XRF	45.68-64.21	n.d.-2.41	12.05-24.24	1.39-16.78	n.d.-0.67	0.55-26.13	0.25-12.79	0.36-13.38	1.40-17.63	n.d.-1.14
Kyme - Turkey ( <i>Miriello et al. 2011</i> )	Natural poz.	SEM-EDS	63.75-84.78	0.28-1.01	5.95-17.66	0.16-3.70	n.d.-0.18	0.82-4.30	0.41-4.38	0.95-4.03	1.02-7.35	0.11-0.73
Roman villa - Mošnje (Slovenia) ( <i>Kramar et al. 2011</i> )	Artificial poz.	ICP-OES	0.21-2.70	0.001-0.023	0.10-3.24	0.13-0.62	0.012-0.033	4.33-12.87	28.97-43.00	0.023-0.043	0.039-0.258	0.055-0.442

Table 3.10. Trace elements compositions of pozzolans determined by XRF (ppm)

<b>Sample Type</b>	<b>P</b>	<b>S</b>	<b>Cr</b>	<b>Ga</b>	<b>Sr</b>	<b>Y</b>	<b>Zr</b>	<b>Mo</b>	<b>Cd</b>	<b>Ba</b>
Natural pozzolans of lime mortars from Aigai (A1, A2, A3, A6, A7, A9, A12)	41 - 240	214 - 505	282 - 520	43 - 72	175 - 288	23 - 44	122 - 428	13 - 180	49 - 232	288 - 700
	200 (ave.)	311(ave.)	395(ave.)	62(ave.)	231(ave.)	35(ave.)	256(ave.)	80(ave.)	108(ave.)	459(ave.)
Natural pozzolans of lime mortars from Nysa (N3, N4, N7, N10, N12, N13, N16, N17, N21, N23)	68 - 548	256 - 417	300 - 555	44 - 132	67 - 378	67 - 378	268 - 546	54 - 180	53 - 270	300 - 703
	216(ave.)	337(ave.)	446(ave.)	74(ave.)	143(ave.)	61(ave.)	400(ave.)	100(ave.)	143(ave.)	469(ave.)
Artificial pozzolans of lime mortars from Aigai (A5, A10, A11)	217 - 327	246 - 340	216 - 401	67 - 72	312 - 352	26 - 70	269 - 380	86 - 190	79 - 160	621 - 1038
	261(ave.)	285(ave.)	297(ave.)	70 (ave.)	333(ave.)	62(ave.)	328(ave.)	152(ave.)	130(ave.)	837(ave.)
Artificial pozzolans of lime mortars from Nysa (N1, N2, N5, N6, N8, N9, N11, N14, N15(1), N15(2), N20, N22, N24)	217 - 878	278 - 332	217 - 750	32 - 70	68 - 138	42 - 87	243 - 435	15 - 111	55 - 158	169 - 668
	374(ave.)	277(ave.)	445(ave.)	54(ave.)	98(ave.)	61(ave.)	334(ave.)	62(ave.)	90(ave.)	350(ave.)

In detail, XRF results of major chemical compositions of natural and artificial pozzolans (Table 3.8) were processed by hierarchical clustering analyses in order to identify the samples with similar compositions into homogenous groups and to distinguish them from those which have instead far different values. For this purpose, hierarchical clustering was implemented by employing a distance measure using Average Linkage Method and the Euclidean distance for each element detected by XRF.

The results of hierarchical clustering analyses revealed that among other elements, only CaO was distinctive to generate clusters. Two distinct classes were easily observable on the dendrogram of CaO, where the members of the first group were the pozzolans used in the mortars of Aigai with a high level of CaO with an average of 2.5 %; and the second group was rather characterized by a low level of CaO with an average of 0.6 % by the pozzolans used in the lime mortars of Nysa (Figure 3.17). However, SiO<sub>2</sub>, TiO<sub>2</sub>, Al<sub>2</sub>O<sub>3</sub>, Fe<sub>2</sub>O<sub>3</sub>, MgO, Na<sub>2</sub>O and K<sub>2</sub>O could not be used to generate clusters since distinct groups were not observed on their dendrograms (Figure 3.18-3.24).

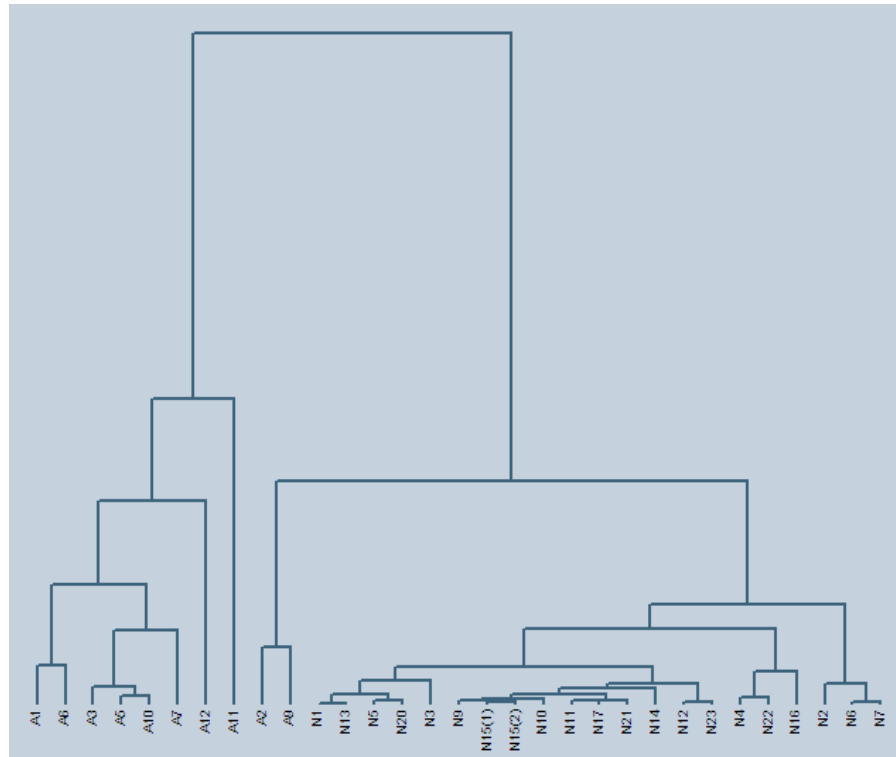


Figure 3.17. The dendrogram graph of CaO

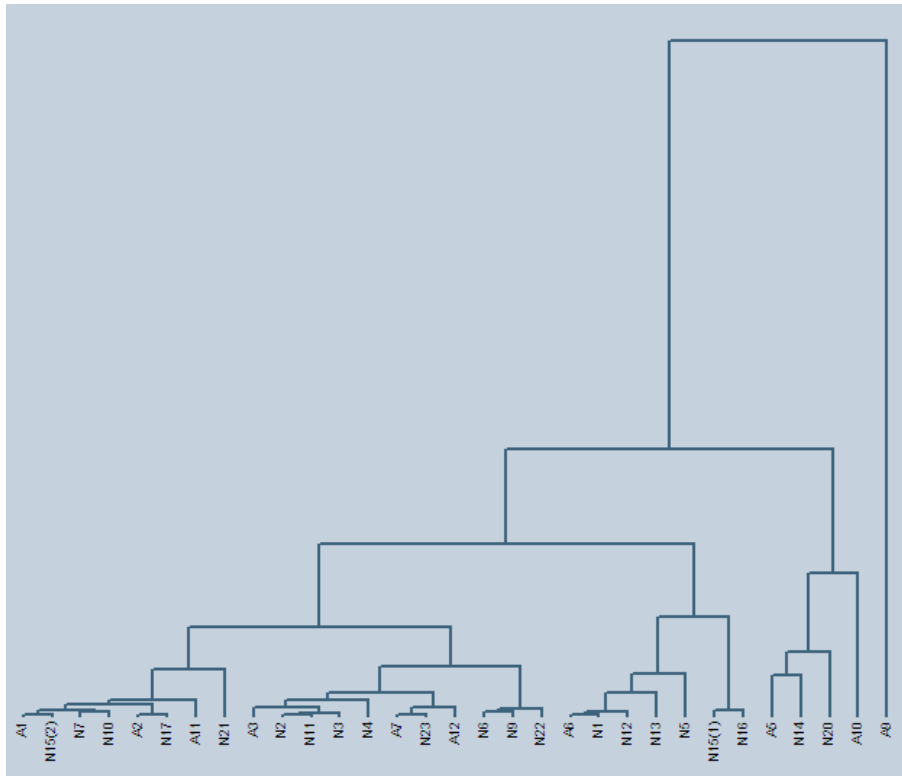


Figure 3.18. The dendrogram graph of SiO<sub>2</sub>

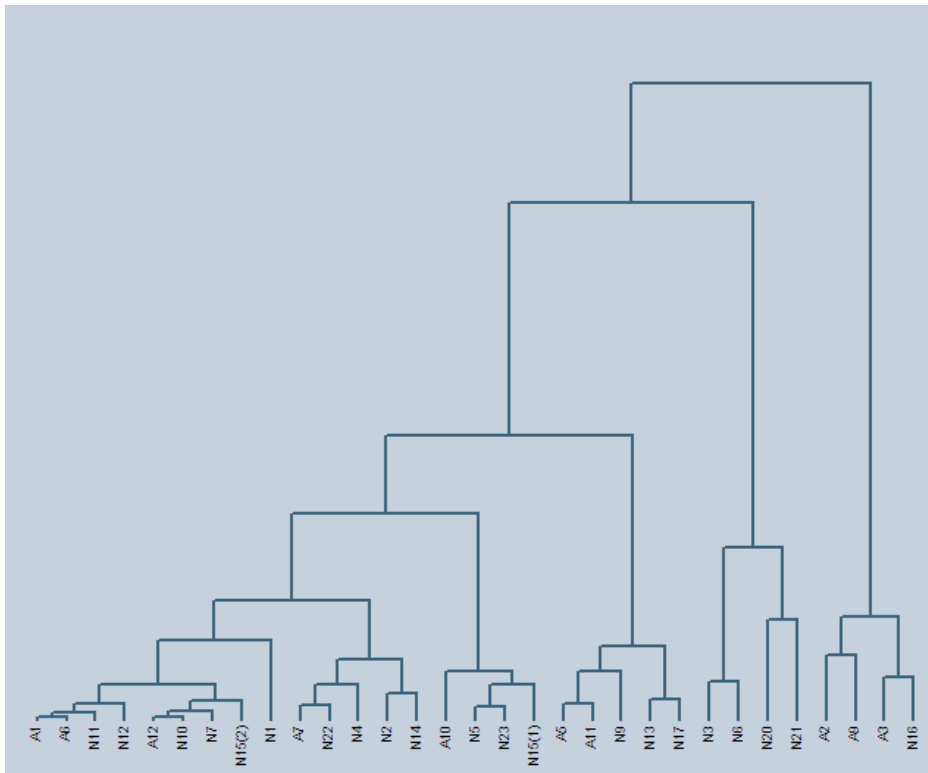


Figure 3.19. The dendrogram graph of TiO<sub>2</sub>



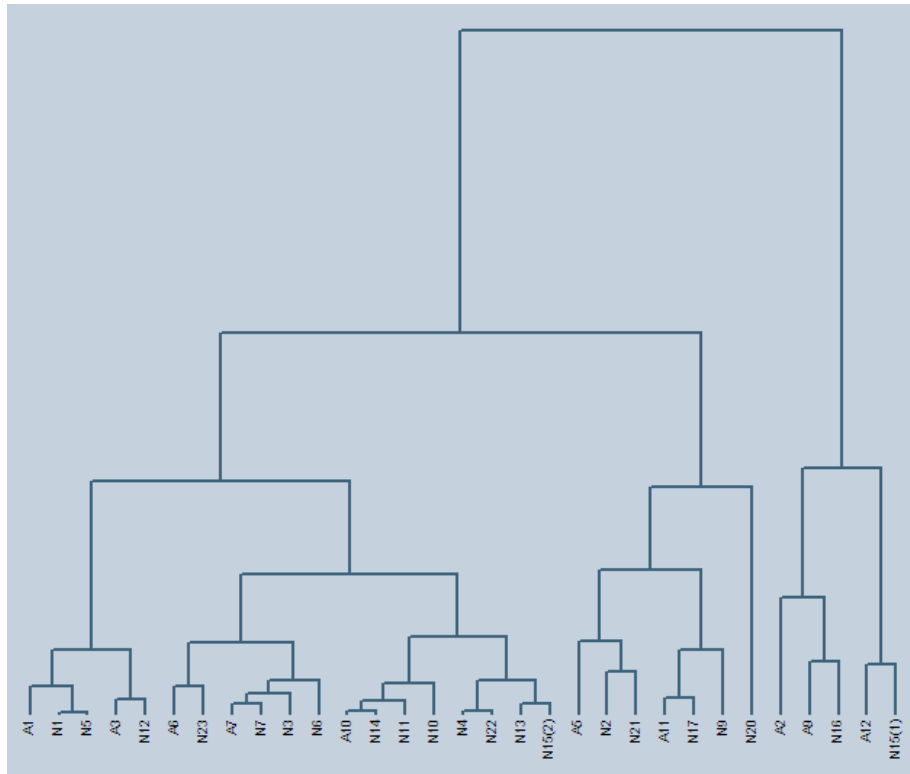


Figure 3.20. The dendrogram graph of  $Al_2O_3$

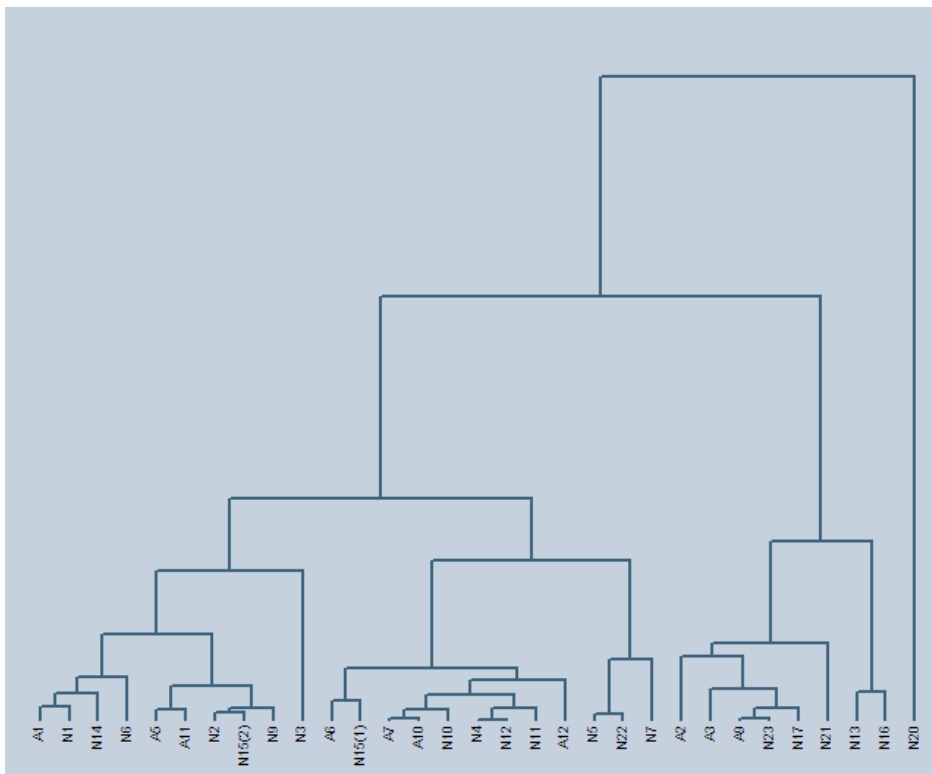


Figure 3.21. The dendrogram graph of  $Fe_2O_3$

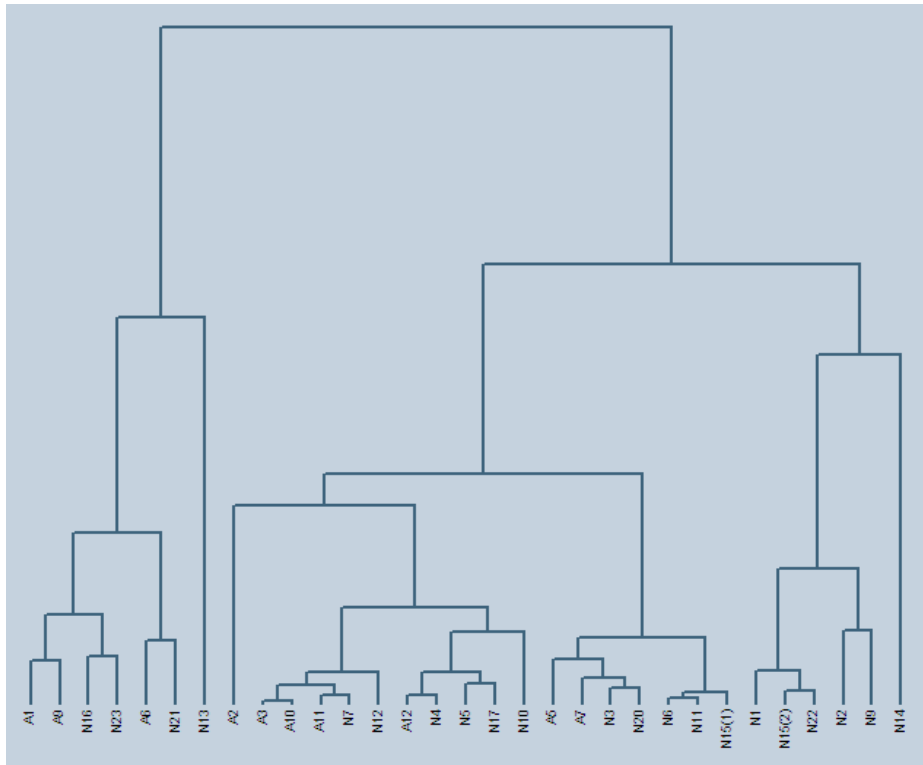


Figure 3.22. The dendrogram graph of MgO

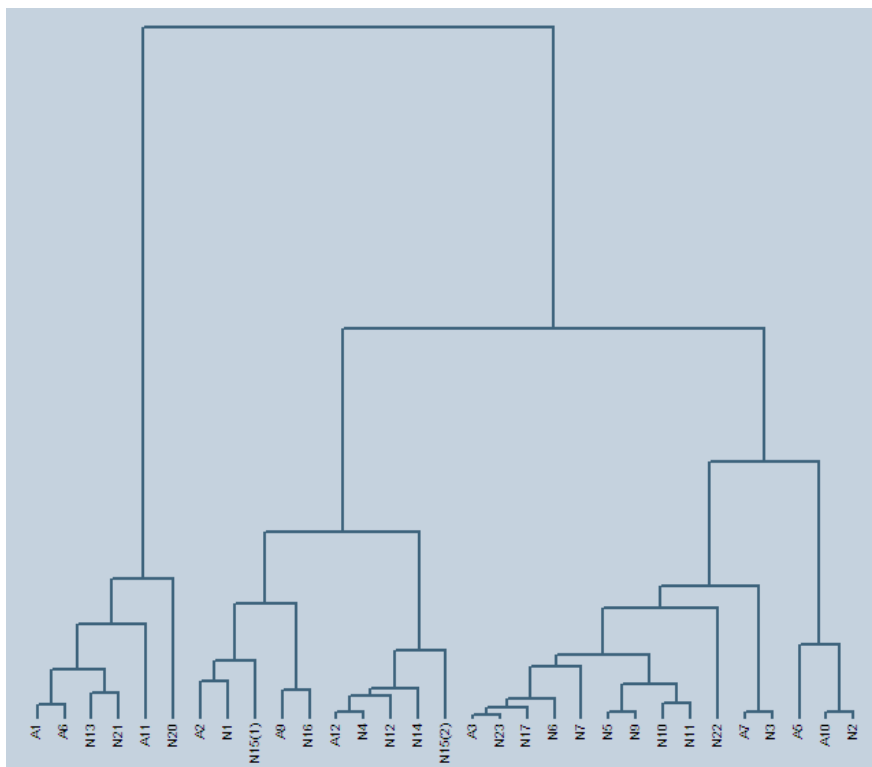


Figure 3.23 The dendrogram graph of Na<sub>2</sub>O

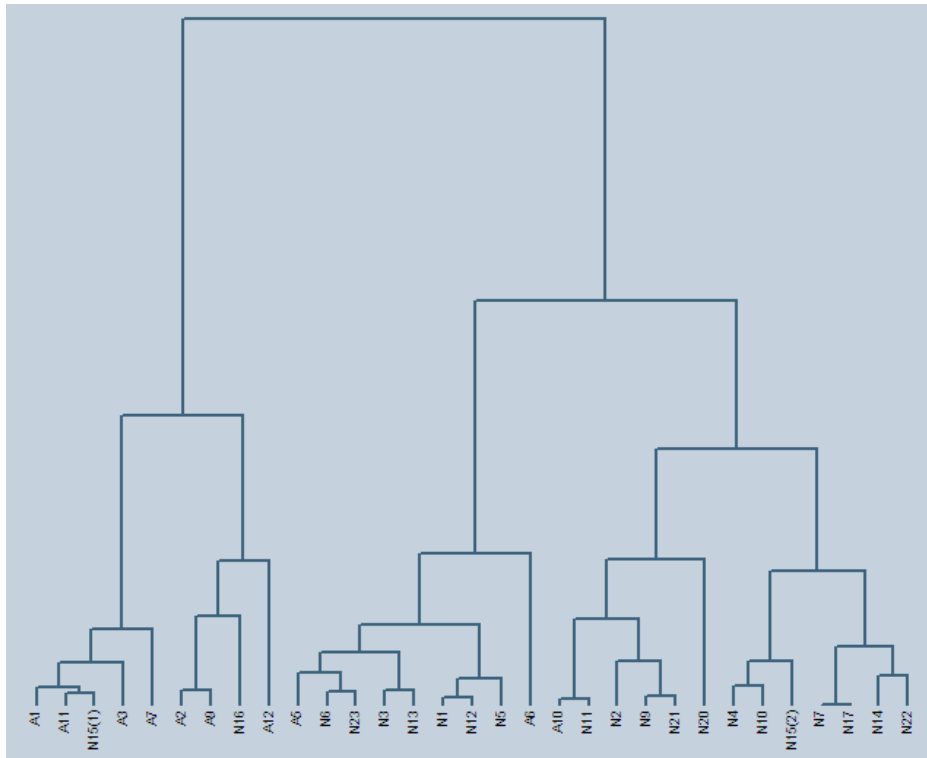


Figure 3.24 The dendrogram graph of  $K_2O$

To support these results also from an inferential point of view, various statistical tests including student t-test, Anova, Kruskall Wallis and Mann-Whitney tests were implemented in order to test formally whether or not the means (or medians) of these two groups generated by CaO were significantly different from each other. The reason for using several tests rather than focusing only on one test was to check the robustness of the results with respect to different testing methodologies developed in the literature. Moreover, the reason to use median values next to ‘mean’ was a purely technical issue since Kruskall-Wallis and Mann Whitney tests were based on testing the median values in the software package (EViews 4.1) used for these analyses.

The results presented in Table 3.11 verified that different means and medians across two groups were strongly evident according to the statistical test methods used. P-values which were the widely accepted indicators to assess significant differences in the means/medians across two groups were calculated for each test. In each of these tests, p-values were far below 1 % level which indicated the fact that differences in the mean/medians across two groups were marginally different from zero.

This finding was evident and robust across different methodologies namely clustering analysis and inferential tests. Therefore, it could be argued that CaO was a

distinctive element to attest that different raw material sources were used for the manufacturing of pozzolanic aggregates in Aigai and Nysa.

Table 3.11. Equality tests of mean/median of clusters

<b>Mean</b>	<b>Test statistic</b>	<b>P-value</b>
t-test	20.0***	0.0000
Anova F-statistic	401.8***	0.0000
<b>Median</b>		
Kruskal-Wallis	16.8***	0.0000
Wilcoxon/Mann-Whitney	4.07***	0.0000

\*\*\* : 1 % or better, \*\*: 5 %, \*: 10%

The small differences in the major and trace element compositions of pozzolans from Aigai and Nysa revealed that different sources with similar chemical compositions had been used for pozzolan production in these cities. This could also indicate that the centralization to make better quality of the pozzolans during Roman period (Ward-Perkins 1974) may be achieved in Anatolia.

### 3.5.4. Microstructural Properties of Pozzolans

Microstructural properties of natural and artificial pozzolans used as aggregates in Roman lime mortars were determined by the investigation of small sized particles <53  $\mu\text{m}$  of pozzolans used in the binder parts through SEM-EDS analyses.

SEM images indicated that natural pozzolans had irregular morphology; and were composed of small sized amorphous particles (Figure 3.25-3.30). The higher magnifications of amorphous particles presented the rod-shaped nano particles that increased the surface area of pozzolan (Figure 3.29). High specific surface area could be considered as an effective factor to enhance the reactivity of pozzolan with lime. Among the investigated samples, N17 had a different morphology with a sponge-like appearance (Figure 3.30).

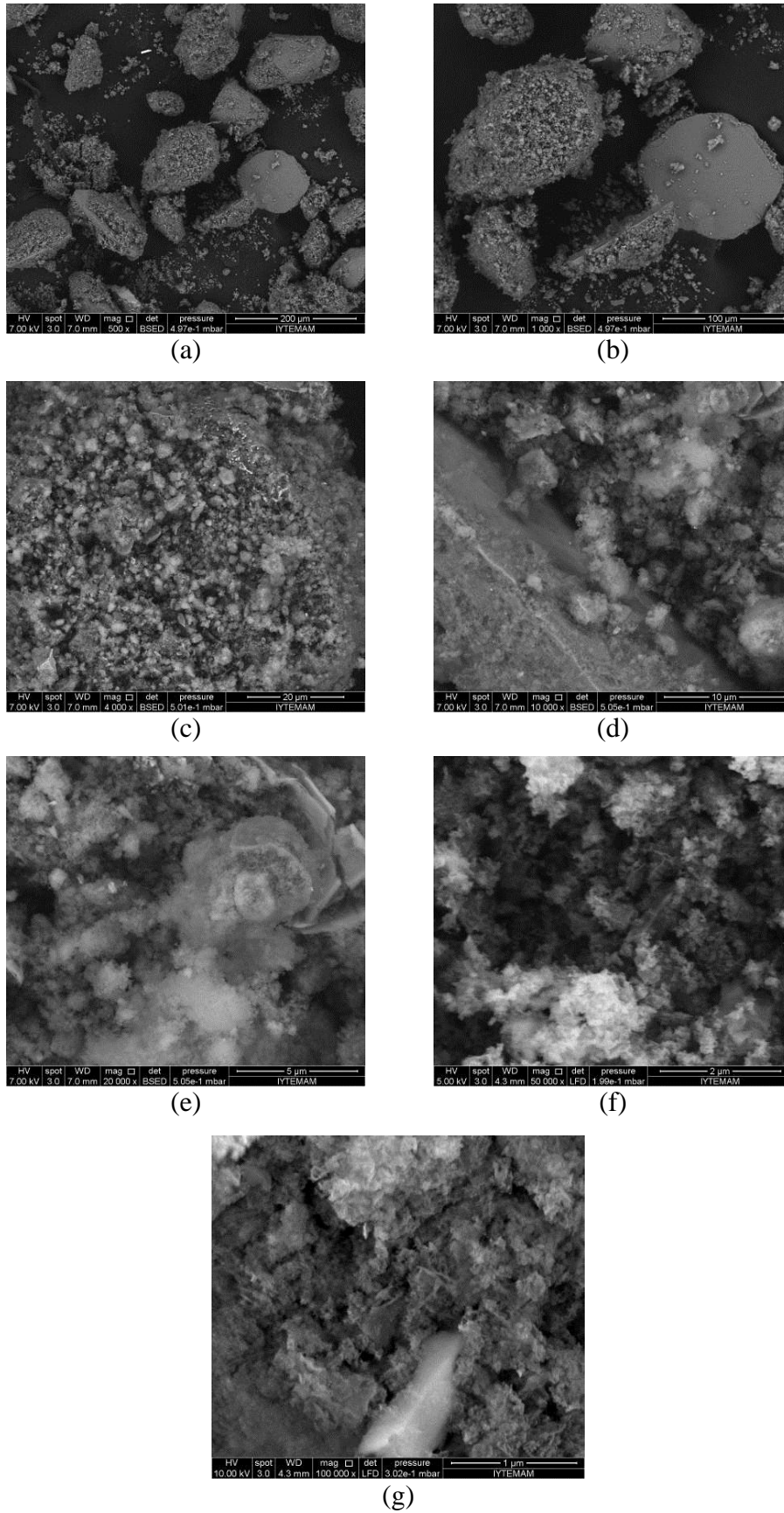


Figure 3.25. SEM-EDS images of natural pozzolans used in A1 at magnifications of 500 (a), 1000 (b), 4000 (c), 10000 (d), 20000 (e), 50000 (f), 100000 (g)

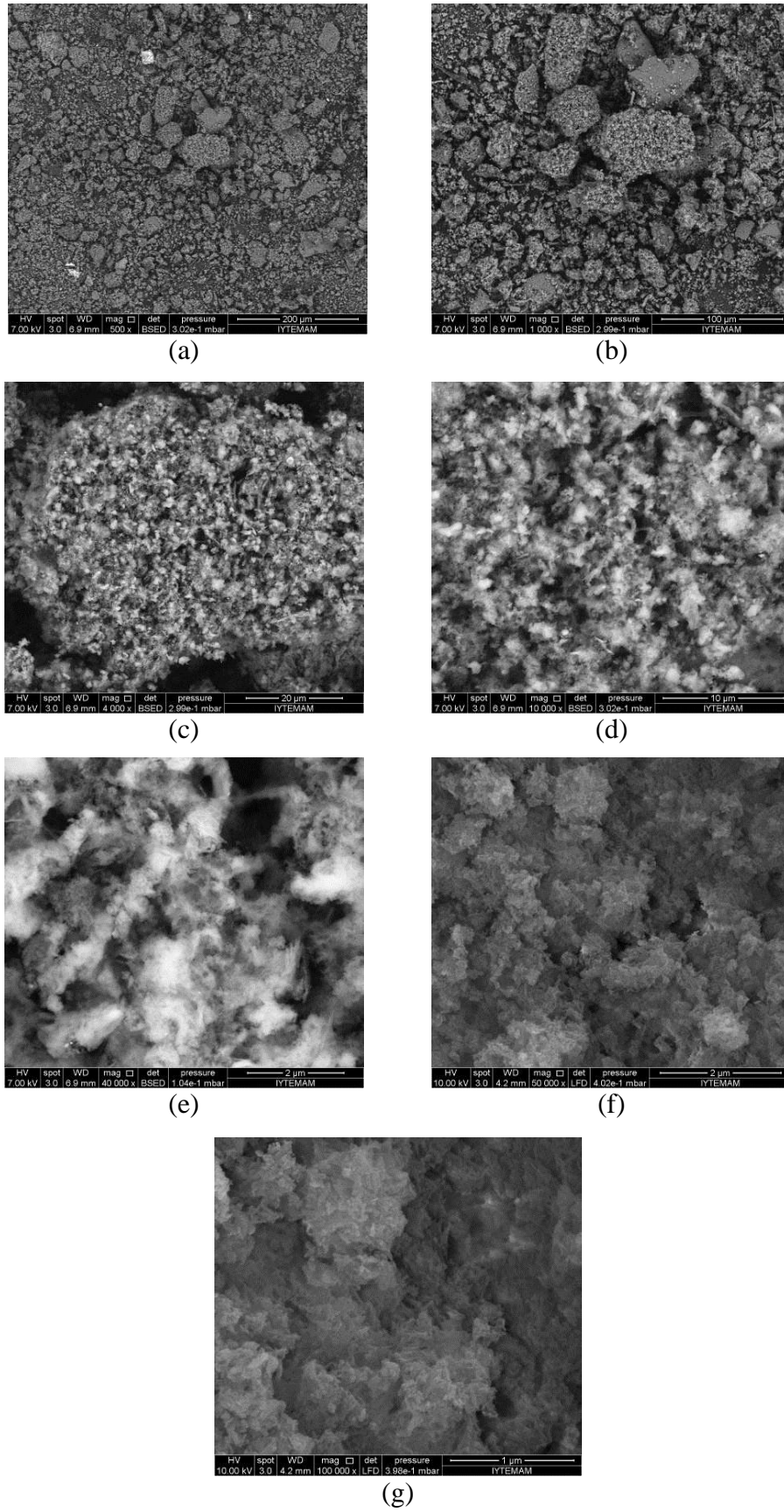
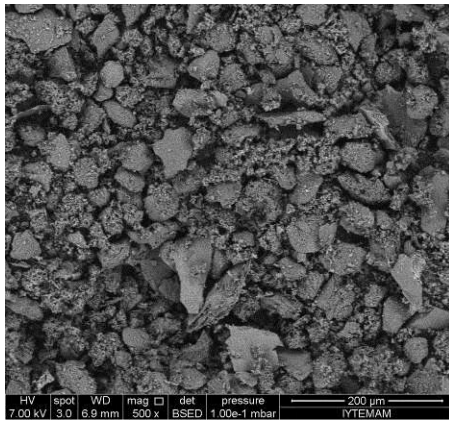
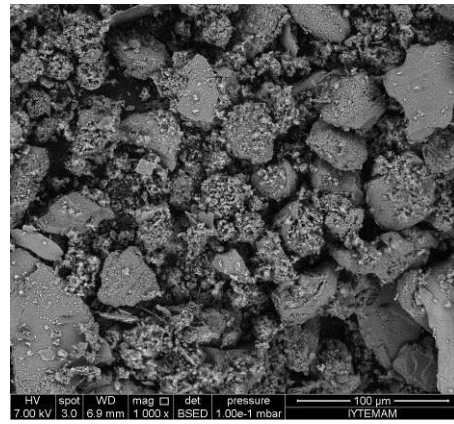


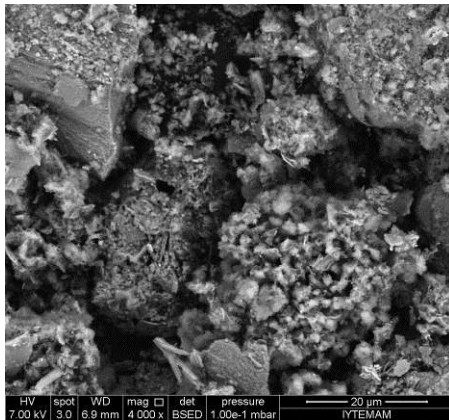
Figure 3.26. SEM-EDS images of natural pozzolans used in A2 at magnifications of 500 (a), 1000 (b), 4000 (c), 10000 (d), 20000 (e), 50000 (f), 100000 (g)



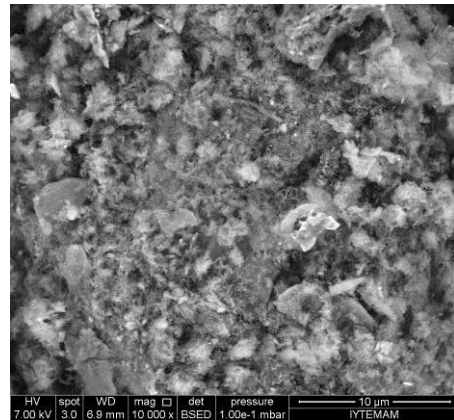
(a)



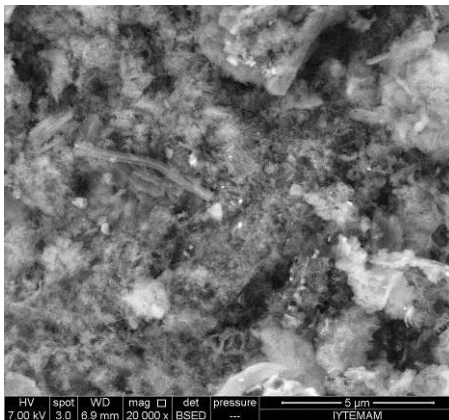
(b)



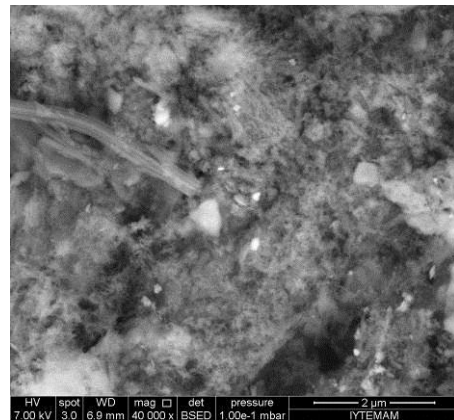
(c)



(d)



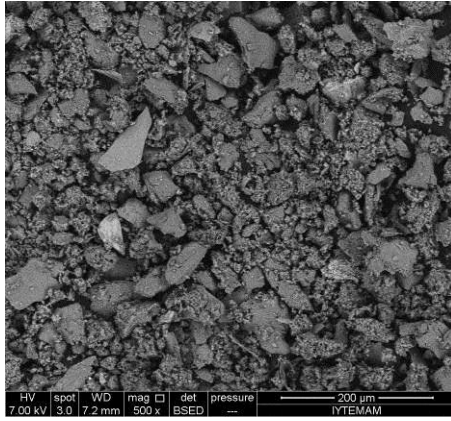
(e)



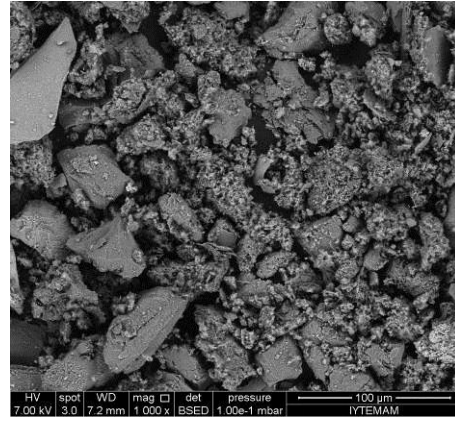
(f)

Figure 3.27. SEM-EDS images of natural pozzolans used in N3 at magnifications of 500 (a), 1000 (b), 4000 (c), 10000 (d), 20000 (e), 40000 (f)

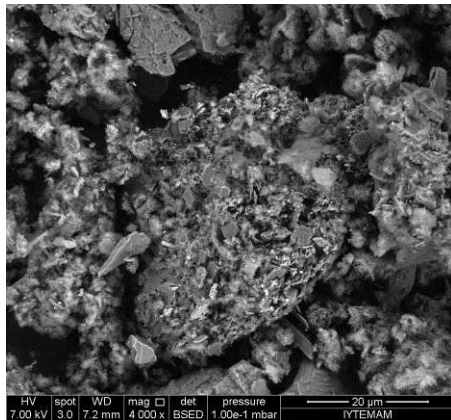




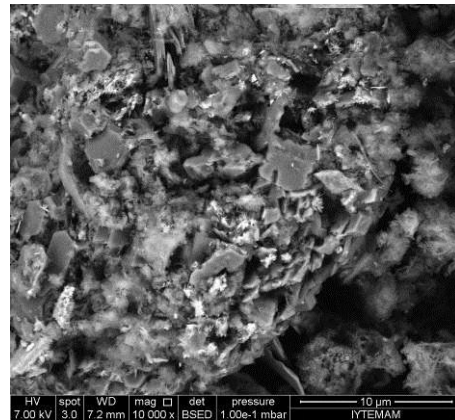
(a)



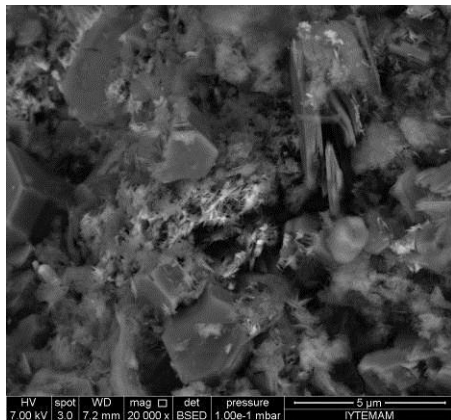
(b)



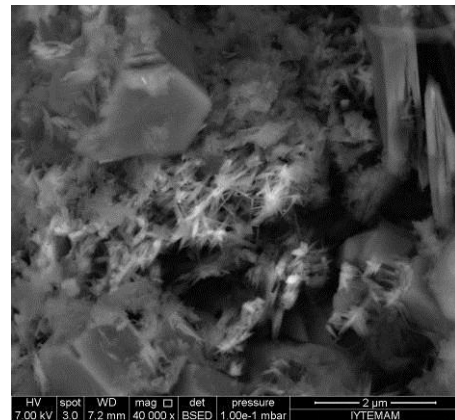
(c)



(d)



(e)



(f)

Figure 3.28. SEM-EDS images of natural pozzolans used in N7 at magnifications of 500 (a), 1000 (b), 4000 (c), 10000 (d), 20000 (e), 40000 (f)

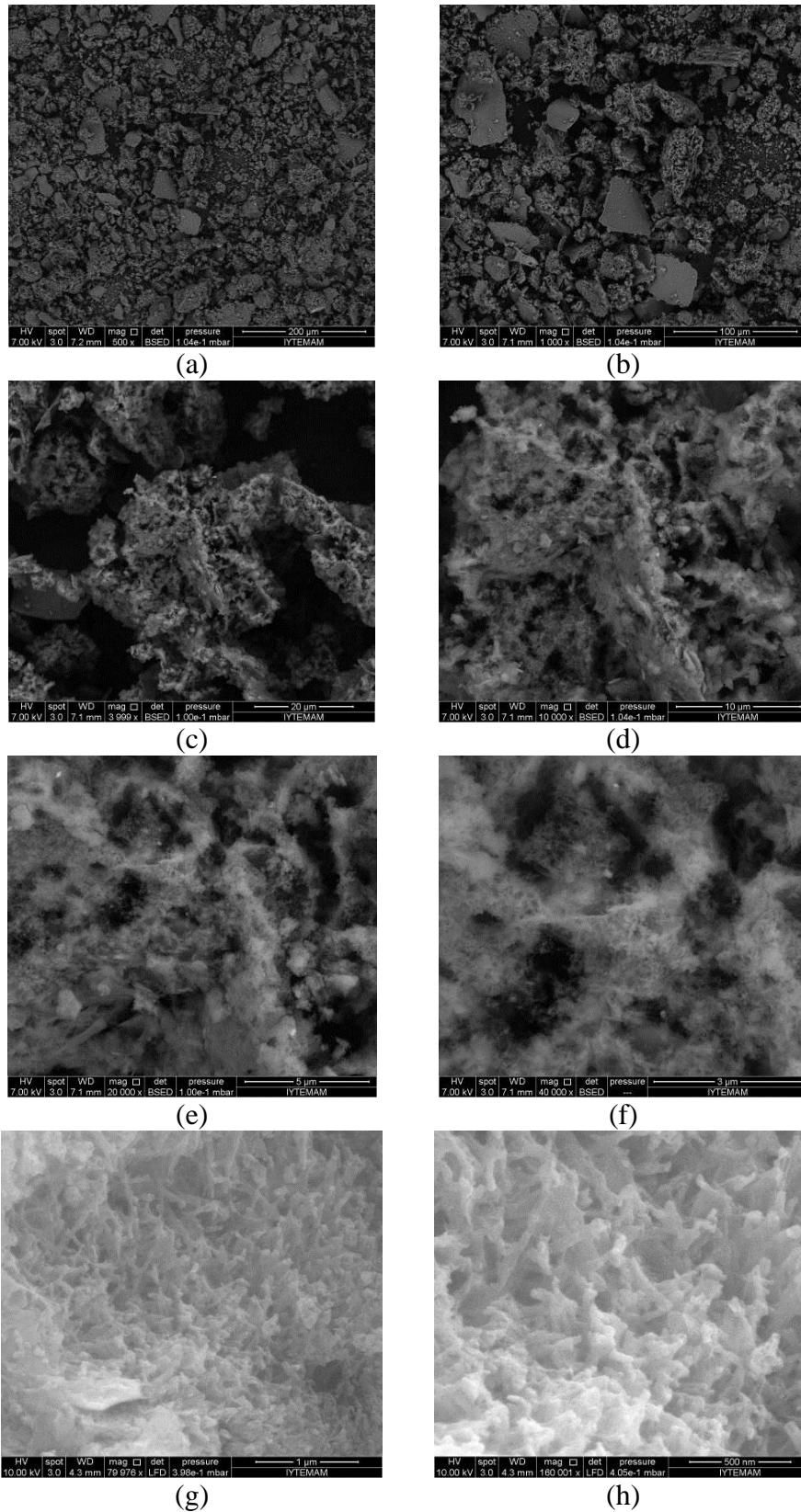
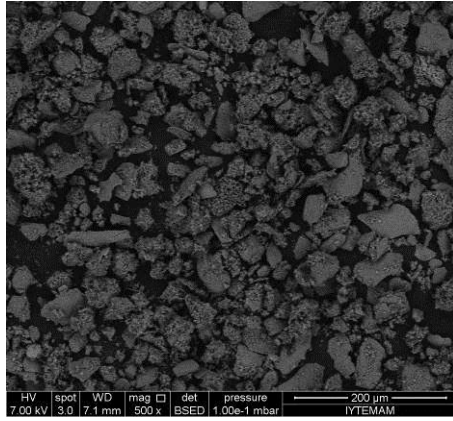
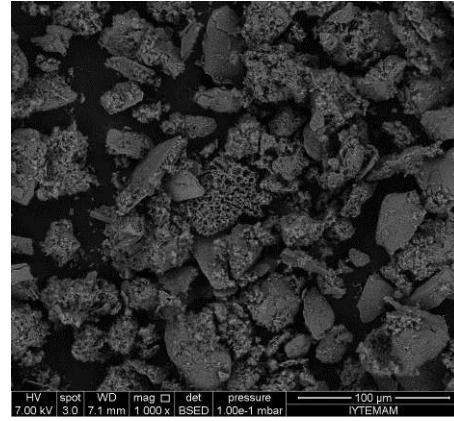


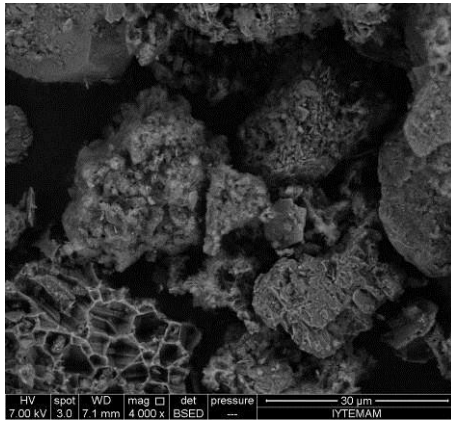
Figure 3.29. SEM-EDS images of natural pozzolans used in N13 at magnifications of 500 (a), 1000 (b), 4000 (c), 10000 (d), 20000 (e), 40000 (f), 80000 (g), 160000 (h)



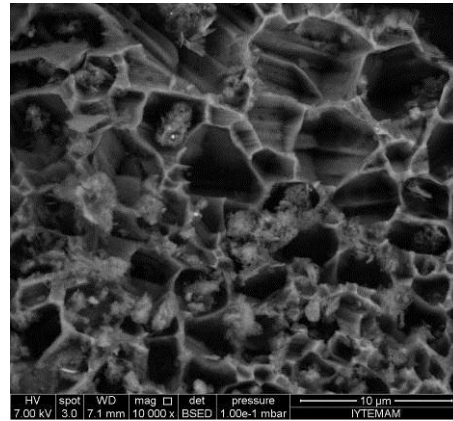
(a)



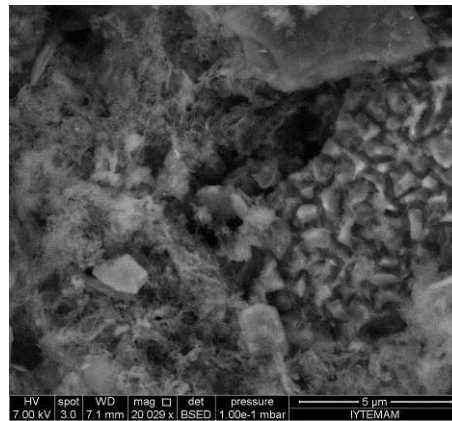
(b)



(c)



(d)



(e)

Figure 3.30. SEM-EDS images of natural pozzolans used in N17 at magnifications of 500 (a), 1000 (b), 4000 (c), 10000 (d), 20000 (e)

Microstructure of artificial pozzolans consisted of amorphous particles (Figure 3.31, 3.32) indicating little vitrification that suggested low heating temperatures ( $< 950$  °C) during their production. This finding also supported XRD analyses (Figure 3.12-3.14) that high temperature mineral phases like mullite and cristobalite were not identified (Cardiano et al. 2004).

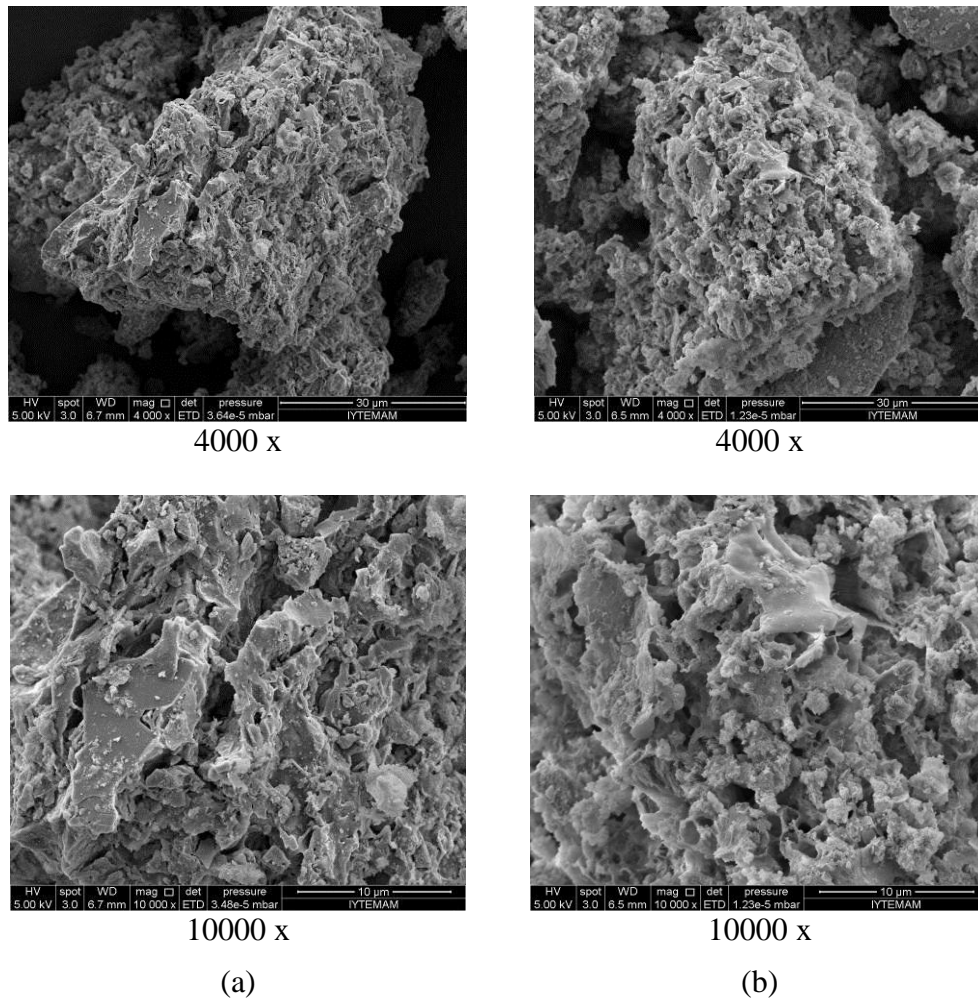


Figure 3.31. SEM-EDS images of artificial pozzolans used in A5 (a), N1 (b)

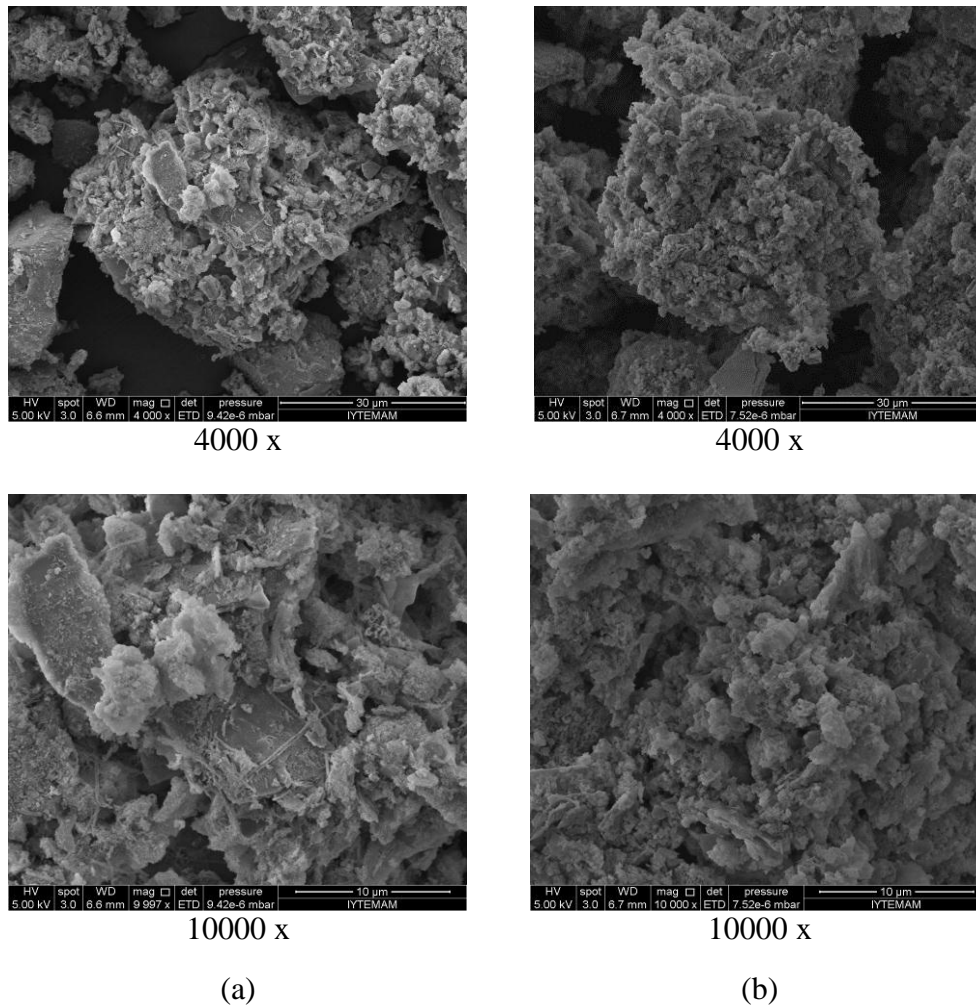


Figure 3.32. SEM-EDS images of artificial pozzolans used in N11 (a), N15(1) (b)

### 3.6. Characteristics of Binders

Fine mortar matrices ( $< 63 \mu\text{m}$ ) which were composed of small grain sized aggregates and carbonated lime ( $\text{CaCO}_3$ ) were defined as “binder” (Bakolas et al. 1995, Middendorf et al. 2005). Binders were considered as the main part that gave hydraulic character and high strength to the mortar (Bakolas et al. 1995, Middendorf et al. 2005). Mineralogical and chemical compositions, microstructural and hydraulic properties of binders of Roman mortars were determined by XRD, SEM-EDS and TGA analyses.

### 3.6.1. Mineralogical and Chemical Compositions of Binders

Mineralogical compositions of binders were determined by XRD analysis. XRD patterns indicated that binders of lime mortars produced by natural pozzolans from Aigai were mainly composed of calcite ( $\text{CaCO}_3$ ), quartz ( $\text{SiO}_2$ ), albite ( $\text{Na(AlSi}_3\text{O}_8)$ ) and anorthite ( $\text{CaAl}_2\text{Si}_2\text{O}_8$ ) minerals (Figure 3.33). In addition to calcite, quartz and albite, muscovite ( $\text{KAl}_2(\text{Si}_3\text{Al})\text{O}_{10}(\text{OH,F})_2$ ) was the other mineral phase detected in the XRD patterns of binders of lime mortars produced by natural pozzolans from Nysa (Figure 3.34).

XRD analysis revealed that lime mortars produced by artificial pozzolans from Aigai were found to be composed of calcite, albite, anorthite and quartz (Figure 3.35). Similarly, calcite, quartz, muscovite, anorthite and albite minerals were observed on the XRD patterns of lime mortars produced by artificial pozzolans from Nysa (Figure 3.36, 3.37).

Among the minerals detected in the binders both produced by natural and artificial pozzolans by XRD, calcite was originated from carbonated lime whereas the others were from aggregates.

The expected peaks of the pozzolanic minerals like amorphous silica and the hydraulic products formed as a result of the reaction between lime and pozzolanic aggregates, like calcium silicate hydrate and calcium aluminate hydrate were not observed on the XRD patterns of binders due to their amorphous structure (Haga et al. 2002).

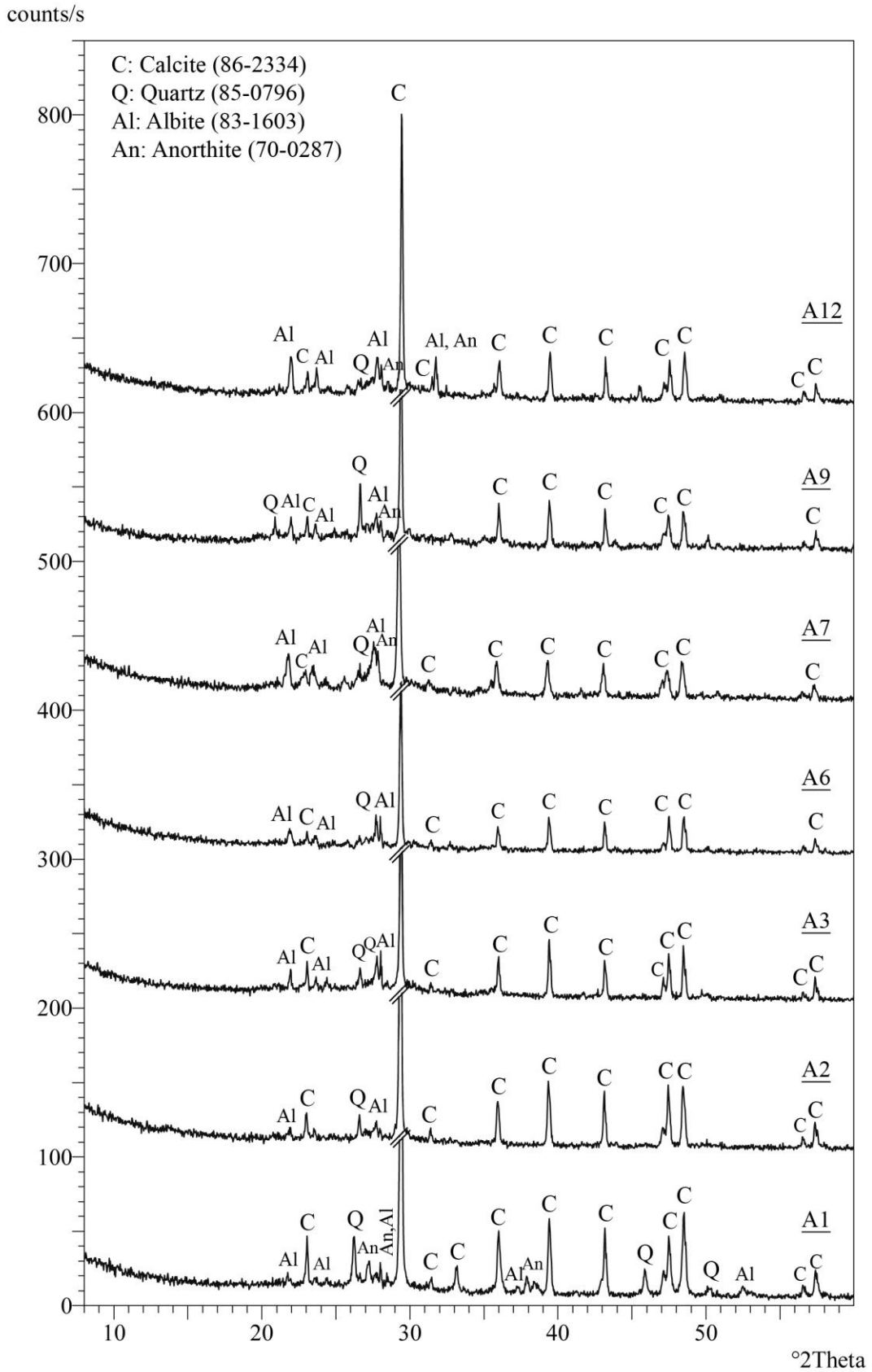


Figure 3.33. XRD patterns of binders produced by natural pozzolans from Aigai



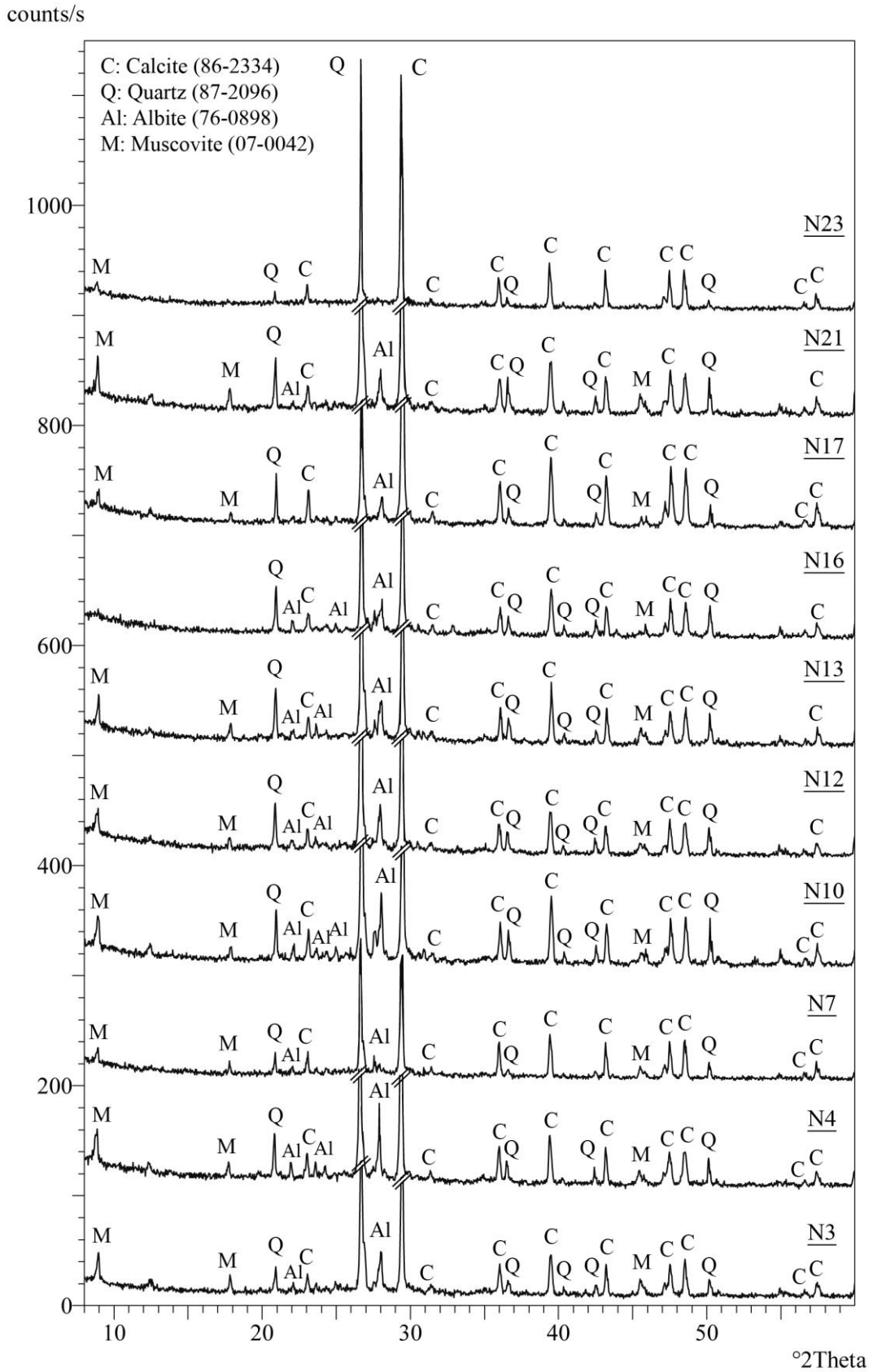


Figure 3.34. XRD patterns of binders produced by natural pozzolans from Nysa

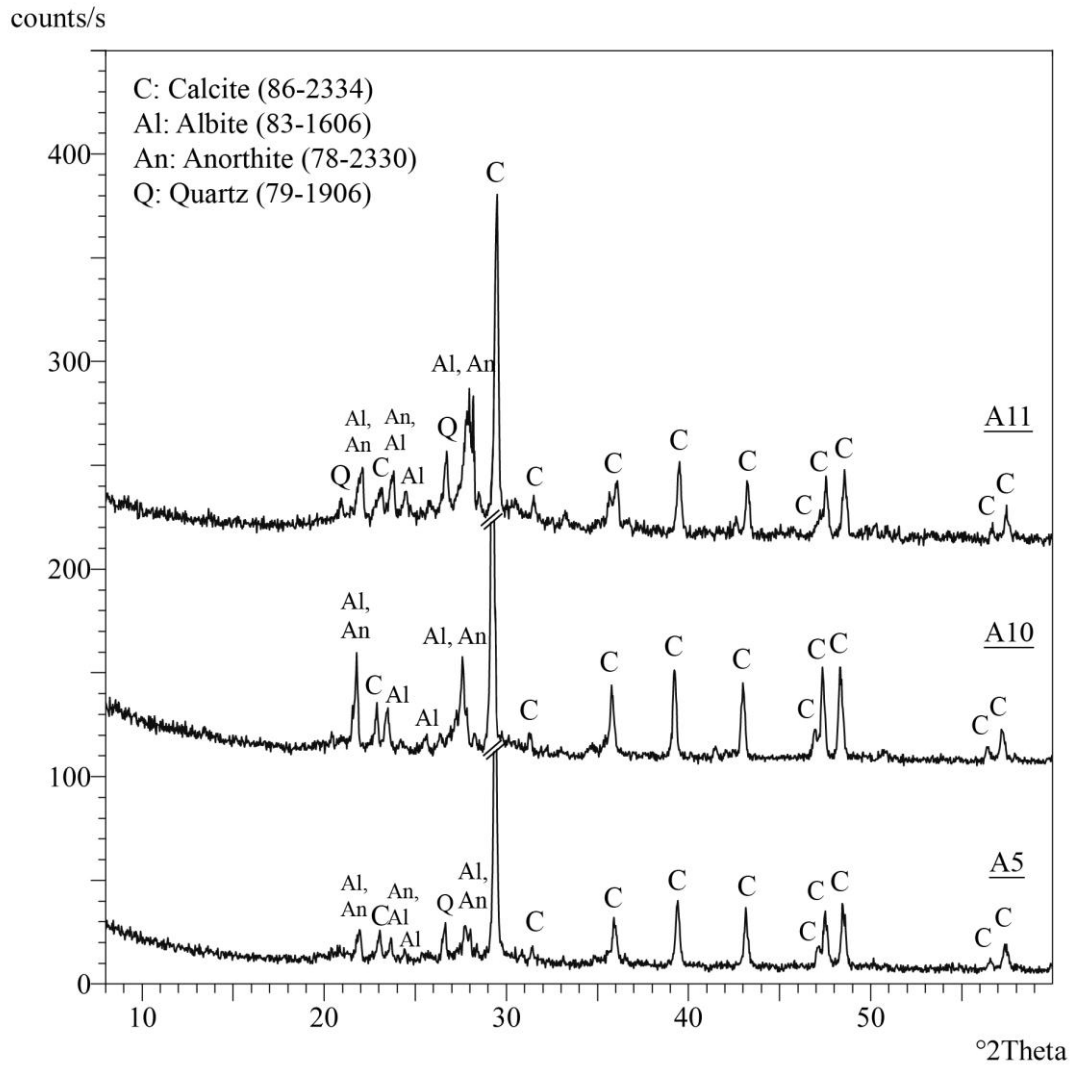


Figure 3.35. XRD patterns of binders produced by artificial pozzolans from Aigai

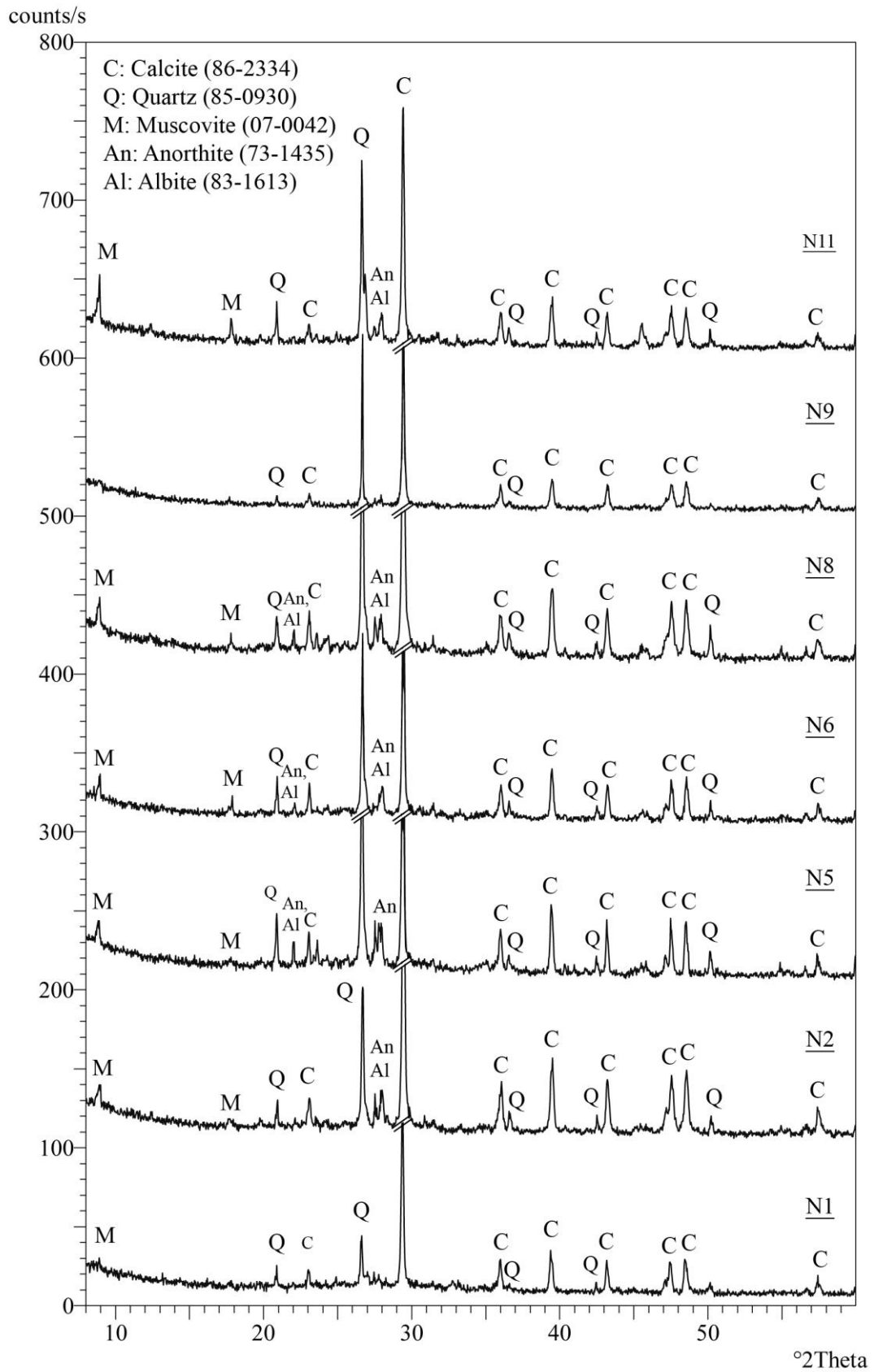


Figure 3.36. XRD patterns of binders produced by artificial pozzolans from Nysa (I)

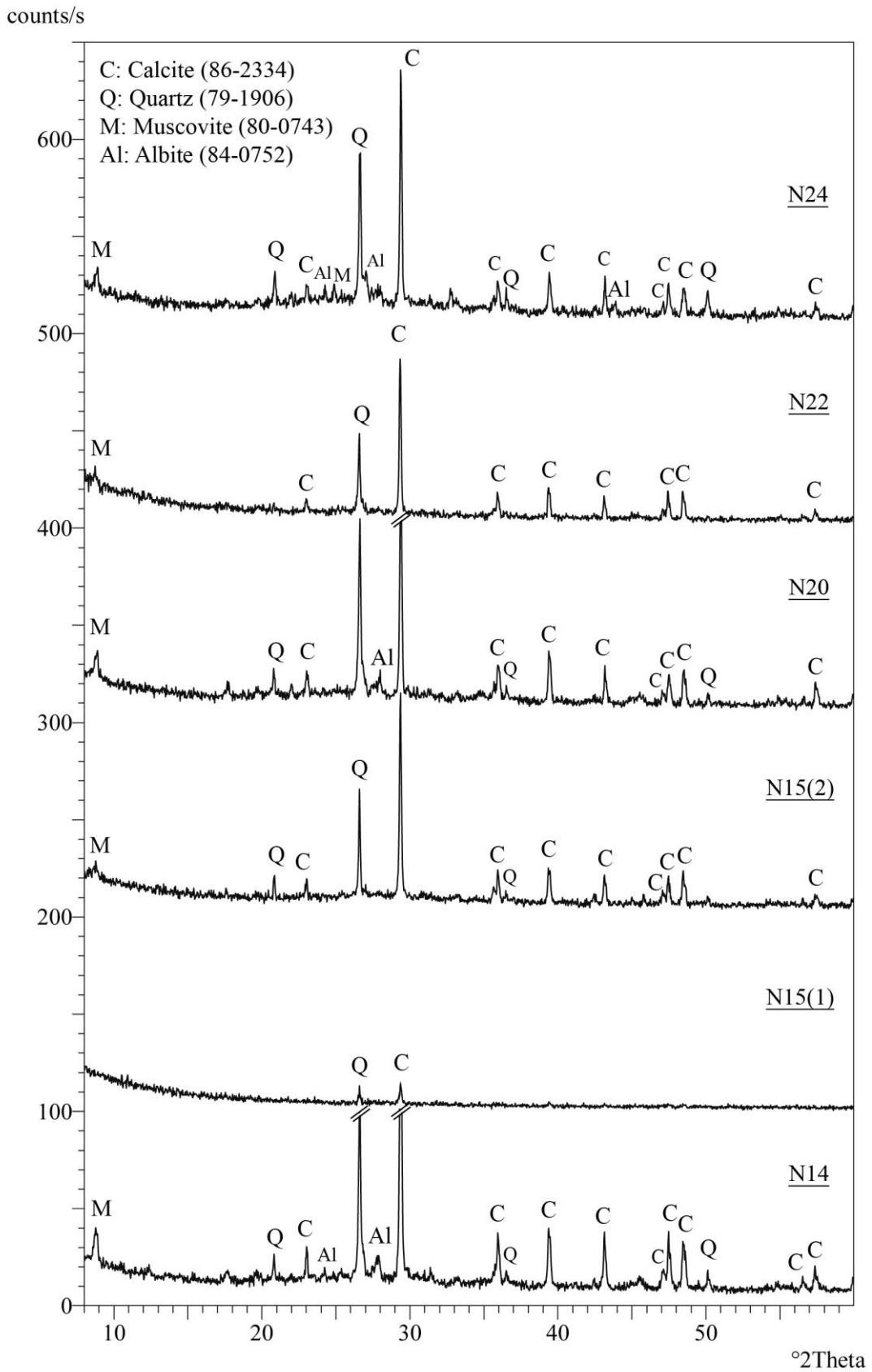


Figure 3.37. XRD patterns of binders produced by artificial pozzolans from Nysa (II)

Some of the previous studies defined mineralogical compositions of Roman lime mortars through the investigation of binder part of the mortars by XRD analysis (Degryse et al. 2002, Genestar et al. 2006, Jackson et al. 2009, Robador et al. 2010, Jackson et al. 2011, Kramar et al. 2011); whereas some other previous studies carried out mineralogical compositions analysis on the whole of mortar samples by mostly XRD (Benedetti et al. 2004, Sánchez-Moral et al. 2005, Velosa et al. 2007, Franquelo et al. 2008, Miriello et al. 2010, Robador et al. 2010, Miriello et al. 2011).

Binders of Roman period lime mortars were found to be composed of mainly calcite, quartz, anorthite and muscovite similar to the binders of lime mortars from Aigai and Nysa. But further, analcime, diopside, strätlingite, sanidine, leucite, vaterite were the other minerals determined by previous studies (Table 3.12).

The most common minerals detected in the compositions of mortars were calcite, quartz, anorthite, albite and muscovite (Table 3.13).

Table 3.12. Mineralogical compositions of binders of Roman lime mortars determined by previous studies

<b>Roman Building/Site (Reference)</b>	<b>Aggregate Type of Mortar</b>	<b>Method</b>	<b>Minerals</b>
Sagalassos - Turkey ( <i>Degryse et al. 2002</i> )	Natural poz.	XRD	Sanidine, anorthite, amorphous glass phase
The Markets of Trajan - Rome (Italy) ( <i>Jackson et al. 2009</i> )	Natural poz.	XRD	Calcite, diopside, sanidine, leucite, analcime, clay mineral, strätlingite
The Theatre of Marcellus - Rome (Italy) ( <i>Jackson et al. 2011</i> )	Natural poz.	XRD	Calcite, analcime, leucite, diopside, vaterite, strätlingite
The Forum and residences of Pollentia - Mallorca (Spain) ( <i>Genestar et al. 2006</i> )	Artificial poz.	XRD	Calcite, quartz
Mithraeum House - Spain ( <i>Robador et al. 2010</i> )	Artificial poz.	XRD	Calcite, quartz, anorthite, mica
Roman villa - Mošnje (Slovenia) ( <i>Kramar et al. 2011</i> )	Artificial poz.	XRD	Calcite, dolomite, quartz, muscovite

Table 3.13. Mineralogical compositions of Roman lime mortars determined by previous studies

<b>Roman Building/Site (Reference)</b>	<b>Aggregate Type of Mortar</b>	<b>Method</b>	<b>Minerals</b>
Roman Villa in Sorrento of Pollio Felice - Naples (Italy) ( <i>Benedetti et al. 2004</i> )	Natural poz.	XRD <sup>2</sup>	Calcite, sanidine, aragonite, graphite, amorphous materials
Saint Callistus and Domitilla catacombs - Rome (Italy) ( <i>Sánchez-Moral et al. 2005</i> )	Natural poz.	XRD	Calcite, phyllosilicate, analcime, augite, feldspar ( <i>trace</i> ), quartz ( <i>trace</i> )
Houses in Pompeii - Italy ( <i>Miriello et al. 2010</i> )	Natural poz.	XRD, petrographic analysis	Calcite, anorthite, analcime, leucite, sanidine, augite, phlogopite, albite, sillimanite, goethite, cowlesite, wollastonite, zircon, ludwigite, CSH phases (hillebrandite, okenite, tobermorite, xonotlite)
Kyme - Turkey ( <i>Miriello et al. 2011</i> )	Natural poz.	XRPD, SEM-EDS	Calcite, anorthite, quartz, goethite, muscovite, vaterite, chlorite, albite
Roman Villa in Sorrento of Pollio Felice - Naples (Italy) ( <i>Benedetti et al. 2004</i> )	Artificial poz.	XRD	Calcite, quartz, muscovite, hematite, periclase, diopside, analcime, labradorite, pyrope
Augustan and Trajan Baths - Conímbriga (Portugal) ( <i>Velosa et al. 2007</i> )	Artificial poz.	XRD	Quartz, calcite, feldspar, phyllosilicates, dolomite ( <i>trace</i> ), magnesite ( <i>trace</i> ), pyrite ( <i>trace</i> )
Mithraeum House - Spain ( <i>Franquelo et al. 2008</i> )	Artificial poz.	XRD	Quartz, calcite, mica, anorthite
Houses in Pompeii - Italy ( <i>Miriello et al. 2010</i> )	Artificial poz.	XRD, petrographic analysis	Calcite, quartz, albite, tobermorite, montmorillonite, andradite, augite, phlogopite, sanidine, nepheline, dypingite, plagioclase
Mithraeum House - Spain ( <i>Robador et al. 2010</i> )	Artificial poz.	XRD	Quartz, calcite, anorthite, hematite

Major chemical compositions of binders of Roman lime mortars were determined by SEM-EDS analysis. The analysis results revealed that binders of lime mortars produced by natural pozzolans were composed of high amounts of SiO<sub>2</sub> (37.83-52.71 %), CaO (22.51-35.84 %), moderate amounts of Al<sub>2</sub>O<sub>3</sub> (9.89-15.70 %), and lower amounts of Fe<sub>2</sub>O<sub>3</sub> (1.54-6.13 %), Na<sub>2</sub>O (1.08-5.65 %), K<sub>2</sub>O (1.33-5.55 %), TiO<sub>2</sub> (0.31-1.18 %) (Table 3.14). Chemical compositions of binders with natural pozzolans from Aigai and Nysa resembled each other except Fe<sub>2</sub>O<sub>3</sub> and MgO which were relatively higher in Nysa samples.

Binders of lime mortars produced by artificial pozzolans also consisted of high amounts of SiO<sub>2</sub> (23.73-55.59 %), CaO (13.13-60.82 %), moderate amounts of Al<sub>2</sub>O<sub>3</sub> (8.57-21.70 %), and lower amounts of Fe<sub>2</sub>O<sub>3</sub> (2.11-6.97 %), Na<sub>2</sub>O (0.84-2.10 %), K<sub>2</sub>O (1.10-3.51 %), TiO<sub>2</sub> (0.21-1.30 %) (Table 3.14). Al<sub>2</sub>O<sub>3</sub> and MgO content of Nysa samples were detected higher than those of Aigai samples.

Fe<sub>2</sub>O<sub>3</sub> and Al<sub>2</sub>O<sub>3</sub> content differences may be due to the pozzolans, and difference of MgO content may be due to lime used for the production of mortars.

Major chemical compositions of binders with natural pozzolans from Aigai and Nysa were almost similar to the compositions of same type of binders and mortars which were determined by previous studies (Table 3.15, 3.16). On the other hand, chemical compositions of binders of Aigai and Nysa samples with artificial pozzolans were identified slightly different from the chemical compositions of mortars determined by previous studies.

Trace elements compositions of binders were not investigated since it was not possible to determine the source of trace elements in such a composite structure consisted of lime and pozzolans.

Table 3.14. Major chemical compositions of binders of Roman lime mortars determined by SEM-EDS

<b>Sample Type</b>	<b>SiO<sub>2</sub></b>	<b>TiO<sub>2</sub></b>	<b>Al<sub>2</sub>O<sub>3</sub></b>	<b>Fe<sub>2</sub>O<sub>3</sub></b>	<b>MgO</b>	<b>CaO</b>	<b>Na<sub>2</sub>O</b>	<b>K<sub>2</sub>O</b>
Lime mortars with natural pozzolanic aggregates from Aigai (A1, A2, A3, A6, A7, A9, A12)	37.83 - 52.71	0.32 - 0.64	10.02 - 13.54	1.54 - 2.51	1.69 - 2.76	25.30 - 31.34	1.21 - 5.65	1.33 - 5.55
	47.65 (ave.)	0.44 (ave.)	11.92 (ave.)	2.12 (ave.)	2.35 (ave.)	29.99 (ave.)	2.19 (ave.)	2.55 (ave.)
Lime mortars with natural pozzolanic aggregates from Nysa (N3, N4, N7, N10, N12, N13, N16, N17, N21, N23)	38.26 - 51.30	0.31 - 1.18	9.89 - 15.70	3.40 - 6.13	2.29 - 5.03	22.51 - 35.84	1.08 - 2.55	1.50 - 3.85
	45.24 (ave.)	1.80 (ave.)	12.90 (ave.)	4.50 (ave.)	3.64 (ave.)	27.88 (ave.)	1.64 (ave.)	2.21 (ave.)
Lime mortars with artificial pozzolanic aggregates from Aigai (A5, A10, A12)	23.73 - 52.32	0.54 - 0.77	8.57 - 17.05	2.18 - 4.80	1.66 - 2.25	19.93 - 60.82	1.19 - 1.58	1.10 - 2.25
	37.17 (ave.)	0.64 (ave.)	12.60 (ave.)	3.66 (ave.)	1.92 (ave.)	41.02 (ave.)	1.38 (ave.)	1.60 (ave.)
Lime mortars with artificial pozzolanic aggregates from Nysa (N1, N2, N5, N6, N8, N9, N11, N14, N15(1), N15(2), N20, N22, N24)	24.78 - 55.59	0.21 - 1.30	12.18 - 21.70	2.11 - 6.97	2.78 - 7.68	13.13 - 50.45	0.84 - 2.10	1.24 - 3.51
	39.78 (ave.)	0.83 (ave.)	15.94 (ave.)	4.71 (ave.)	4.16 (ave.)	30.72 (ave.)	1.35 (ave.)	2.52 (ave.)



Table 3.15. Major chemical compositions of binders (%) determined by previous studies

<b>Roman Building/Site (Reference)</b>	<b>Agg. Type of Mortar</b>	<b>Method</b>	<b>SiO<sub>2</sub></b>	<b>TiO<sub>2</sub></b>	<b>Al<sub>2</sub>O<sub>3</sub></b>	<b>Fe<sub>2</sub>O<sub>3</sub></b>	<b>MnO</b>	<b>MgO</b>	<b>CaO</b>	<b>Na<sub>2</sub>O</b>	<b>K<sub>2</sub>O</b>	<b>P<sub>2</sub>O<sub>5</sub></b>
Houses in Pompeii - Italy (Miriello et al. 2010)	Natural poz.	SEM-EDS	15.21-50.79	n.d.-0.90	5.01-15.74	0.97-4.16	-	1.83-13.14	18.08-74.16	n.d.-1.59	0.77-4.33	-
Kyme - Turkey (Miriello et al. 2011)	Natural poz.	SEM-EDS	3.81-15.11	n.d.-0.32	1.22-4.38	0.40-0.80	n.d.-0.41	1.39-1.97	74.95-90.63	0.77-1.39	0.32-0.81	0.87-1.15
The Markets of Trajan - Rome (Jackson et al. 2009)	Natural poz.	XRF	30.65-35.71	0.44-0.65	11.08-12.61	4.38-6.98	0.11-0.14	1.76-3.93	20.29-21.70	0.78-1.24	2.51-3.69	0.29-0.48
Rome - Italy (Jackson et al. 2010)	Natural poz.	SEM-EDS	34.19-34.77	0.64-0.66	11.48-11.74	7.09-7.35	0.14	3.06-3.32	16.13-19.71	0.48-1.16	4.19-4.35	0.6-1.28
The Theatre of Marcellus - Rome (Jackson et al. 2011)	Natural poz.	Plasma mass spec.	27.44-38.62	0.36-0.52	9.84-12.80	4.10-6.00	0.10-0.15	2.04-2.43	14.30-26.80	1.63-1.88	0.79-2.28	0.32-0.47
Houses in Pompeii - Italy (Miriello et al. 2010)	Artificial poz.	SEM-EDS	5.19-14.28	0.06-0.26	1.55-4.58	0.28-1.16	-	2.29-6.34	71.77-90.62	0.28-0.90	0.26-0.71	-

Table 3.16. Major chemical compositions of mortars (%) determined by previous studies

<b>Roman Building/Site (Reference)</b>	<b>Agg. Type of Mortar</b>	<b>Method</b>	<b>SiO<sub>2</sub></b>	<b>TiO<sub>2</sub></b>	<b>Al<sub>2</sub>O<sub>3</sub></b>	<b>Fe<sub>2</sub>O<sub>3</sub></b>	<b>MnO</b>	<b>MgO</b>	<b>CaO</b>	<b>Na<sub>2</sub>O</b>	<b>K<sub>2</sub>O</b>	<b>P<sub>2</sub>O<sub>5</sub></b>
Houses in Pompeii - Italy (Miriello et al. 2010)	Natural poz.	XRF	32.31-45.06	0.52-0.86	9.95-14.73	5.11-7.35	0.10-0.14	2.88-8.44	12.15-27.50	1.27-3.47	2.40-5.00	0.18-0.48
Kyme - Turkey (Miriello et al. 2011)	Natural poz.	XRF	30.60-42.46	0.37-0.51	6.80-9.34	1.67-2.86	0.07-0.09	1.72-2.15	21.36-30.67	0.27-0.40	1.16-2.01	0.19-0.31
Saint Callistus and Domitilla catacombs - Rome (Italy) (Sánchez-Moral et al. 2005)	Natural poz.	AAS, EMPA	27.55-35.32	0.33-0.43	10.11-12.31	3.53-3.73	0.10-0.15	1.95-1.99	19.39-28.98	1.23-1.95	1.22-1.25	0.15-0.29
Houses in Pompeii - Italy (Miriello et al. 2010)	Artificial poz.	XRF	34.95-42.94	0.66-0.80	11.14-14.61	6.13-7.24	0.12-0.15	3.94-5.23	16.80-24.65	1.03-1.30	2.08-2.40	0.26-0.32
Mithraeum House - Spain (Robador et al. 2010)	Artificial poz.	XRF	54.4-57.9	0.004-0.005	2.6-3.4	3.8-5.1	-	0-0.005	18.5-19.5	0.1	0.6	-
Augustan and Trajan Baths - Portugal (Velosa et al. 2007)	Artificial poz.	XRF	28.42-51.21	0.34-0.63	7.52-11.31	2.29-3.59	0.02-0.04	1.46-4.48	12.95-22.05	0.27-0.69	0.70-1.36	0.22-0.35

### **3.6.2. Quantitative Determination of CaCO<sub>3</sub> and SiO<sub>2</sub> Content in Binders**

“Binder” part of the mortars were defined as the fine matrices (< 63 µm) composed of small grain sized silica (SiO<sub>2</sub>) and carbonated lime (CaCO<sub>3</sub>) and considered as the main part that gave hydraulic character and high strength to the mortar (Bakolas et al. 1995, Middendorf et al. 2005). Compositions of binders were investigated by many studies as a part of lime mortar characterization by using several different techniques such as XRD, SEM-EDS, XRF, AAS and LIBS (Bakolas et al. 1995, Barba et al. 2009, Miriello et al. 2011).

XRD is suitable for identification of minerals in crystalline structure. Amorphous substances and organic additives can not be detected by XRD. However, FTIR can be used for the identification of amorphous minerals and organic additives, and also for their quantification.

Scanning Electron Microscope (SEM) is used for determination of microstructural properties of binders. It is also used for determination of chemical compositions if it is equipped with X-Ray Energy Dispersive System (EDS).

X-ray Fluorescence (XRF) and Atomic Absorption Spectroscopy (AAS) are more precise methods than SEM-EDS for determination of chemical compositions of binders. But these analyses need experience, complex sample preparation, and takes a long time (Reig 2002). Moreover, binder analyses do not require the use of very sensitive analysis due to their non-homogeneous characteristics.

Laser Induced Breakdown Spectroscopy, LIBS (Radziemski and Cremers 1986), has emerged in the last two decades as an elemental analysis technique for the determination of chemical composition of the various cultural heritage objects (Anglos and Miller 2006). LIBS, with its ability to make multielement and on-line analysis, offers several advantages over commonly employed atomic spectrometric techniques.

In this study, a relatively fast and easy method for the quantitative determination of CaCO<sub>3</sub> and SiO<sub>2</sub> content in binder compositions was proposed by using FTIR, LIBS, SEM-EDS and XRD analyses.

For this purpose, a series of standard mixtures of CaCO<sub>3</sub> and SiO<sub>2</sub> were prepared in ten combinations of varying weight ratios from 0.5 to 5.0, to generate calibration curves for FTIR, SEM-EDS, XRD and LIBS analysis. XRD, SEM-EDS, FTIR and LIBS analysis were then carried out for the prepared binder samples to find out the

weight ratios of  $\text{CaCO}_3$  to  $\text{SiO}_2$  by using calibration equations obtained from standard mixtures analyses.

### 3.6.2.1. FTIR, SEM-EDS, LIBS and XRD Analysis of Standard Mixtures of $\text{CaCO}_3$ and $\text{SiO}_2$

FTIR, SEM-EDS, LIBS and XRD analysis of standard mixtures were carried out and the calibration curves were generated. Details of each analysis are given below.

*FTIR Analysis:* FTIR spectra of standard mixtures showed the characteristics of  $\text{CaCO}_3$  and  $\text{SiO}_2$  bands. The main  $\text{CaCO}_3$  bands at  $1432\text{ cm}^{-1}$  (C-O stretching), 876 and  $712\text{ cm}^{-1}$  (C-O bending) and  $\text{SiO}_2$  bands at  $1100\text{ cm}^{-1}$  (Si-O stretching) and  $470\text{ cm}^{-1}$  (Si-O bending) were indicated (Figure 3.38).

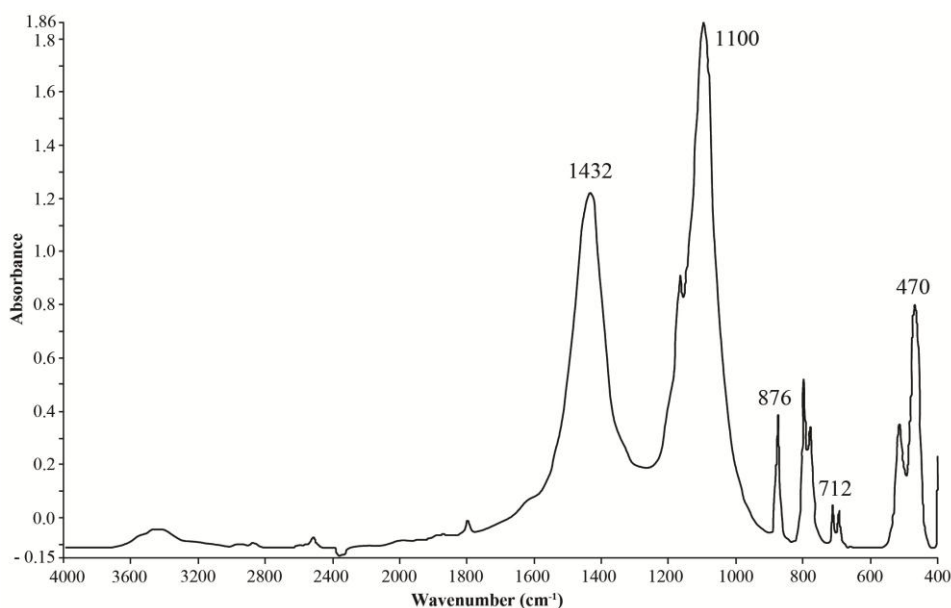


Figure 3.38. FTIR spectra of a standard mixture ( $\text{CaCO}_3/\text{SiO}_2$ :1/1)

The FTIR spectrum of the  $\text{CaCO}_3$  and  $\text{SiO}_2$  mixtures demonstrated that there is no interference between the bands of the two components. Hence, in the preparation of calibration curves, stretching bands of  $\text{CaCO}_3$  and  $\text{SiO}_2$  were used. The weak bands of bending vibrations of  $\text{CaCO}_3$  and  $\text{SiO}_2$  were not used due to low sensitivity values when compared to the bands of the stretching ones. As it is seen in Figure 3.39, calibration

curve showed the linear relationship with good correlation coefficient. The error bars shown on the graph were obtained from the standard deviation of three replicate FTIR measurements and the error in terms of the relative standard deviation (RSD) of measurements were calculated to be around 8 %.

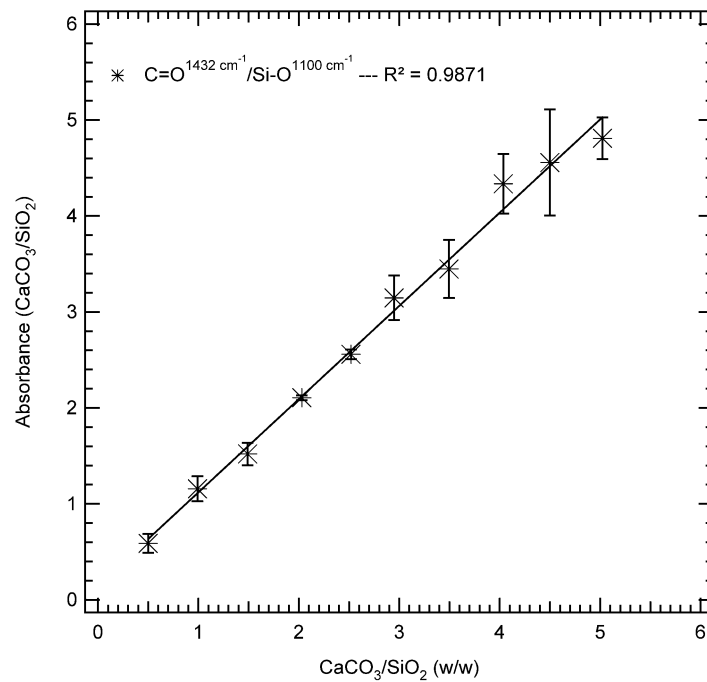


Figure 3.39. Calibration curve for FTIR analysis results of standard mixtures

*SEM-EDS analysis:* The chemical compositions of the standard mixtures were determined by SEM-EDS analysis and the weight ratios of CaCO<sub>3</sub> and SiO<sub>2</sub> were used in the preparation of the calibration curve. Calibration curve showed the linear relationship with good correlation coefficient (Figure 3.40). The error bars shown on the graph were obtained from the standard deviations of the measurements, and the average error (RSD) was estimated to be around 7.7 %.

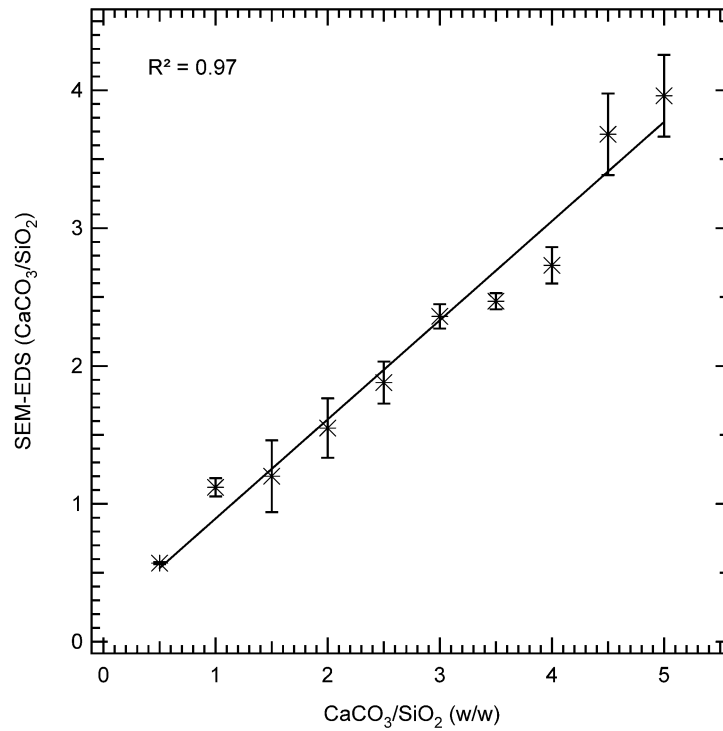


Figure 3.40. Calibration curve for SEM-EDS analysis results of standard mixtures

LIBS analysis: The LIBS spectra of standard mixtures of CaCO<sub>3</sub> and SiO<sub>2</sub> showed neutral Ca(I) at 504.2, 534.9, 714.8 and 720.2 nm and neutral Si(I) at 288.15 nm (Figure 3.41).

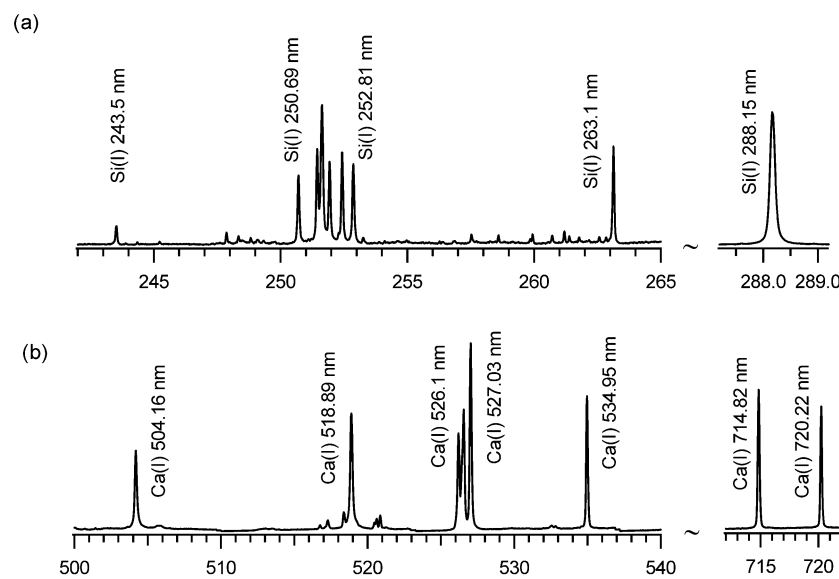


Figure 3.41. LIBS spectra of a standard mixture (CaCO<sub>3</sub>/SiO<sub>2</sub>:1/1)

They were used to generate calibration curves against their weight ratios. The calibration graphs present linear relationships in signal intensities versus Ca/Si weight ratios with good correlation coefficients (Figure 3.42). However, Ca(I) line emission at 504.16 nm presents higher sensitivity compared to other Ca(I) emissions at 714.8 nm and 720.2 nm due to the higher spectral sensitivity of the spectrograph at that wavelength. The error bars shown in the graph were obtained from the standard deviation of ten sequential LIBS measurements, and the error was estimated to be around 10%.

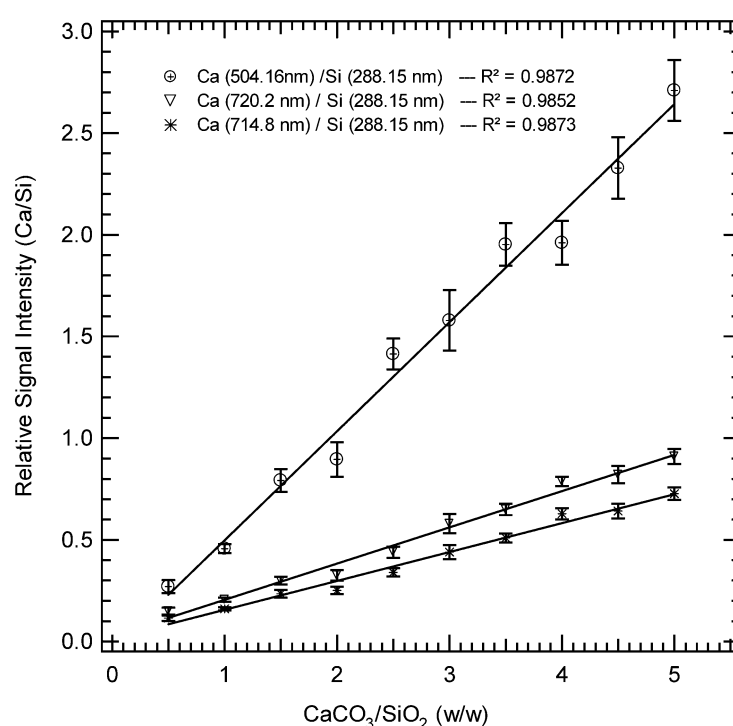


Figure 3.42. Calibration curve for LIBS analysis results of standard mixtures

XRD analysis : In the XRD patterns of the standard samples, the main CaCO<sub>3</sub> peaks at 2-thetas of 22.9, 29.3, 39.3, 43.1, 47.4° and SiO<sub>2</sub> peaks at 2 thetas of 22.9, 29.3, 39.3, 43.1, 47.4° were indicated (Figure 3.43).

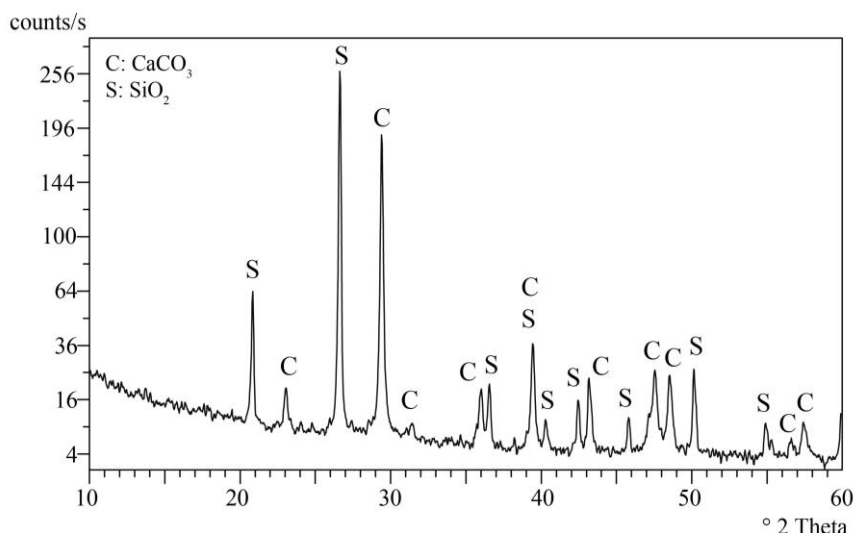


Figure 3.43. XRD pattern of a standard mixture (CaCO<sub>3</sub>/SiO<sub>2</sub>:1/1)

The CaCO<sub>3</sub> and SiO<sub>2</sub> peaks were then analyzed using X'Pert High Score Plus analysis software to find weight percent of CaCO<sub>3</sub> and SiO<sub>2</sub> in the mixtures by Rietveld method. The weight percent of CaCO<sub>3</sub> and SiO<sub>2</sub> were used to generate a calibration curve against their standard concentration ratios (Figure 3.44). As it is seen in Figure 3.44, calibration curve showed the linear relationship with good correlation coefficient. The observed errors ranged between 7 % and 10 %.

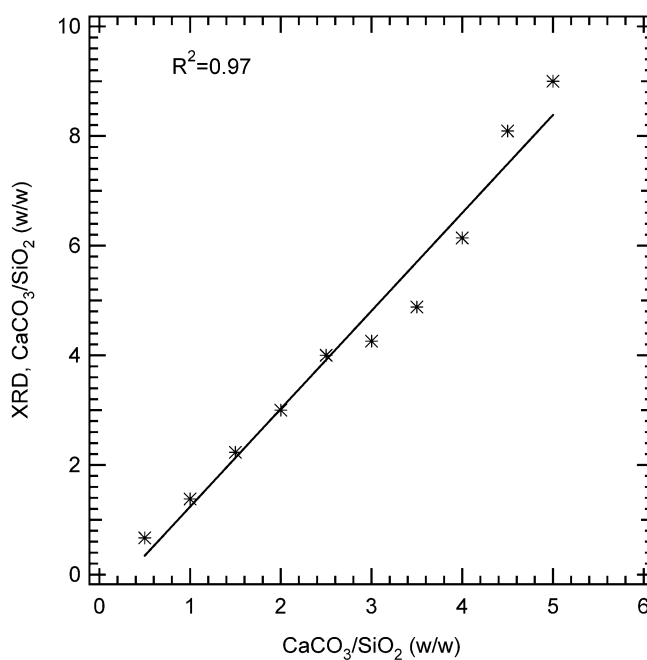


Figure 3.44. Calibration curve for XRD analysis results of standard mixtures



### 3.6.2.2. Determination of CaCO<sub>3</sub>/SiO<sub>2</sub> Ratio in the Binders of Roman Mortar Samples by FTIR, SEM-EDS, LIBS and XRD Analysis

The binders of the mortars collected from Roman buildings were mainly composed of CaCO<sub>3</sub> and SiO<sub>2</sub>. They are hard, fine grained and compact due to strong adherence between silica and lime.

*FTIR analysis:* The FTIR spectrum of the binders showed the bands of stretching and bending vibrations of CaCO<sub>3</sub> (~1430 cm<sup>-1</sup>, 874 cm<sup>-1</sup>, 712 cm<sup>-1</sup>) and SiO<sub>2</sub> (~1031 cm<sup>-1</sup>, ~470 cm<sup>-1</sup>) (Figure 3.45).

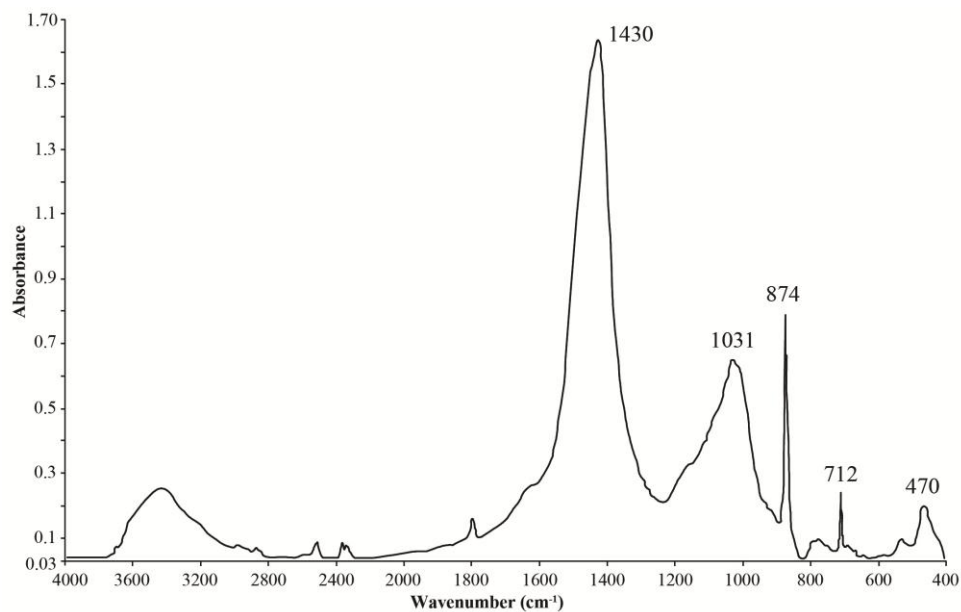


Figure 3.45. FTIR spectrum of a Roman binder sample (N2)

The areas of absorption of CaCO<sub>3</sub> (1430 cm<sup>-1</sup>) and SiO<sub>2</sub> (1031 cm<sup>-1</sup>) were used in the determination of weight ratios of CaCO<sub>3</sub> to SiO<sub>2</sub> by using the line equation of FTIR analysis (Figure 3.39). The results indicated that the CaCO<sub>3</sub>/SiO<sub>2</sub> ratio was between 0.5 and 2.2 in the binders of the mortars compositions (Table 3.17).

Table 3.17 CaCO<sub>3</sub>/SiO<sub>2</sub> ratio in the binders of Roman mortar samples by FT-IR, SEM-EDS, XRD and LIBS analysis

Sample	CaCO <sub>3</sub> /SiO <sub>2</sub>			
	FTIR	SEM-EDS	LIBS	XRD
A1	1.9	1.9	2.2	0.7
A2	1.2	1.3	1.5	20.5
A3	0.6	0.6	0.7	6.0
A7	1.3	1.6	1.0	18.4
N4	0.6	0.5	0.7	1.8
N10	2.2	2.2	1.6	3.5
N12	0.6	0.8	0.8	1.8
N13	0.5	0.6	0.6	1.7

*SEM-EDS analysis:* The elemental compositions of the binders expressed as the percent oxide were determined by SEM-EDS analysis. The results indicated that binders contain high amounts of CaO and SiO<sub>2</sub> and low amounts of Al<sub>2</sub>O<sub>3</sub> and Fe<sub>2</sub>O<sub>3</sub> (Table 3.18).

Table 3.18 Elemental compositions of binders of Roman mortars

Sample	Na <sub>2</sub> O	K <sub>2</sub> O	CaO	MgO	SiO <sub>2</sub>	Al <sub>2</sub> O <sub>3</sub>	Fe <sub>2</sub> O <sub>3</sub>	TiO <sub>2</sub>
A1	1.6±0.2	1.7±0.1	42.5±1.8	2.2±0.1	40.4±1.2	9.4±0.1	1.7±0.4	0.6±0.2
A2	1.9±0.1	2.2±0.3	32.6±0.6	2.5±0.4	46.5±0.8	11.7±0.4	2.1±0.4	0.5±0.1
A3	2.2±0.6	2.0±0.2	19.7±0.7	4.4±0.7	56.9±1.1	12.4±0.7	2.1±0.2	0.4±0.3
A7	1.2±0.0	2.4±0.1	39.1±0.6	3.2±0.3	42.4±0.7	9.0±0.3	2.4±0.4	0.4±0.0
N4	2.2±0.2	2.3±0.3	15.7±1.4	3.5±0.3	55.2±0.7	18.3±0.6	1.8±0.1	1.1±0.2
N10	2.2±0.6	1.9±0.1	41.5±4.9	4.6±1.0	33.9±2.9	12.1±1.1	3.3±1.4	0.5±0.5
N12	1.9±0.2	2.8±0.2	22.4±0.3	3.7±0.3	51.0±1.4	13.2±0.3	4.1±1.4	0.9±0.9
N13	2.1±0.3	2.0±0.2	18.1±1.9	3.7±0.5	54.4±2.3	15.3±1.1	3.0±1.8	1.6±0.5

The percent CaO and SiO<sub>2</sub> were used in the determination of weight ratios of CaCO<sub>3</sub> to SiO<sub>2</sub> by using the line equation of SEM-EDS analysis (Figure 3.40). The

results indicated that the  $\text{CaCO}_3/\text{SiO}_2$  ratio was between 0.5 and 2.2 in the binders of the mortars compositions (Table 3.17).

*LIBS analysis:* LIBS spectrum of the binders showed the strong Ca and Si lines together with weak Mg and Al lines. A full and detailed spectra of the sample (N2) is shown in Figure 3.46.

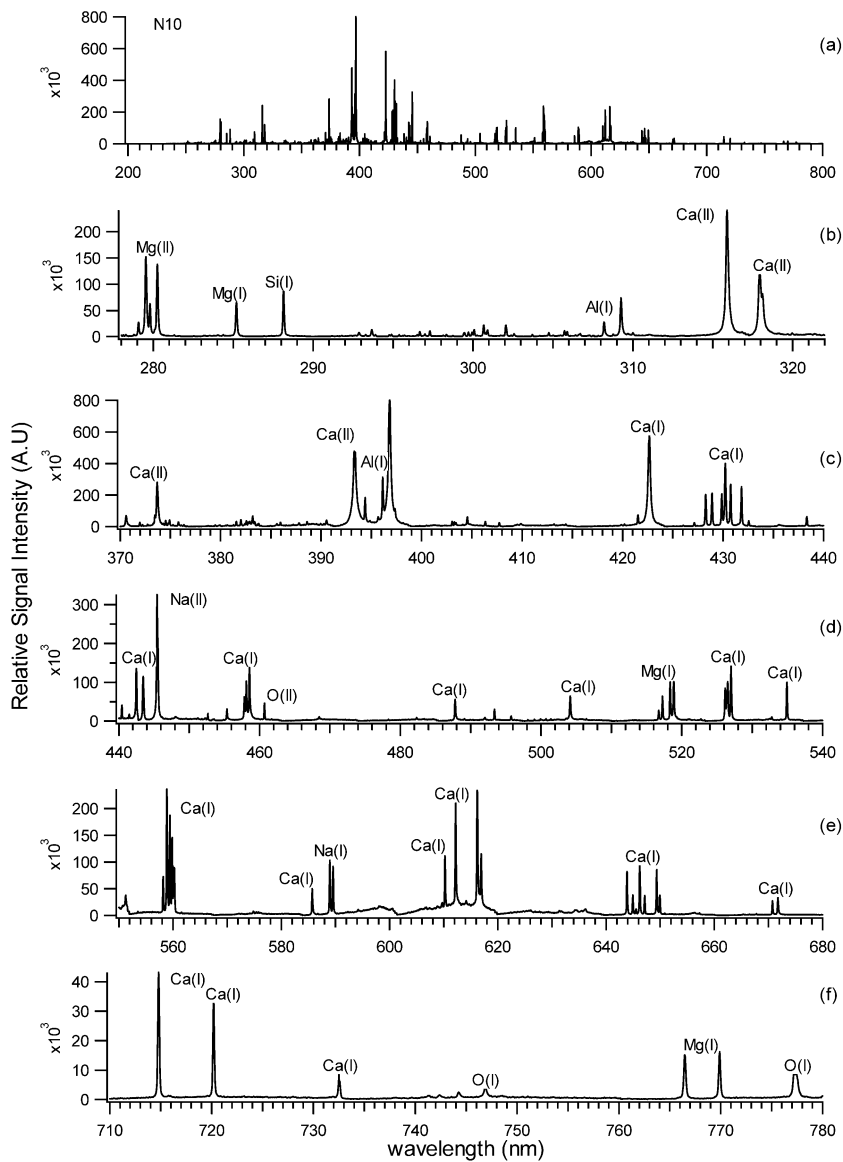


Figure 3.46. LIBS spectra of a Roman binder sample (N10)

The line intensities of Ca observed at 504.16 nm and Si at 288.15 nm were used in the determination of the weight ratios of  $\text{CaCO}_3$  to  $\text{SiO}_2$  in the binders of the mortars by using the line equation of LIBS analysis (Figure 3.16). The results showed that the  $\text{CaCO}_3/\text{SiO}_2$  ratio was between 0.6 and 2.2 in the binders of the mortars compositions (Table 3.17).

XRD analysis: X-ray diffraction patterns of the binders of the mortars indicated that they were mainly composed of  $\text{CaCO}_3$  and  $\text{SiO}_2$  (Figure 3.47).

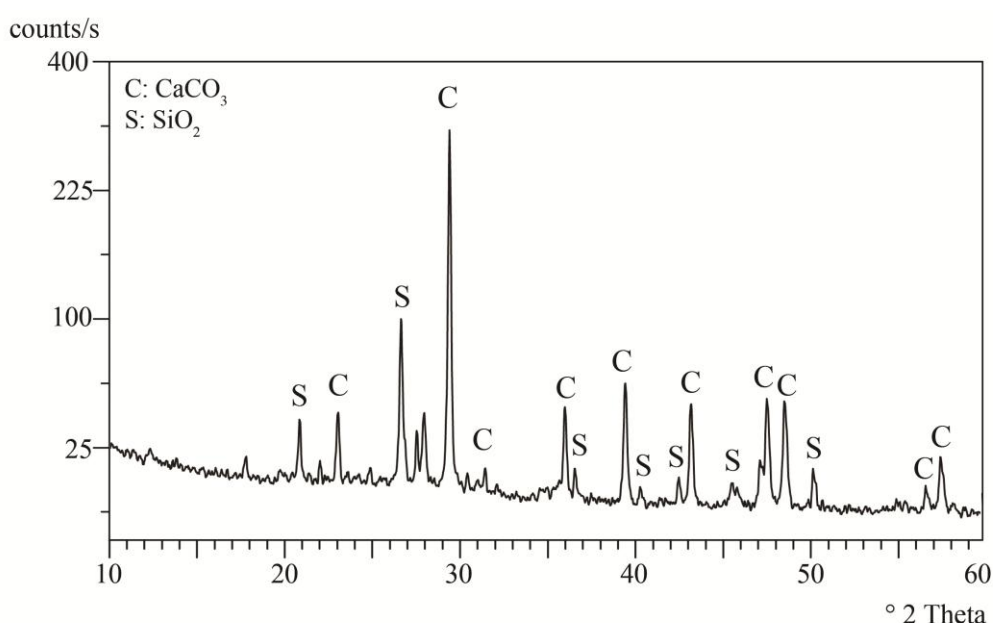


Figure 3.47. XRD spectrum of a Roman binder sample (N10)

Their patterns were analyzed by Rietveld method and their weight ratios were determined by using the line equation of standard mixtures of  $\text{CaCO}_3$  and  $\text{SiO}_2$  (Figure 3.12). XRD analysis did not show consistent results with the ones found by FTIR, SEM-EDS and LIBS analysis (Table 3.17). This can be explained due to the existence of various amounts of amorphous or poor crystalline silica in their composition which cannot be detected by XRD analysis.

### 3.6.2.3. Comparison of the Methods

The methods proposed in this study gave satisfactory results in the determination of weight ratios of  $\text{CaCO}_3$  to  $\text{SiO}_2$  for standard mixtures. The analysis results of Roman binders indicated that these analyses can also be used to evaluate the weight ratios of  $\text{CaCO}_3$  to  $\text{SiO}_2$  for historic lime mortar binders except for XRD analysis due to the existence of amorphous or poor crystalline silica in the binder. As seen in Figure 3.48, the results obtained by FTIR, SEM-EDS and LIBS appear to be in good agreement.

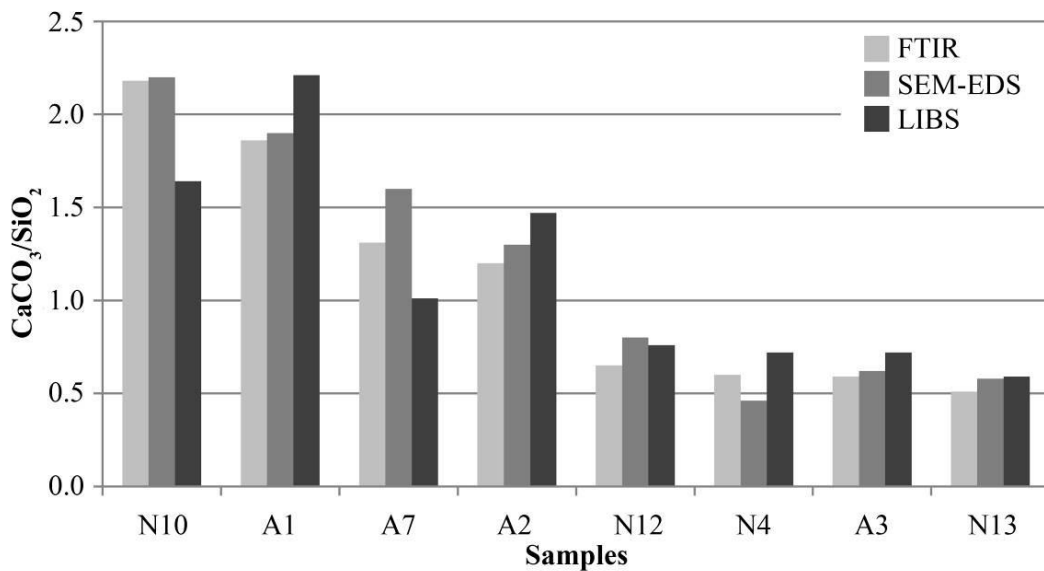


Figure 3.48. Weight ratios of  $\text{CaCO}_3/\text{SiO}_2$  obtained by FTIR, SEM-EDS, LIBS methods in binders of Roman mortars

These results showed that the FTIR, SEM-EDS and LIBS analysis can be safely used to determine the lime and fine silica content in the binder of historic lime mortars. But, XRD analysis can not be used for historic mortars due to the varied amounts of amorphous or poor crystalline silica in their compositions.

However, there are some factors that influence the analysis. Particle size, polymorphism and orientation are the main factors that affect the quantitative IR analysis. The effects of polymorphism and orientation are negligible for the analysis of inorganic substances (Böke et al. 2004). Particle size of the sample is also significant, but it can be eliminated by well grinding processes.

In the quantitative analysis of the substances by SEM-EDS and LIBS analysis, the samples must be in small analytic volume and homogeneous on the microscopic scale (Goldstein et al. 2003). Hence, in the quantification of carbonated lime and silica content in the historic mortars, the samples must be well ground and homogenized.

### 3.6.3. Microstructural Properties of Binders

Microstructural properties of mortar matrices and binders were identified by SEM-EDS analyses. Strong adhesion between pozzolanic aggregates and lime were identified in the SEM-EDS images (Figure 3.49). This adhesion led the mortars to be stiff, hard and compact.

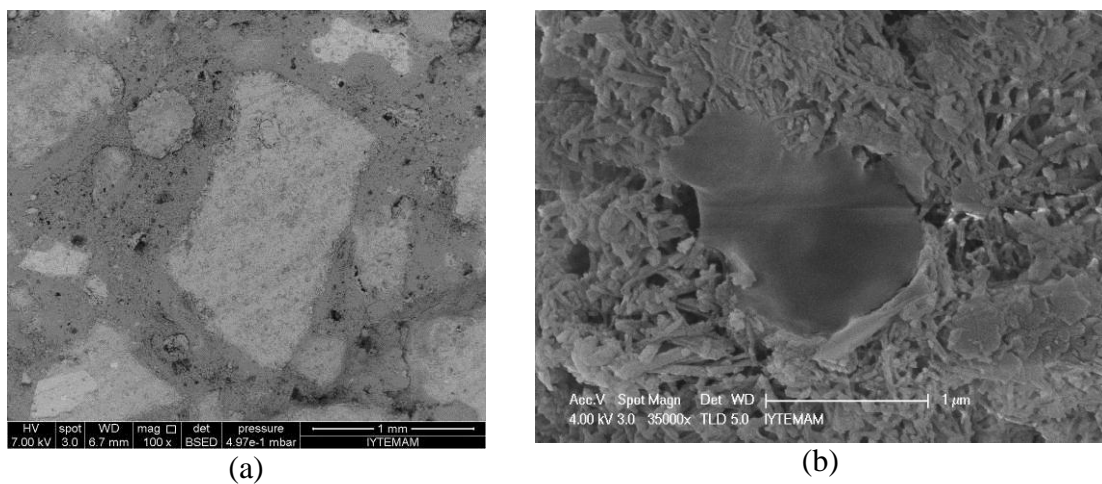


Figure 3.49. SEM images showing strong adhesion between pozzolans and lime in A2 (a) and N16 (b)

Pozzolan-lime interfaces were free from microcracks (Figure 3.50 (a)). The widths of the interfaces were determined to be between 35-50 μm (Figure 3.50 (b)).

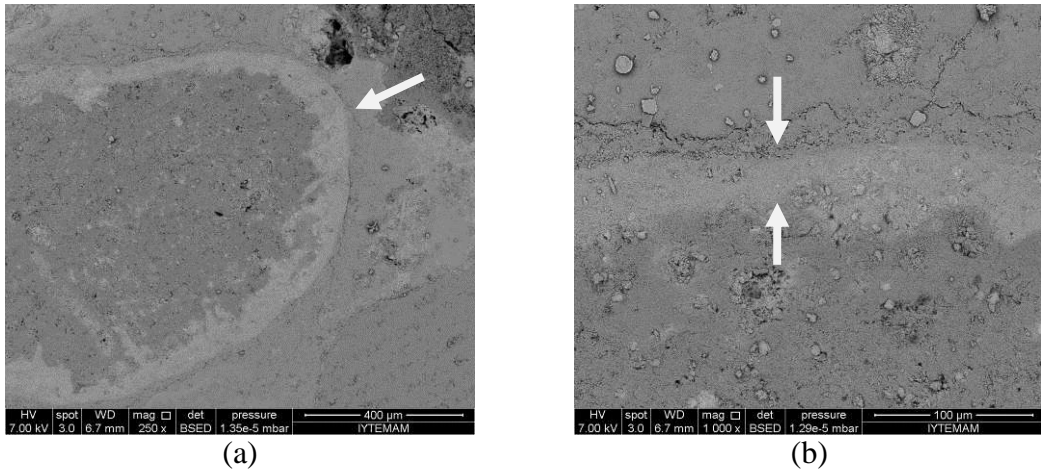


Figure 3.50. SEM images of pozzolan-lime interface at 250x (a) and 1000x (b) (A2)

Binders composed of small grain sized pozzolans and lime revealed a uniform structure in which calcite crystals and pozzolans were well mixed with each other (Figure 3.51, 3.52). This uniform structure may indicate the thorough mixing carried out during the production of mortars.

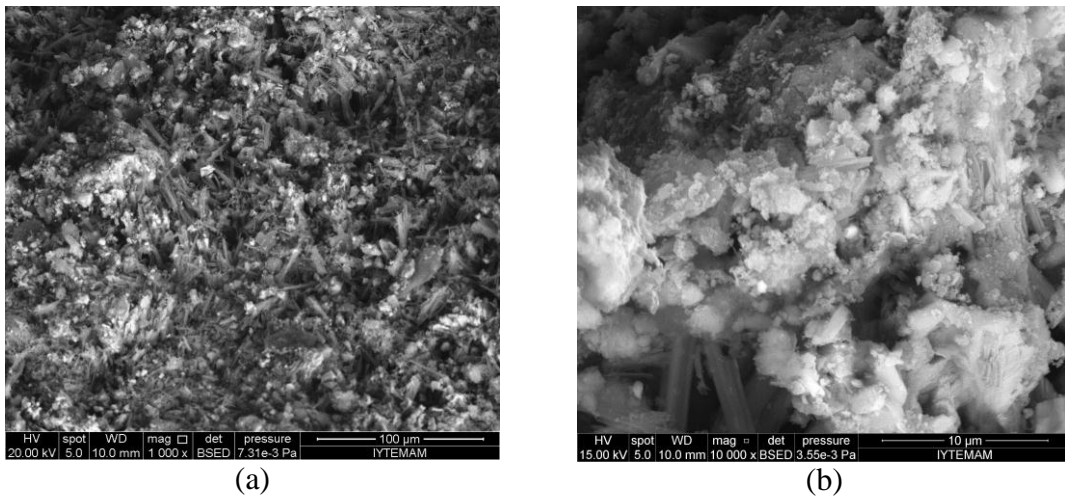


Figure 3.51. SEM images of the binder of A9 at magnifications of 1000 (a) and 10000 (b)

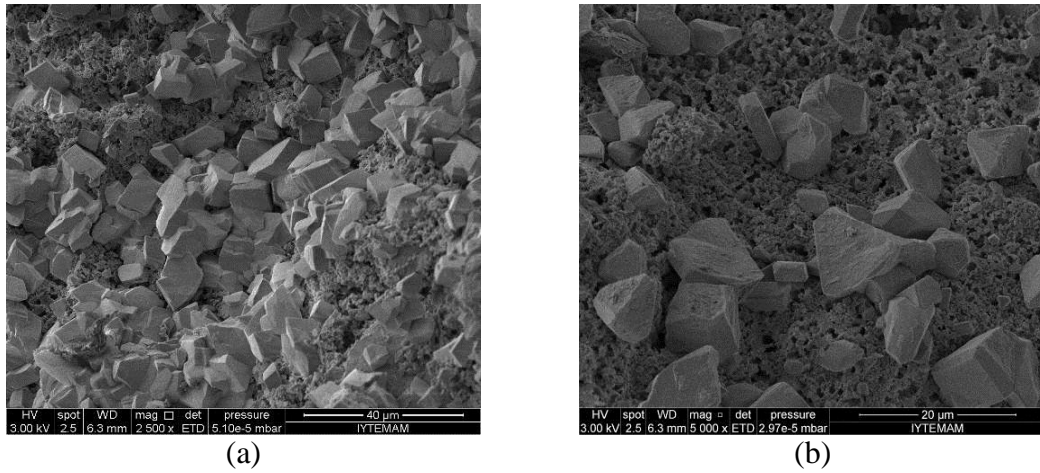


Figure 3.52. SEM images of binder of N13 at magnifications of 1000 (a) and 10000 (b)

Within the binders, needle-like formations with a thickness of nearly 30 nm were also observed (Figure 3.53).

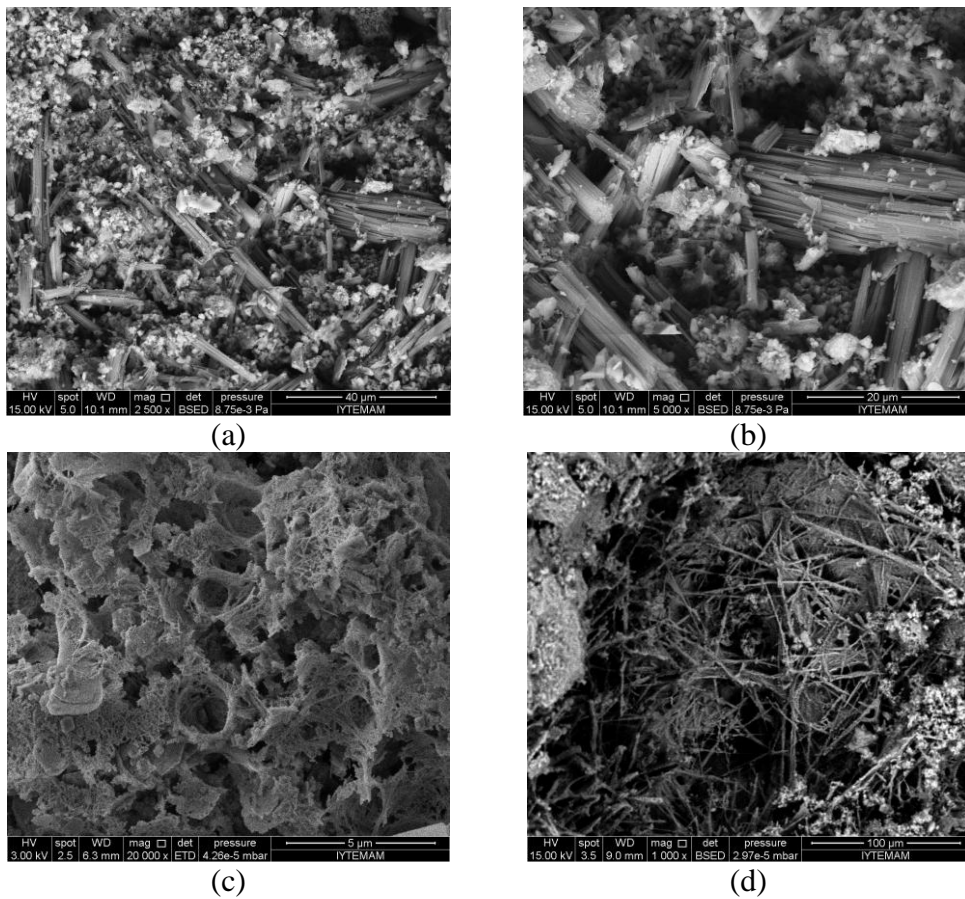


Figure 3.53. SEM images of CSH and CAH formations in A12 (a, b), N13 (c) and N15(1) (d)

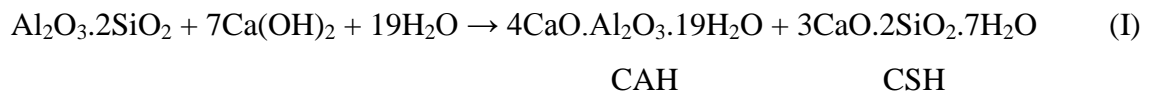


These formations were found to be composed of mainly calcium, silicon and aluminum by EDS analyses performed on seven different selected areas of these formations (Table 3.19).

Table 3.19. Chemical compositions of CSH and CAH formations

<b>Chemical Composition (%)</b>							
<b>CaO</b>	<b>SiO<sub>2</sub></b>	<b>Al<sub>2</sub>O<sub>3</sub></b>	<b>Na<sub>2</sub>O</b>	<b>MgO</b>	<b>P<sub>2</sub>O<sub>5</sub></b>	<b>K<sub>2</sub>O</b>	<b>FeO</b>
24.1 - 54.0	32.3 - 56.0	10.1 - 16.6	0 - 0.3	0.4 - 0.6	0.0 - 0.7	1.0 - 1.5	0.1 - 0.7

This may indicate that these formations were the calcium silicate hydrate (CSH) and calcium aluminate hydrates (CAH) which were the hydraulic products of the reaction between lime and pozzolans (Haga et al. 2002) (Reaction I).



CSH and CAH formations (Figure 3.54) provided durability and stiffness to the mortar since they generated strong adhesion bonds between pozzolans and lime.

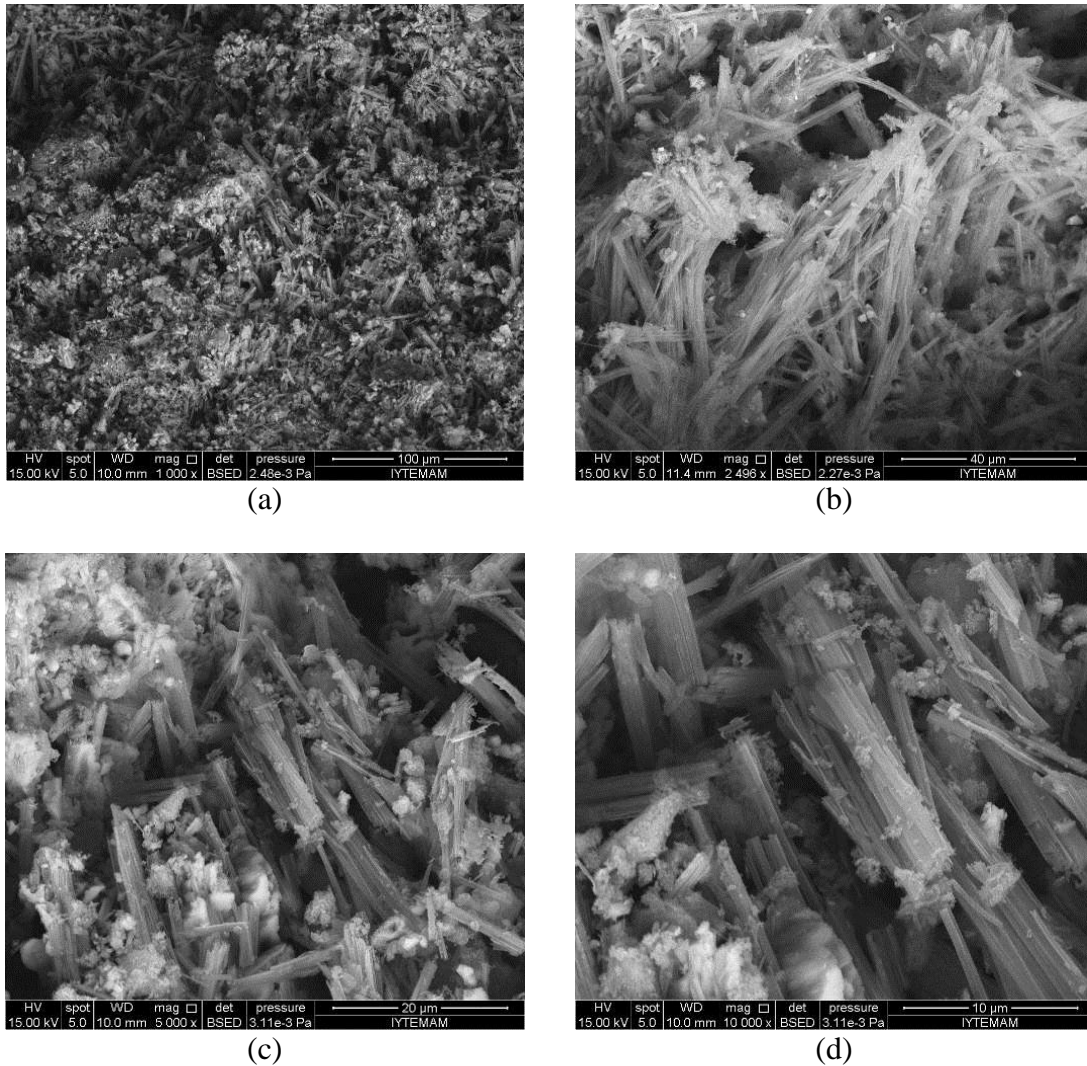


Figure 3.54. SEM images of CSH and CAH formations in Aigai sample (A9) at different magnifications 1000x (a), 2500x (b), 5000x (c), 10000x (d)

### 3.6.4. Hydraulic Properties of Binders

Hydraulic properties of Roman lime mortars were determined by thermo gravimetric analyses (TGA) of binders which gave hydraulic character to mortars (Bakolas et al. 1995, Middendorf et al. 2005). Weight losses of binder parts of mortars ( $< 63 \mu\text{m}$ ) between 200-600 °C were due to the structurally bound water of hydraulic products; and the weight losses between 600-900°C were due to the loss of carbon dioxide ( $\text{CO}_2$ ) released during the decomposition of carbonated lime. The ratio of the percent of weight losses due to  $\text{CO}_2$ / structurally bound water ( $\text{H}_2\text{O}$ ) between 1 and 10

indicated the hydraulic character of the mortar (Bakolas et al. 1998, Moropoulou et al. 2000).

CO<sub>2</sub>/H<sub>2</sub>O ratios of lime mortars produced by using natural pozzolans were found in the range of 1.12-3.77 for Aigai mortars, 2.99-6.41 for Nysa mortars (Table 3.20, Appendix F). Similarly, CO<sub>2</sub>/H<sub>2</sub>O ratios of lime mortars comprised of artificial pozzolans ranged between 1.88-4.78 in Aigai samples, 2.73-6.41 in Nysa samples (Table 3.20, Appendix F). These results revealed that all the Roman lime mortars from Aigai and Nysa could be regarded as hydraulic.

Table 3.20. Structural H<sub>2</sub>O and CO<sub>2</sub> amounts and CO<sub>2</sub>/H<sub>2</sub>O values of Roman lime mortars

Sample Type	Weight Losses (%)		CO <sub>2</sub> /H <sub>2</sub> O
	200-600 °C (Struc. H <sub>2</sub> O)	600-900 °C (CO <sub>2</sub> )	
Lime mortars with natural pozzolanic aggregates from Aigai (A1, A2, A3, A6, A7, A9, A12)	3.43 - 9.86	10.92 - 19.90	1.12 - 3.77
Lime mortars with natural pozzolanic aggregates from Nysa (N3, N4, N7, N10, N12, N13, N16, N17, N21, N23)	2.85 - 4.38	10.73 - 22.05	2.99 - 6.41
Lime mortars with artificial pozzolanic aggregates from Aigai (A5, A10, A11)	3.58 - 4.08	7.66 - 18.50	1.88 - 4.78
Lime mortars with artificial pozzolanic aggregates from Nysa (N1, N2, N5, N6, N8, N9, N11, N14, N15(1), N15(2), N20, N22, N24)	2.85 - 5.48	12.85 - 21.94	2.73 - 6.41

Hydraulic character of Roman lime mortars did not differ according to their uses in the structure. CO<sub>2</sub>/H<sub>2</sub>O ratios of all lime mortars were determined to be similar to each other (Table 3.21).

Table 3.21. CO<sub>2</sub>/Structural H<sub>2</sub>O of Roman lime mortars used for different purposes

Use of Mortar	CO <sub>2</sub> /H <sub>2</sub> O
Rubble core of the wall (A2, A3, A10, A12)	1.12 - 4.78
Wall - Mortared rubble throughout (N2, N3, N4, N5, N7, N11, N16, N17, N21, N23)	1.46 - 6.41
Wall - Mortared ashlar throughout (A1, A7)	2.76 - 3.28
Arch, Vault (A6, N10, N12, N13, N22)	2.99 - 5.03
Supporting for coverings, mosaics (A9, A11, N1, N6, N14, N20)	1.72 - 5.23
Plaster (A5, N8, N9, N15(1), N15(2), N24)	2.76 - 4.94

CO<sub>2</sub>/H<sub>2</sub>O values of lime mortars from Aigai and Nysa were similar to the lime mortars from different Roman period buildings which possessed CO<sub>2</sub>/H<sub>2</sub>O values varying between 0.29-7.5 (Silva et al. 2005, Genestar et al. 2006, Özkaya and Böke 2009) (Table 3.22.). These results indicated that the Roman period mortars were hydraulic. Hydraulic character of Roman lime mortars was due to the use of natural or artificial pozzolanic aggregates during their manufacturing.

Table 3.22. Structural H<sub>2</sub>O and CO<sub>2</sub> ratios of Roman lime mortars determined by previous studies

Roman Building/Site (Reference)	Aggregate Type of Mortar	Weight Losses (%)		CO <sub>2</sub> /H <sub>2</sub> O
		200-600 °C (Struc. H <sub>2</sub> O)	600-900 °C (CO <sub>2</sub> )	
Colosseum - Rome, cistern -Albano Laziale (Italy) (Silva et al. 2005)	Natural poz.	5.62-7.84	2.25 - 11.88	0.29 - 2.11
Serapis Temple - Turkey (Özkaya and Böke 2009)	Natural poz.	2.33	6.87	2.95
The Forum and residences of Pollentia - Mallorca (Spain) (Genestar et al. 2006)	Natural poz.	4.3	31.9	7.5
	Artificial poz.	5.1	21.5	4.3

## CHAPTER 4

### CONCLUSIONS

In this study, characteristics of lime mortars produced by using natural and artificial pozzolans from several Roman period buildings in Aigai and Nysa which were two of the eastern provinces of Roman Empire in Anatolia were investigated in order to understand technology of Roman period lime mortars used in Anatolia.

Basic physical properties, raw material compositions, mineralogical and chemical compositions, microstructural and hydraulic properties of Roman lime mortars of Aigai and Nysa; and mineralogical and chemical compositions, microstructural properties and pozzolanic activities of natural and artificial pozzolans used as aggregates in these mortars were determined.

In both cities, mortars produced from natural pozzolans were generally used in wall constructions, arches and vaults whereas mortars produced from artificial pozzolans were generally used as plaster, paving and supporting for mosaics and marble coverings.

They were low density and high porosity materials with a high percent of macro pores. Lime mortars produced by artificial pozzolans were slightly lower in density and higher in porosity than the mortars produced by natural pozzolans. Basic physical properties of mortars did not differ depending on their use in structural elements like wall constructions, arches and vaults or in non-structural elements like plasters, supporting for covering or mosaics.

Roman lime mortars were mainly produced by using non-hydraulic high calcium lime and highly pozzolanic aggregates. Lime/aggregate ratios of mortars produced by artificial pozzolans (0.55) were found higher than mortars produced by natural pozzolans (0.30). Lime/aggregate ratios of plasters were higher than mortars used for structural purposes like wall construction, arches and vaults.

Lime used in the production of mortars could be classified as high calcium lime since it contained higher than 90 % CaO. Lime composed of small size of micritic crystals may indicate the use of porous limestones in their production and also aging of lime putty before it was used in the mortar.

Pozzolans were mainly composed of amorphous silicates, quartz, albite, anorthite and muscovite minerals. Chemical compositions of pozzolans were comprised of high amounts of SiO<sub>2</sub>, moderate amounts of Al<sub>2</sub>O<sub>3</sub>, Fe<sub>2</sub>O<sub>3</sub>, and low amounts of MgO, CaO, Na<sub>2</sub>O, K<sub>2</sub>O and TiO<sub>2</sub>.

Natural pozzolans from Aigai and Nysa were distinctively separated by their CaO and Y contents. Artificial pozzolans were also differentiated by their alkaline earth metal contents (Ba, Sr, Ca). The small differences in the major and trace element compositions of pozzolans revealed that different sources with similar chemical compositions had been used for pozzolan production in Aigai and Nysa.

Natural pozzolans were composed of small sized amorphous particles with high specific surface area that enhanced the reactivity of pozzolan with lime. Artificial pozzolans were also consisted of amorphous particles indicating little vitrification that suggested the use of low heating temperatures (< 950 °C) during their production.

Binders of the mortars defined as the fine matrices (< 63 μm) composed of small grain sized silica (SiO<sub>2</sub>) and carbonated lime (CaCO<sub>3</sub>) were considered as the main part that gave hydraulic character and high strength to the mortar.

Binders of all mortars were hydraulic due to the use of pozzolans in their production. They were composed of mainly calcite originating from carbonated lime; and silicas originating from the pozzolans.

In this study, a relatively fast and easy method was developed for the quantitative determination of CaCO<sub>3</sub> and SiO<sub>2</sub> content in the binder compositions of mortars by using FTIR, LIBS, SEM-EDS and XRD analyses. FTIR, SEM-EDS and LIBS analysis were found as suitable methods to determine the lime and fine silica content in the binders of historic lime mortars. But, XRD analysis could not be used for historic mortars due to the varied amounts of amorphous or poor crystalline silica in their compositions.

## REFERENCES

- Adam, J.P. 2005. *Roman Building Materials and Techniques*. (First published in 1937). Translated by Anthony Mathews. London and New York: Routledge.
- Akman, M.S., A. Güner, and I.H. Aksoy. 1986. "The History and Properties of Khorasan Mortar and Concrete." In the proceedings of II. International Congress on the History of Turkish and Islamic Science and Technology, Vol I: Turkish and Islamic Science and Technology in the 16<sup>th</sup> Century, 101-112. İstanbul: İTÜ Research Center of History of Science and Technology.
- Alberti, L.B. 1986. *The Ten Books on Architecture - The 1755 Leoni Edition*. New York: Dover Publications, INC.
- Akurgal, E. 2001. *Ancient Civilizations and Ruins of Turkey*. İstanbul: Net Yayıncılık.
- Bakolas, A., G. Biscontin, A. Moropoulou, and E. Zendri. 1995. "Characterization of the Lumps in the Mortars of Historic Masonry." *Thermochimica Acta* 269-270: 809-816. doi: 10.1016/0040-6031(95)02573-1.
- Bakolas, A., G. Biscontin, A. Moropoulou, and E. Zendri. 1998. "Characterization of Structural Byzantine Mortars by Thermogravimetric Analysis." *Thermochimica Acta* 321: 151-160. doi: 10.1016/S0040-6031(98)00454-7.
- Barba, L., J. Blancas, L.R. Manzanilla, A. Ortiz, D. Barca, G.M. Crisci, D. Miriello and A. Pecci. 2009. "Provenance of the Limestone Used in Teotihuacan (Mexico): A Methodological Approach." *Archaeometry* 51: 525-545. doi: 10.1111/j.1475-4754.2008.00430.x.
- Bean, G.E. 1989. *Turkey Beyond the Meander*. (First published in 1971) London: John Murray Publishers Limited.
- Boynton, R.S. 1980. *Chemistry and Technology of Lime and Limestone*, 2<sup>nd</sup> Edition. New York: John Wiley & Sons.
- Benedetti, D., S. Valetti, E. Bontempi, C. Piccioli, and L.E. Depero. 2004. "Study of Ancient Mortars from the Roman Villa of Pollio Felice in Sorrento (Naples)." *Applied Physics A* 79: 341-345. doi: 10.1007/s00339-004-2529-x.
- Böke, H., S. Akkurt, S. Özdemir, E.H. Göktürk, and E.N. Caner Saltik. (2004). "Quantification of CaCO<sub>3</sub>-CaSO<sub>3</sub>-0.5H<sub>2</sub>O-CaSO<sub>4</sub>-2H<sub>2</sub>O Mixtures by FTIR

- Analysis and its ANN Model.” *Materials Letters* 58: 723-726. doi: 10.1016/j.matlet.2003.07.008.
- Bruni, S., F. Cariati, P. Fermo, P. Cariati, G. Alessandrini, and L. Toniolo. (1997). “White Lumps in Fifth to Seventeenth Century AD Mortars from Northern Italy.” *Archaeometry* 39(1): 1-7. doi: 10.1111/j.1475-4754.1997.tb00786.x.
- Cardiano, P., S. Ioppola, C.D. Stefano, A. Pettignano, S. Sergi, and P. Piraino. 2004. “Study and Characterization of the Ancient Bricks of Monastery of "San Filippo di Fragalá" in Frazzanò (Sicily).” *Analytica Chimica Acta* 519: 103-111. doi: 10.1016/j.aca.2004.05.042.
- Caron, P, and M.F. Lynch, 1988. “Making Mud Plaster.” *APT Bulletin* 4: 7-9.
- Carretero, M.I., M. Dondi, B. Fabbri, and M. Raimondo. 2002. “The Influence of Shaping and Firing Technology on Ceramic Properties of Calcareous and Non-Calcareous Illitic-Chloritic Clays.” *Applied Clay Science* 20: 301- 306. doi: 10.1016/S0169-1317(01)00076-X.
- Coulton, J.J. 1980. *Greek Architecture in Architecture of the Western World (Edited by Michael Raeburn)*. New York: Rizzoli International Publications Inc.
- Cowan, H.J. 1977. *The Master Builders: A History of Structural and Environmental Design from Ancient Egypt to the Nineteenth Century*. New York: John Willey & Sons.
- Cowper, A. 1998. *Lime and Lime Mortars*. (First published in 1927 for the Building Research Station by HM Stationery Office, London) Dorset: Donhead Publishing Ltd.
- Cultrone, G., E. Sebastián, K. Elert, M.J. de la Torre, O. Cazalla, and C. Rodriguez-Navarro. 2004. “Influence of Mineralogy and Firing Temperature on the Porosity of Bricks.” *Journal of the European Ceramic Society* 24: 547-564. doi: 10.1016/S0955-2219(03)00249-8.
- Davey, N. 1961. *A History of Building Materials*, London: Phoenix House.
- Degryse, P., J. Elsen, and M. Waelkens. 2002. “Study of Ancient Mortars from Sagalassos (Turkey) in View of Their Conservation.” *Cement and Concrete Research* 32: 1457-1463. doi: 10.1016/S0008-8846(02)00807-4.
- Doğer, E. 2007. Aigai 2004-2006 Yılı Kazıları. In *29. Kazı Sonuçları Toplantısı I*. 28 May-01 June 2007.



- Elsen, J., A. Brutsaert, M. Deckers, and R. Brulet. 2004. "Microscopical Study of Ancient Mortars from Tournai (Belgium)." *Material Characterization* 53: 289-294. doi: 10.1016/j.matchar.2004.10.004.
- Farci, A., D. Floris, and P. Meloni. 2005. "Water Permeability vs. Porosity in Samples of Roman Mortars." *Journal of Cultural Heritage* 6: 55-59. doi: doi:10.1016/j.culher.2004.08.002.
- Franquelo, M.L., M.D. Robador, V. Ramírez-Valle, A. Durán, A. Durán and J. L. Pérez-Rodríguez. 2008. "Roman Ceramics of Hydraulic Mortars Used to Build the Mithraeum House of Mérida (Spain)" *Journal of Thermal Analysis and Calorimetry* 92(1): 331-335. doi: 10.1007/s10973-007-8810-4.
- Genestar, C., C. Pons, and A. Más. 2006. "Analytical Characterisation of Ancient Mortars from the Archaeological Roman City of Pollentia (Balearic Islands, Spain)." *Analytica Chimica Acta* 557:373-379. doi: 10.1016/j.aca.2005.10.058.
- Goldstein, J., D.E. Newbury, D.C. Joy, C.E. Lyman, P. Echlin, E. Lifshin, L. Sawyer, and J.R. Michal. 2003. *Scanning Electron Microscopy and X-Ray Microanalysis (3<sup>rd</sup> Edition)*. New York: Springer.
- Goldsworthy, H., and Z. Min. 2009. "Mortar Studies Towards the Replication of Roman Concrete." *Archaeometry* 51(6): 932-946. doi: 10.1111/j.14754754.2009.00450.x.
- Grant, M. 1980. *Roman Architecture in Architecture of the Western World (Edited by Michael Raeburn)*. New York: Rizzoli International Publications.
- Güleç, A., and T. Tulun. 1997. "Physico-Chemical and Petrographical Studies of Old Mortars and Plasters of Anatolia." *Cement and Concrete Research* 27(2): 227-234. doi: 10.1016/S0008-8846(97)00005-7.
- Haga, K., M. Shibata, M. Hironaga, S. Tanaka, and S. Nagazaki. 2002. "Silicate Anion Structural Change in Calcium Silicate Hydrate Gel on Dissolution of Hydrated Cement" *Journal of Nuclear Science and Technology* 39(5): 540-547. doi: 10.1080/18811248.2002.9715232.
- Herodotus. 1890. *The History of Herodotus* (Translated into English by G.C. Macaulay.) London and New York: MacMillan and Co.
- İdil, V. 1999. *Nysa ve Akharaka*. İstanbul: Yaşar Eğitim ve Kültür Vakfı.
- Jackson, M. D., J.M. Logan, B.E. Scheetz, D.D. Deocampo, C.G. Cawood, F. Marra, M. Vitti, and L. Ungaro. 2009. "Assessment of Material Characteristics of Ancient

- Concretes, Grand Aula, Markets of Trajan, Rome.” *Journal of Archaeological Science* 36: 2481-2492. doi: 10.1016/j.jas.2009.07.011.
- Jackson, M.D., P. Ciancio Rossetto, C.K. Kosso, M. Buonfiglio, and F. Marra. 2011. “Building Materials of the Theatre of Marcellus, Rome.” *Archaeometry* 53(4):728-742. doi: 10.1111/j.1475-4754.2010.00570.x.
- Jedrzejewska, H. 1981. “Ancient Mortars as Criterion in Analysis of Old Architecture.” Proceedings of Symposium on Mortars, Cements and Grouts Used in the Conservation of Historic Buildings, Rome, 311-329.
- Kirby, R.S., S. Withington, A. B. Darling, and F.G. Kilgour. 1990. *Engineering in History*. (First published in 1956) New York: Dover Publications, Inc.
- Kramar, S., V. Zalar, M. Urosevic, W. Körner, A. Mauko, B. Mirtič, J. Lux, and A. Mladenović. 2011. “Mineralogical and Microstructural Studies of Mortars from the Bath Complex of the Roman Villa Rustica near Mošnje (Slovenia)” *Materials Characterization* 62: 1042-1057. doi: 10.1016/j.matchar.2011.07.019.
- Luxán, M.P., F. Madruga, and J. Saavedra. 1989. “Rapid Evaluation of Pozzolanic Activity of Natural Products of Conductivity Measurement.” *Cement and Concrete Research* 19: 63-68. doi: 10.1016/0008-8846(89)90066-5.
- MacDonald, and W. 1965. *The Architecture of the Roman Empire*. New Haven and London: Yale University Press.
- Massazza, F., and M. Pezzuoli. 1981. Some Teachings of Roman Concrete Mortars. Proceedings of Symposium on Mortars, Cements and Grouts Used in the Conservation of Historic Buildings. Rome, November 3-6.
- Middendorf, B., J.J. Hughes, K. Callebaut, G. Baronio, and I. Papayianni. 2005. “Investigative Methods for the Characterisation of Historic Mortars- Part 2: Chemical Characterisation.” *Materials and Structures* 38: 771-780. doi: 10.1617/14282.
- Mirioollo, D., A. Bloise, G.M. Crisci, C. Apollaro, and A. La Marca. 2011. “Characterisation of Archaeological Mortars and Plasters from Kyme (Turkey).” *Journal of Archaeological Science* 38: 794-804. doi: 10.1016/j.jas.2010.11.002.
- Mirioollo, D., D. Barca, A. Bloise, A. Ciarallo, G.M. Crisci, T. De Rose, C. Gattuso, F. Gazineo, and M.F. La Russa. 2010. “Characterisation of Archaeological Mortars from Pompeii (Campania, Italy) and Identification of Construction Phases by Compositional Data Analysis.” *Journal of Archaeological Science* 37: 2207-2223. doi: 10.1016/j.jas.2010.03.019.

- Mommsen, H. 2001. "Provenance Determination of Pottery by Trace Element Analysis: Problems, Solutions and Applications." *Journal of Radioanalytical and Nuclear Chemistry* 247(3): 657-662. doi: 10.1016/0305-4403(92)90018-X.
- Montjoye.net Châteaux & Patrimoine. "Thésée, Site-gallo romain, Opus Spicatum, Tasciaca." Accessed April 25, 2012. <http://www.montjoye.net/patrimoine/thesee-site-gallo-romain-opus-spicatum-tasciaca>.
- Moropoulou, A., A. Bakolas, and K. Bisbikou. 2000. "Investigation of the Technology of Historic Mortars." *Journal of Cultural Heritage* 1: 45-58.
- Moropoulou, A., A. Bakolas, and E. Aggelakopoulou. 2001. "The Effects of Limestone Characteristics and Calcination Temperature to the Reactivity of the Quicklime." *Cement and Concrete Research* 31: 633-639. doi: 10.1016/S0008-8846(00)00490-7.
- Moropoulou A., Th. Tsiourva, K. Bisbikou, G. Biscontin, A. Bakolas, and E. Zendri. 1996. "Hot Lime Technology Imparting High Strength to Historic Mortars." *Construction and Building Materials* 10/2: 151-159. doi: 10.1016/0950-0618(95)00022-4.
- Ostia Harbour City of Ancient Rome. "Topographical Dictionary - Building Glossary." Accessed April 25, 2012. <http://www.ostia-antica.org/dict/topics/glossary.htm>
- Pavía, S., and S. Caro. 2008. "An Investigation of Roman Mortar Technology Through the Petrographic Analysis of Archaeological Material." *Construction and Building Materials* 22: 1807-1811. doi: 10.1016/j.conbuildmat.2007.05.003.
- Pearson, G. 1994. *Conservation of Clay and Chalk Buildings*. Dorset: Donhead Publishing Ltd.
- Ramsay, W.M. 1881. Contributions to the History of Southern Aeolis. *The Journal Hellenic Studies* 2: 271-308.
- RILEM. "Tests Defining the Structure" *Materials and Construction*, Vol. 13, No. 73, 1980.
- Robador, M.D., J.L. Perez-Rodriguez, and A. Duran. 2010. "Hydraulic Structures of the Roman Mithraeum House in Augusta Emerita, Spain." *Journal of Archaeological Science* 37: 2426-2430. doi: 10.1016/j.jas.2010.05.003.
- Rodriguez-Navarro, C., E. Hansen, and W.S. Ginell. 1998. "Calcium Hydroxide Crystal Evolution Upon Ageing of Lime Putty." *Journal of the American Ceramic Society* 81(11): 3032-3034. doi: 10.1111/j.1151-2916.1998.tb02735.x.

- Sánchez-Moral, S., L. Luque, Juan-Carlos Cañaveras, V. Soler, J. Garcia-Guinea, and A. Aparicio. 2005. "Lime Pozzolana Mortars in Roman Catacombs: Composition, Structures and Restoration" *Cement and Concrete Research* 35(8): 1555-1565. doi: 10.1016/j.cemconres.2004.08.009.
- Silva, D.A., H.R. Wenk, and P.J.M. Monteiro. 2005. "Comparative Investigation of Mortars from Roman Colosseum and Cistern." *Thermochimica Acta* 438: 35-40. doi:10.1016/j.tca.2005.03.003.
- Stierlin, H. 2002. *The Roman Empire from the Etruscans to the Decline of the Roman Empire*. Köln: Taschen GmbH.
- Strabon. 2005. *Antik Anadolu Coğrafyası - Geographika*. İstanbul: Arkeoloji ve Sanat Yayınları.
- The University of Texas at Austin. "Masonry Analysis and Building Techniques at Ostia." Accessed April 25, 2012. [http://www.utexas.edu/research/isac/web/OSMAP/OSMAP\\_Masonry2.html](http://www.utexas.edu/research/isac/web/OSMAP/OSMAP_Masonry2.html).
- Umar, B. 2002. *Aiolis*. İstanbul: İnkılâp Kitabevi.
- Vicat, L.J. 2003. *Mortars and Cements*. (First published in 1837 by John Weale, High Holborn, London) Dorset: Donhead Publishing Ltd.
- Vitruvius, P. 1960. *The Ten Books on Architecture*. (First published in 1914. Edited by M.H. Morgan) New York: Dover Publications.
- Velosa, A.L., J. Coroado, M.R. Veiga, and F. Rocha. 2007. "Characterisation of Roman Mortars from Conímbriga with Respect to Their Repair." *Materials Characterization* 58: 1208–1216. doi: 10.1016/j.matchar.2007.06.017.
- Ward-Perkins, J.B. 1974. *Roman Architecture*. New York: H.N. Abrams.
- Ward-Perkins, J.B. 1981. *Roman Imperial Architecture*. New Haven and London: Yale University Press.
- Zamba, I.C., M.G. Stamatakis, F.A. Cooper, P.G. Themelis, and C.G. Zambas. 2007. "Characterization of Mortars used for the Construction of Saithidai Heroon Podium (1<sup>st</sup> century AD) in Ancient Messene, Peloponnesus, Greece." *Materials Characterization* 58: 1229-1239. doi: 10.1016/j.matchar.2007.07.004.

## APPENDIX A

### BASIC PHYSICAL PROPERTIES OF ROMAN LIME MORTARS

Sample Type	Sample Name	Apparent Density (g/cm <sup>3</sup> )	Porosity (by volume - %)
Lime mortars with natural pozzolanic aggregates from Aigai	A1	1.58 ± 0.01	36.12 ± 0.15
	A2	1.72 ± 0.46	31.05 ± 15.05
	A3	1.51 ± 0.06	36.40 ± 2.78
	A6	1.56 ± 0.14	35.31 ± 5.68
	A7	1.74 ± 0.24	28.84 ± 6.79
	A9	1.40 ± 0.01	41.96 ± 1.22
	A12	1.41 ± 0.09	40.29 ± 3.75
Lime mortars with natural pozzolanic aggregates from Nysa	N3	1.76 ± 0.01	32.23 ± 0.08
	N4	1.64 ± 0.01	35.92 ± 0.51
	N7	1.84 ± 0.03	24.79 ± 1.18
	N10	1.62 ± 0.08	35.56 ± 2.83
	N12	1.75 ± 0.00	29.97 ± 1.50
	N13	1.91 ± 0.20	24.97 ± 7.13
	N16	1.72 ± 0.00	32.48 ± 0.35
	N17	1.64 ± 0.03	35.54 ± 1.51
	N21	1.53 ± 0.03	39.40 ± 0.78
	N23	1.39 ± 0.01	44.55 ± 1.03
Lime mortars with artificial pozzolanic aggregates from Aigai	A5	1.44 ± 0.01	42.33 ± 0.00
	A10	1.48 ± 0.11	40.10 ± 4.88
	A11	1.63 ± 0.01	33.50 ± 2.04

<b>Sample Type</b>	<b>Sample Name</b>	<b>Apparent Density (g/cm<sup>3</sup>)</b>	<b>Porosity (by volume - %)</b>
Lime mortars with artificial pozzolanic aggregates from Nysa	N1	1.23 ± 0.01	48.15 ± 0.52
	N2	1.69 ± 0.02	33.51 ± 0.17
	N5	1.63 ± 0.01	36.16 ± 0.30
	N6	1.56 ± 0.00	37.22 ± 0.72
	N8	1.40 ± 0.51	44.08 ± 19.02
	N9	1.38 ± 0.16	44.40 ± 5.18
	N11	1.77 ± 0.01	25.59 ± 1.31
	N14	1.23 ± 0.01	50.84 ± 0.06
	N15(1)	1.33 ± 0.04	45.27 ± 0.90
	N15(2)	1.34 ± 0.04	39.90 ± 1.06
	N20	1.40 ± 0.00	44.50 ± 0.02
	N22	1.10 ± 0.00	55.55 ± 1.54
	N24	1.23 ± 0.03	49.18 ± 2.90

## APPENDIX B

### DRYING RATES OF ROMAN LIME MORTARS

Sample	Vapor Flow Rate (kg/m <sup>2</sup> s)							
	15 min.	30 min.	60 min.	2 h.	3 h.	17 h.	24 h.	2 days
<b>A1</b>	0.1988 ±0.0028	0.0985 ±0.0014	0.0482 ±0.0007	0.0232 ±0.0004	0.0174 ±0.0038	0.0010 ±0.0000	0.0003 ±0.0000	0.0000 ±0.0000
<b>A3</b>	0.2301	0.1140	0.0556	0.0268	0.0171	0.0016	0.0009	0.0003
<b>A11</b>	0.2274 ±0.0035	0.1125 ±0.0018	0.0548 ±0.0011	0.0261 ±0.0005	0.0165 ±0.0004	0.0015 ±0.0001	0.0008 ±0.0001	0.0003 ±0.0001
<b>N1</b>	0.2687 ±0.0269	0.1332 ±0.0134	0.0652 ±0.0064	0.0315 ±0.0030	0.0202 ±0.0019	0.0019 ±0.0001	0.0009 ±0.0001	0.0002 ±0.0000
<b>N4</b>	0.1901 ±0.0015	0.0942 ±0.0008	0.0459 ±0.0005	0.0220 ±0.0003	0.0140 ±0.0002	0.0009 ±0.0001	0.0003 ±0.0001	0.0000 ±0.0000
<b>N5</b>	0.1911 ±0.0139	0.0945 ±0.0068	0.0460 ±0.0032	0.0220 ±0.0015	0.0140 ±0.0009	0.0010 ±0.0000	0.0005 ±0.0000	0.0001 ±0.0000
<b>N10</b>	0.2185 ±0.0015	0.1076 ±0.0008	0.0517 ±0.0004	0.0243 ±0.0004	0.0151 ±0.0003	0.0006 ±0.0001	0.0002 ±0.0000	0.0000 ±0.0000
<b>N12</b>	0.2028 ±0.0023	0.0989 ±0.0005	0.0478 ±0.0002	0.0272 ±0.0064	0.0101 ±0.0058	0.0008 ±0.0000	0.0004 ±0.0000	0.0001 ±0.0000
<b>N13</b>	0.2753 ±0.0201	0.1356 ±0.0100	0.0654 ±0.0048	0.0307 ±0.0022	0.0191 ±0.0014	0.0009 ±0.0001	0.0004 ±0.0000	0.0001 ±0.0000
<b>N17</b>	0.1760 ±0.0023	0.0871 ±0.0042	0.0425 ±0.0021	0.0205 ±0.0011	0.0131 ±0.0007	0.0011 ±0.0002	0.0004 ±0.0001	0.0000 ±0.0000
<b>N20</b>	0.2074 ±0.0046	0.1026 ±0.0024	0.0499 ±0.0010	0.0240 ±0.0005	0.0154 ±0.0003	0.0013 ±0.0000	0.0005 ±0.0000	0.0001 ±0.0000
<b>N21</b>	0.2601 ±0.0180	0.1284 ±0.0089	0.0623 ±0.0041	0.0296 ±0.0018	0.0187 ±0.0010	0.0187 ±0.0001	0.0004 ±0.0001	0.0001 ±0.0000

## APPENDIX C

### LIME/AGGREGATE RATIOS OF ROMAN LIME MORTARS

Sample Type	Sample Name	Lime (%)	Aggregate (%)	Lime/Aggregate
Lime mortars with natural pozzolanic aggregates from Aigai	A1	20.47 ± 0.74	79.53 ± 0.74	0.26 ± 0.01
	A2	22.49 ± 1.16	77.51 ± 1.16	0.29 ± 0.02
	A3	16.31 ± 0.16	77.51 ± 0.16	0.19 ± 0.00
	A6	26.67 ± 1.36	73.33 ± 1.36	0.36 ± 0.03
	A7	22.17 ± 0.95	77.83 ± 0.95	0.28 ± 0.02
	A9	26.06 ± 2.11	73.94 ± 2.11	0.35 ± 0.04
	A12	25.08 ± 1.63	74.92 ± 1.63	0.33 ± 0.03
Lime mortars with natural pozzolanic aggregates from Nysa	N3	18.08 ± 1.57	81.82 ± 1.57	0.22 ± 0.02
	N4	20.14 ± 0.12	79.86 ± 0.12	0.25 ± 0.00
	N7	22.51 ± 5.56	77.49 ± 5.56	0.29 ± 0.09
	N10	23.28 ± 2.48	76.72 ± 2.48	0.30 ± 0.04
	N12	19.22 ± 1.13	80.78 ± 1.13	0.24 ± 0.02
	N13	19.17 ± 0.71	80.83 ± 0.71	0.24 ± 0.01
	N16	34.69 ± 3.41	65.31 ± 3.41	0.53 ± 0.08
	N17	39.04 ± 1.29	60.96 ± 1.29	0.64 ± 0.03
	N21	24.96 ± 4.92	75.04 ± 4.92	0.33 ± 0.09
	N23	19.93 ± 1.54	80.07 ± 1.54	0.25 ± 0.02
Lime mortars with artificial pozzolanic aggregates from Aigai	A5	28.92 ± 0.94	71.08 ± 0.94	0.41 ± 0.02
	A10	54.27 ± 17.08	45.73 ± 17.08	1.19 ± 0.88
	A11	17.06 ± 1.48	82.94 ± 1.48	0.21 ± 0.02



<b>Sample Type</b>	<b>Sample Name</b>	<b>Lime (%)</b>	<b>Aggregate (%)</b>	<b>Lime/Aggregate</b>
Lime mortars with artificial pozzolanic aggregates from Nysa	N1	38.29 ± 1.88	61.71 ± 1.88	0.62 ± 0.05
	N2	33.93 ± 0.98	66.07 ± 0.98	0.51 ± 0.02
	N5	21.20 ± 1.79	78.80 ± 1.79	0.27 ± 0.03
	N6	19.29 ± 1.49	80.71 ± 1.49	0.24 ± 0.02
	N8	<i>Can not be determined due to insufficient sample size.</i>		
	N9	40.69 ± 8.59	59.31 ± 8.59	0.69 ± 0.25
	N11	22.91 ± 2.05	77.09 ± 2.05	0.30 ± 0.03
	N14	19.59 ± 2.25	80.41 ± 2.25	0.24 ± 0.03
	N15(1)	42.50 ± 0.28	57.50 ± 0.28	0.74 ± 0.01
	N15(2)	46.95 ± 0.12	53.05 ± 0.12	0.89 ± 0.00
	N20	20.19 ± 3.93	79.81 ± 3.93	0.25 ± 0.06
	N22	32.86 ± 3.27	67.14 ± 3.27	0.49 ± 0.07
	N24	<i>Can not be determined due to insufficient sample size.</i>		

## APPENDIX D

### PARTICLE SIZE DISTRIBUTION OF AGGREGATES

Sample Type	Sample Name	1180 $\mu$ m (%)	500 $\mu$ m (%)	250 $\mu$ m (%)	125 $\mu$ m (%)	53 $\mu$ m (%)	<53 $\mu$ m (%)
Lime mortars with natural pozzolanic aggregates from Aigai	A1	27.9 $\pm$ 1.5	22.0 $\pm$ 3.8	18.3 $\pm$ 1.2	8.1 $\pm$ 1.2	2.6 $\pm$ 0.8	0.9 $\pm$ 0.0
	A2	40.8 $\pm$ 1.0	26.2 $\pm$ 0.6	6.6 $\pm$ 1.2	2.6 $\pm$ 1.4	0.8 $\pm$ 0.8	0.6 $\pm$ 0.1
	A3	29.5 $\pm$ 1.9	37.5 $\pm$ 0.2	11.5 $\pm$ 0.9	3.4 $\pm$ 0.6	1.3 $\pm$ 0.2	0.8 $\pm$ 0.1
	A6	11.2 $\pm$ 2.1	28.3 $\pm$ 0.3	23.4 $\pm$ 2.5	8.0 $\pm$ 1.1	2.1 $\pm$ 0.2	0.8 $\pm$ 0.0
	A7	44.6 $\pm$ 0.6	20.8 $\pm$ 0.4	7.0 $\pm$ 0.7	3.4 $\pm$ 0.2	1.5 $\pm$ 0.1	1.0 $\pm$ 0.1
	A9	30.4 $\pm$ 5.6	29.9 $\pm$ 1.8	8.5 $\pm$ 1.0	2.9 $\pm$ 0.4	1.4 $\pm$ 0.2	0.5 $\pm$ 0.3
	A12	45.1 $\pm$ 3.0	19.0 $\pm$ 0.6	6.7 $\pm$ 0.4	2.6 $\pm$ 0.1	1.2 $\pm$ 0.1	0.9 $\pm$ 0.4
Lime mortars with natural pozzolanic aggregates from Nysa	N3	39.9 $\pm$ 1.9	19.6 $\pm$ 1.8	11.1 $\pm$ 2.1	6.7 $\pm$ 2.0	3.5 $\pm$ 0.8	1.4 $\pm$ 0.5
	N4	35.2 $\pm$ 4.3	23.7 $\pm$ 1.6	11.0 $\pm$ 1.3	5.5 $\pm$ 0.7	3.3 $\pm$ 0.4	1.6 $\pm$ 0.4
	N7	41.0 $\pm$ 1.5	16.5 $\pm$ 0.5	9.6 $\pm$ 3.1	6.5 $\pm$ 3.0	2.9 $\pm$ 0.1	1.1 $\pm$ 0.1
	N10	31.3 $\pm$ 2.6	22.9 $\pm$ 0.3	13.4 $\pm$ 0.6	6.3 $\pm$ 0.1	2.4 $\pm$ 0.3	0.8 $\pm$ 0.2
	N12	45.5 $\pm$ 1.6	18.9 $\pm$ 0.9	7.9 $\pm$ 0.0	4.7 $\pm$ 0.1	2.9 $\pm$ 0.1	1.3 $\pm$ 0.0
	N13	34.9 $\pm$ 0.8	15.8 $\pm$ 1.4	9.4 $\pm$ 0.1	9.3 $\pm$ 1.1	8.0 $\pm$ 2.2	3.1 $\pm$ 0.8
	N16	41.0 $\pm$ 8.5	11.6 $\pm$ 1.3	5.9 $\pm$ 2.0	3.5 $\pm$ 0.7	2.3 $\pm$ 0.6	1.5 $\pm$ 0.3
	N17	22.0 $\pm$ 1.3	14.3 $\pm$ 1.8	10.6 $\pm$ 0.9	7.9 $\pm$ 0.6	3.6 $\pm$ 0.0	1.2 $\pm$ 0.1
	N21	38.0 $\pm$ 7.6	17.2 $\pm$ 0.4	9.9 $\pm$ 0.5	5.6 $\pm$ 0.7	3.0 $\pm$ 1.1	1.4 $\pm$ 0.4
N23	38.0 $\pm$ 0.8	22.7 $\pm$ 0.5	9.9 $\pm$ 0.2	5.4 $\pm$ 0.0	3.1 $\pm$ 0.1	1.4 $\pm$ 0.1	

Sample Type	Sample Name	1180 $\mu$ m (%)	500 $\mu$ m (%)	250 $\mu$ m (%)	125 $\mu$ m (%)	53 $\mu$ m (%)	<53 $\mu$ m (%)
Lime mortars with artificial pozzolanic aggregates from Aigai	A5	29.2 $\pm$ 1.1	12.9 $\pm$ 0.9	8.9 $\pm$ 1.5	8.4 $\pm$ 0.6	7.0 $\pm$ 0.6	4.7 $\pm$ 2.2
	A10	18.5 $\pm$ 6.6	11.8 $\pm$ 9.0	7.7 $\pm$ 1.3	3.7 $\pm$ 0.1	2.0 $\pm$ 0.2	2.0 $\pm$ 0.1
	A11	65.1 $\pm$ 3.3	9.1 $\pm$ 0.3	4.0 $\pm$ 0.4	2.5 $\pm$ 0.5	1.7 $\pm$ 0.3	0.9 $\pm$ 0.2
Lime mortars with artificial pozzolanic aggregates from Nysa	N1	37.8 $\pm$ 2.7	13.4 $\pm$ 0.7	4.9 $\pm$ 0.3	2.6 $\pm$ 0.4	2.2 $\pm$ 0.5	1.5 $\pm$ 0.4
	N2	13.3 $\pm$ 1.0	26.2 $\pm$ 1.4	13.9 $\pm$ 0.6	6.6 $\pm$ 0.3	3.6 $\pm$ 0.0	2.2 $\pm$ 0.1
	N5	37.0 $\pm$ 1.3	23.4 $\pm$ 0.7	10.6 $\pm$ 0.9	4.7 $\pm$ 0.0	2.4 $\pm$ 0.0	1.1 $\pm$ 0.1
	N6	38.0 $\pm$ 1.5	19.2 $\pm$ 1.6	12.1 $\pm$ 1.0	6.6 $\pm$ 0.5	3.5 $\pm$ 0.2	1.8 $\pm$ 0.4
	N8	<i>Can not be determined due to insufficient sample size.</i>					
	N9	26.3 $\pm$ 3.6	12.6 $\pm$ 3.4	10.8 $\pm$ 0.7	5.1 $\pm$ 3.6	3.6 $\pm$ 0.5	1.4 $\pm$ 0.0
	N11	37.3 $\pm$ 4.4	17.6 $\pm$ 0.1	10.4 $\pm$ 0.9	6.9 $\pm$ 0.9	3.7 $\pm$ 0.3	1.3 $\pm$ 0.2
	N14	38.6 $\pm$ 4.8	19.2 $\pm$ 0.5	10.8 $\pm$ 0.9	6.2 $\pm$ 0.6	4.4 $\pm$ 0.6	1.6 $\pm$ 0.2
	N15(1)	42.9 $\pm$ 1.0	7.1 $\pm$ 0.6	3.0 $\pm$ 0.3	2.1 $\pm$ 0.2	1.7 $\pm$ 0.2	1.6 $\pm$ 0.2
	N15(2)	18.6 $\pm$ 1.5	17.2 $\pm$ 2.3	6.6 $\pm$ 0.1	4.8 $\pm$ 0.5	3.9 $\pm$ 0.6	3.2 $\pm$ 1.2
	N20	38.0 $\pm$ 4.9	20.5 $\pm$ 1.0	10.6 $\pm$ 0.3	5.6 $\pm$ 0.2	3.6 $\pm$ 0.4	2.0 $\pm$ 0.2
	N22	40.2 $\pm$ 2.6	11.5 $\pm$ 2.1	6.2 $\pm$ 0.3	4.1 $\pm$ 0.4	3.7 $\pm$ 1.2	1.9 $\pm$ 0.0
N24	<i>Can not be determined due to insufficient sample size.</i>						

## APPENDIX E

### POZZOLANIC ACTIVITIES OF AGGREGATES

Sample Type	Sample Name	Electrical Conductivity (mS/cm)		Difference in Electrical Conductivity (mS/cm)
		Before	After	
Lime mortars with natural pozzolanic aggregates from Aigai	A1	7.89	0.98	6.91
	A2	7.97	0.33	7.64
	A3	8.29	3.18	5.11
	A6	8.07	1.32	6.75
	A7	7.90	0.66	7.24
	A9	8.50	1.85	6.65
	A12	8.22	0.37	7.85
Lime mortars with natural pozzolanic aggregates from Nysa	N3	8.09	3.99	4.10
	N4	8.35	3.62	4.73
	N7	8.23	4.98	3.25
	N10	7.98	3.49	4.49
	N12	8.00	4.44	3.56
	N13	8.17	3.77	4.40
	N16	7.98	1.96	6.02
	N17	8.20	4.09	4.11
	N21	8.20	4.52	3.68
	N23	8.09	2.21	5.88

Sample Type	Sample Name	Electrical Conductivity (mS/cm)		Difference in Electrical Conductivity (mS/cm)
		Before	After	
Lime mortars with artificial pozzolanic aggregates from Aigai	A5	7.98	4.48	3.50
	A10	8.29	4.73	3.56
	A11	8.00	1.31	6.69
Lime mortars with artificial pozzolanic aggregates from Nysa	N1	8.00	1.76	6.24
	N2	7.95	3.78	4.17
	N5	8.02	2.01	6.01
	N6	7.98	4.03	3.95
	N7	8.23	4.98	3.25
	N9	7.99	2.34	5.65
	N11	8.21	3.11	5.10
	N14	8.07	2.22	5.85
	N15(1)	8.32	1.04	7.28
	N15(2)	8.22	2.41	5.81
	N20	8.27	1.86	6.42
	N22	8.14	2.47	5.67
	N24	8.42	0.34	8.09

## APPENDIX F

### STRUCTURAL H<sub>2</sub>O AND CO<sub>2</sub> RATIOS OF ROMAN LIME MORTARS

Sample Type	Sample Name	Weight Losses (%)		CO <sub>2</sub> /H <sub>2</sub> O
		200-600 °C (Structural H <sub>2</sub> O)	600-900 °C (CO <sub>2</sub> )	
Lime mortars with natural pozzolanic aggregates from Aigai	A1	4.79	13.21	2.76
	A2	5.47	19.90	3.64
	A3	5.41	14.86	2.75
	A6	4.54	17.10	3.77
	A7	3.43	11.24	3.28
	A9	6.34	10.92	1.72
	A12	9.86	11.03	1.12
Lime mortars with natural pozzolanic aggregates from Nysa	N3	4.16	12.96	3.11
	N4	3.54	13.22	3.73
	N7	2.85	18.28	6.41
	N10	4.38	22.05	5.03
	N12	3.64	12.11	3.33
	N13	3.59	10.73	2.99
	N16	4.01	13.17	3.29
	N17	4.16	20.83	5.00
	N21	4.24	14.82	3.49
	N23	3.75	12.84	3.42

Sample Type	Sample Name	Weight Losses (%)		CO <sub>2</sub> /H <sub>2</sub> O
		200-600 °C (Structural H <sub>2</sub> O)	600-900 °C (CO <sub>2</sub> )	
Lime mortars with artificial pozzolanic aggregates from Aigai	A5	3.58	15.62	4.36
	A10	3.87	18.50	4.78
	A11	4.08	7.66	1.88
Lime mortars with artificial pozzolanic aggregates from Nysa	N1	5.48	14.99	2.73
	N2	4.77	20.67	4.34
	N5	2.94	12.85	4.37
	N6	3.87	20.24	5.23
	N7	2.85	18.28	6.41
	N9	4.44	21.94	4.94
	N11	9.16	13.33	1.46
	N14	5.05	12.08	2.39
	N15(1)	5.16	14.24	2.76
	N15(2)	5.89	18.82	3.20
	N20	4.36	11.12	2.55
	N22	3.95	8.00	2.02

# VITA

## Elif UĞURLU SAĞIN

*Date of Birth:*

08.10.1980

*Place of Birth:*

İzmir

*Education:*

B.Arch., Dokuz Eylül University, Department of Architecture (2002)

M.Sc., İzmir Institute of Technology, Department of Architectural Restoration (2005)

Ph.D., İzmir Institute of Technology, Department of Architecture (2012)

*Academic Experience:*

Research Assistant, Department of Architectural Restoration, İzmir Institute of Technology (2002-2005)

Specialist, Department of Architectural Restoration, İzmir Institute of Technology (since 2005)